21136

NATIONAL LIBRARY
OTTAWA

CANADA

BIBLIOTHÈQUE NATIONALE
OTTAWA

NAME OF AUTHOR.....William T. Woloadko.....

TITLE OF THESIS....Physical and Chemical Studies of Rabbit Cardiac Myosin and Subfragments Produced by Limited Papain Digestion

UNIVERSITY..University of Alberta (Edmonton)

DEGREE FOR WHICH THESIS WAS PRESENTED.....Ph.D.....

YEAR THIS DEGREE GRANTED.....1974.....

Permission is hereby granted to THE NATIONAL LIBRARY OF CANADA to microfilm this thesis and to lend or sell copies of the film.

The author reserves other publication rights, and neither the thesis nor extensive extracts from it may be printed or otherwise reproduced without the author's written permission.

(Signed).....W.T. Woloadko.....

PERMANENT ADDRESS:

.....12013-58 St.....
.....Edmonton, Alberta
.....

DATED..December 17, 1973

NL-91 (10-68)

THE UNIVERSITY OF ALBERTA

PHYSICAL AND CHEMICAL STUDIES OF RABBIT CARDIAC MYOSIN AND SUBFRAGMENTS PRODUCED BY LIMITED PAPAIN DIGESTION

by

© WILLIAM T. WOLODKO

A THESIS

SUBMITTED TO THE FACULTY OF GRADUATE STUDIES AND RESEARCH

IN PARTIAL FULFILMENT OF THE REQUIREMENTS FOR THE DEGREE

OF DOCTOR OF PHILOSOPHY

DEPARTMENT OF BIOCHEMISTRY

EDMONTON, ALBERTA

SPRING, 1974

THE UNIVERSITY OF ALBERTA

FACULTY OF GRADUATE STUDIES AND RESEARCH

The undersigned certify that they have read, and recommend to the Faculty of Graduate Studies and Research, for acceptance, a thesis entitled Physical and Chemical Studies of Rabbit Cardiac Myosin and Subfragments Produced by Limited Papain Digestion, submitted by William T. Wolodko in partial fulfilment of the requirements for the degree of Doctor of Philosophy.

Supervisor

External Examiner

Date December 10, 1973.

ABSTRACT

Rabbit cardiac myosin, isolated from frozen tissue, was effectively purified by batchwise treatment with DEAE-cellulose in addition to using dilution-precipitation techniques. An extensive experimental program was subsequently carried out with respect to the enzymic, amino acid, optical, and physicochemical properties of native cardiac myosin. This program has included the following: examination of the effects of pH and varying concentrations of ATP, $CaCl_2$, $MgCl_2$, and PCMB on its ATPase activity; determination of its ultraviolet absorption spectrum and associated extinction coefficient; measurement of its circular dichroic spectrum in solvent buffers at different pH or containing ATP in the absence or presence of Ca^{++} or Mg^{++} ions; study of the concentration dependence of its viscosity and sedimentation velocity at low temperatures; and investigation of its molecular weight by the Archibald method and low- and high-speed sedimentation equilibrium. In brief, the results of these studies were consistent with the interpretation that cardiac myosin is comprised of highly asymmetric, semi-rigid molecules with a molecular weight in the order of 4.7×10^5, which display nonideality even in solvent buffers of high ionic strength at neutral pH. In addition, computer analysis of the high-speed sedimentation equilibrium data has provided evidence for the presence of a self-association reaction at low protein concentration. Even though the specific ATPase activity of cardiac myosin was found to be approximately one-third that reported for skeletal myosin in all cases, it was concluded, on the basis of the essentially analogous physical and chemical properties of rabbit cardiac and skeletal myosin, that the two proteins are very similar in terms of

molecular size, shape, and secondary structure.

This conclusion was augmented by the results of studies using a degradative approach to investigate the substructure of the cardiac molecule. Routine methodology was established for the limited proteolytic digestion of rabbit cardiac myosin with S-MDA-mercuripapain at low temperatures and neutral pH, using moderate enzyme to myosin ratios. Pertinent properties of the insoluble enzyme complex were also examined briefly. Kinetic, ultracentrifugal, and chromatographic observations of the fragmentation process revealed that a single type of lytic reaction occurs during the early stages, predominantly releasing HMM-S1 and myosin rods. With further time of digestion, the rods are additionally cleaved yielding light meromyosin and HMM-S2, and HMM-S1 is found to be partially degraded.

The major proteolytic subfragments were isolated, purified, and characterized with respect to their enzymatic, optical, amino acid, and physicochemical properties. Only HMM-S1 exhibited Ca^{++} ion-activated ATPase activity, and at a level three- to four-fold higher than that of native myosin. Moreover, its hydrodynamic properties suggest that it is globular in structure. On the other hand, LMM-A (which consists mainly of rods) and HMM-S2 appear to be highly asymmetric, rigid, α-helical molecules devoid of the amino acid proline. Strong similarities were evident in all aspects upon comparison of these results with documented information concerning the skeletal system. On the basis of the physical and chemical properties of the proteolytic subfragments relative to that of native myosin, it was further concluded that the cardiac myosin molecule is a double-stranded, α-helical rod ending in two subfragment 1 globules, of which only one may be enzymatically active at a time.

ACKNOWLEDGEMENTS

The author is pleased to express sincere appreciation to Dr. Cyril Kay for his patient guidance and continued encouragement throughout the course of these studies. His generous provision of research facilities and funds has contributed considerably to the success of this work and is most gratefully acknowledged.

The author is indebted to fellow members of Dr. Kay's laboratory for their general assistance, valuable advice, and criticisms. In particular, the author is grateful to Mr. K. Oikawa for performing the circular dichroic measurements, and to Mr. V. Ledsham for his skillful operation of the ultracentrifuge and expert help with the graphics and photography.

Special thanks are due Dr. L.B. Smillie for extending the use of his laboratory facilities for amino acid analysis, and to Mr. M. Natriss for his competent technical assistance in carrying out the analyzer runs.

Personal financial support in the form of a University of Alberta Graduate Teaching Assistantship and a Predoctoral Fellowship from the Muscular Dystrophy Association of Canada, as well as from Dr. Kay during the writing of this dissertation, is gratefully acknowledged.

TABLE OF CONTENTS

	Page
ABSTRACT	iv
ACKNOWLEDGEMENTS	vi
LIST OF TABLES	x
LIST OF FIGURES	xi
GLOSSARY OF PRINCIPAL SYMBOLS AND ABBREVIATIONS	xiv
CHAPTER 1 INTRODUCTION	1
The Substructure of Striated Muscle	1
Current Status of Cardiac Myosin	2
Comparative Features of the Cardiac and Skeletal Molecules	3
The Substructure of Myosin as Revealed by Proteolytic Studies	5
Aims of the Present Investigation	7
CHAPTER 2 GENERAL MATERIALS AND METHODS	9
Laboratory Materials and Procedures	9
Enzymatic Activity and pH-Stat Measurements	11
UV Optical Property Measurements	12
Ultraviolet Absorption	12
Circular Dichroism	13
Protein Concentration Measurements	14
Dry Weight Method	14
Micro-Kjeldahl Method	15
Lowry Method	15

Page

Refractometric Method 17

Amino Acid Analysis 17

Viscometry 18

Ultracentrifugation Studies 21

Determination of Sedimentation Rates and Molecular Homogeneity 22

Molecular Weight Determination by Sedimentation Equilibrium 26

Molecular Weight Determination by the Archibald Method 33

CHAPTER 3 NATIVE CARDIAC MYOSIN 36

Preparation of Rabbit Cardiac Myosin 36

Results 39

Adenosinetriphosphatase Activity 41

Ultraviolet Optical Properties 47

Amino Acid Composition 50

Viscosity 52

Sedimentation Velocity 52

Molecular Weight 54

Discussion 66

CHAPTER 4 PROTEOLYTIC FRAGMENTATION OF CARDIAC MYOSIN WITH PAPAIN 75

Preparative Methods and Procedures 76

Mercuripapain 76

S-MDA Resin 79

S-MDA-mercuripapain 79

Results 82

Page

Studies of S-MDA Resin and S-MDA-mercuripapain . . . 82

General Method of Proteolysis 90

Observations of the Fragmentation Process 92

Kinetic Analysis 100

Discussion 102

CHAPTER 5 THE PROTEOLYTIC SUBFRAGMENTS 107

Methods of Isolation and Purification 107

LMM-A 107

HMM-S1 108

HMM-S2 109

Results 111

Ultraviolet Optical Properties 112

Amino Acid Composition 114

Adenosinetriphosphatase Activity 117

Viscosity 119

Sedimentation Velocity 121

Molecular Weight 121

Discussion 129

CHAPTER 6 FINAL DISCUSSION 139

BIBLIOGRAPHY 149

APPENDICES 155

Computer Programs 155

Appendix 1. SDCF 155

Appendix 2. LSDQM, HSDQM, MNZY2, and LSPFIT 156

Appendix 3. ARCH and RND 164

LIST OF TABLES

Table		Page
I	Amino Acid Composition of Cardiac Myosin	51
II	Molecular Weight of Cardiac Myosin as Determined by High-speed Sedimentation Equilibrium	65
III	Comparison of the Amino Acid Composition of Rabbit Cardiac and Skeletal Myosin	71
IV	Apparent Kinetic Constants Associated with the Esterase Activity of Mercuripapain and S-MDA-Mercuripapain	89
V	Amino Acid Composition of Papain, Mercuripapain, and S-MDA-Mercuripapain	91
VI	Amino Acid Composition of Cardiac Myosin, LMM-A, and Subfragments 1 and 2	118
VII	Comparison of the Amino Acid Composition of Cardiac and Skeletal Subfragment 1	131
VIII	Comparison of the Amino Acid Composition of Rabbit Cardiac and Skeletal LMM-like Fragments and Subfragment 2	135
IX	Physical and Chemical Parameters of Rabbit Cardiac Myosin and the Proteolytic Subfragments	140

LIST OF FIGURES

Figure		Page
1	Schlieren Patterns of Cardiac Myosin Preparations Treated and Not Treated with DEAE-cellulose	40
2	The Ca^{++} Ion-activated ATPase Activity of Cardiac Myosin as a Function of Amount Myosin	40
3	The Effect of Varying $CaCl_2$ Concentration on the Specific ATPase Activity of Cardiac Myosin	43
4	The Effect of Varying $MgCl_2$ Concentration on the Specific ATPase Activity of Cardiac Myosin	43
5	The Effect of Varying ATP Concentration, in the Absence and Presence of $CaCl_2$, on the Specific ATPase Activity of Cardiac Myosin	44
6	Double-reciprocal Plot: Inverse Specific ATPase Activity Against Inverse Varying ATP Concentration, in the Absence and Presence of $CaCl_2$	44
7	The pH Profile of the Ca^{++} Ion-activated Specific ATPase Activity of Cardiac Myosin	46
8	The Effect of Varying PCMB to Protein Ratios on the Ca^{++} Ion-activated Specific ATPase Activity of Cardiac Myosin	46
9	Ultraviolet Absorption Spectrum of Cardiac Myosin . .	48
10	Ultraviolet Circular Dichroic Spectrum of Cardiac Myosin	49
11	Concentration Dependence of the Reduced Specific Viscosity of Cardiac Myosin	53
12	Concentration Dependence of the Corrected Sedimentation Velocity of Cardiac Myosin	53
13	Molecular Weight Study of Cardiac Myosin by the Archibald Method	55
14	Molecular Weight Study of Cardiac Myosin by Low-speed Sedimentation Equilibrium	58
15	Molecular Weight Study of Cardiac Myosin by High-speed Sedimentation Equilibrium	62

Figure		Page
16	Schematic Representation of the Principal Reaction Steps in the Synthesis of S-MDA Resin	80
17	Protein Binding Curve for S-MDA Resin	83
18	Time Course of Binding of Mercuripapain to Diazotized S-MDA Resin	83
19	Apparent Loss of Protein Binding Capacity of Diazotized S-MDA Resin with Time	85
20	The Effect of Storage Time on the Enzymatic Stability of Mercuripapain and S-MDA-Mercuripapain	85
21	Kinetic Study of Mercuripapain	87
22	Kinetic Study of S-MDA-Mercuripapain	88
23	Schlieren Patterns of Trial Digestion Mixtures of Cardiac Myosin Fragmented with Insolubilized Papain .	93
24	Schlieren Patterns of the Water-soluble and Water-insoluble Fractions of a Routine Papain Digest of Cardiac Myosin	93
25	Elution Profiles, upon Gel Filtration, of the Water-soluble and Water-insoluble Fractions in Relation to that of the Total Digest	96
26	Schlieren Patterns of the Water-soluble Fraction after 1, 15, and 30 Minute Times of Digestion . . .	98
27	Apparent Area of the Schlieren Peaks of the Water-soluble Fraction as a Function of Digestion Time . .	98
28	Uptake of Hydroxide Ions During the Proteolytic Digestion of Cardiac Myosin with Insolubilized Papain	101
29	Graphical Analysis of the Adjusted pH-Stat Data Derived from Papain Digestion of Cardiac Myosin . .	101
30	Elution Profile of the Chromatographic Separation of the Water-soluble Subfragments by Gel Filtration . .	110
31	Ultraviolet Absorption Spectra of HMM-S1, HMM-S2, and LMM-A	113
32	Graphical Estimation of the Extinction Coefficients for LMM-A, HMM-S2, and HMM-S1	115

Figure		Page
33	Ultraviolet Circular Dichroic Spectra of HMM-S1, HMM-S2, and LMM-A	116
34	The Effect of Varying $CaCl_2$ Concentration on the Specific ATPase Activity of HMM-S1	120
35	Concentration Dependence of the Reduced Specific Viscosity of LMM-A, HMM-S2, and HMM-S1	120
36	Concentration Dependence of $s_{20,w}$ of the Major Proteolytic Subfragments of Cardiac Myosin	122
37	Molecular Weight Study of Cardiac Subfragment 1 . .	124
38	Molecular Weight Study of Cardiac Subfragment 2 . .	126
39	Molecular Weight Study of LMM-A	128
40	Schematic Representation of the Cardiac Myosin Molecule, Subfragments, and Principal Steps of the Digestion Process	141

GLOSSARY OF PRINCIPAL SYMBOLS AND ABBREVIATIONS

ATP	adenosine triphosphate
B	second virial coefficient
BAEE	α-N-benzoyl-L-arginine ethyl ester
c	concentration
CD	circular dichroism
DEAE-	diethylaminoethyl-
DTT	dithiothreitol
dy	vertical fringe displacement
EDTA	ethylenediaminetetraacetate
$E^{1\%}_{1\ cm}$	extinction coefficient: absorbance of a 1% solution over an optical path length of 1 cm
HMM	heavy meromyosin
HMM-S1, HMM-S2	heavy meromyosin subfragment 1 and subfragment 2
k'	Huggins constant
k_{cat}	kinetic rate constant
K_{mapp}	apparent Michaelis constant
K_s	concentration-dependence constant of the sedimentation coefficient
LMM	light meromyosin
$\bar{M}_n$, $\bar{M}_w$, $\bar{M}_z$, $\bar{M}_{y2}$	number-, weight-, z-, and y_2-average molecular weight
PAB-	p-aminobenzyl-
PCMB	p-chloromercuribenzoate
P_i	inorganic phosphate
r	radial distance from the axis of rotation
R	universal gas constant

S	Svedberg unit of sedimentation velocity (10^{-13} sec)
SDS	sodium dodecyl sulfate
S-MDA	(dialdehyde)-starch-methylenedianiline
$s_{20,w}$	sedimentation coefficient corrected to the viscosity and density of water at 20°C
t	time
T	absolute temperature
TCA	trichloroacetic acid
V_{max}	maximum enzymic velocity
η	viscosity
$[\eta]$	intrinsic viscosity
$[\theta]$	mean residue molecular ellipticity
λ_{max}	wavelength of maximum absorbance
$\bar{\nu}$	partial specific volume
ρ	solution density
ω	angular velocity of rotation

CHAPTER 1

INTRODUCTION

The Substructure of Striated Muscle

When examined with a light microscope, the myofibrils of striated muscle are characterized by a pattern of alternating dark and light transverse markings. The origin of this pattern has been established by electron microscopic investigations of vertebrate skeletal tissue (Huxley, 1953). Striated muscle is comprised principally of two contractile proteins, myosin and actin, which are organized in parallel, interdigitating sets of thick and thin filaments aligned longitudinally in the myofibrils (Hanson and Huxley, 1960). The anisotropic zone of high refractive index (the A-band), observed in the central portion of the sarcomere, arises from the assembled order of the thick filaments, while the isotropic regions of lower refractive index (the I-band), evident to either side of the anisotropic zone, result from the arrangement of the thin filaments. Each thick filament consists primarily of longitudinally oriented molecules of myosin (Huxley, 1963), and each thin filament of globular actin monomers linked in a rigid, double-stranded helical chain (Hanson and Lowy, 1963). In addition, tropomyosin and the components of the troponin complex are physically associated with the thin filaments. These proteins mediate the coupling of excitation and contraction by sensitizing the complex of actin and myosin to the physiological action of calcium ions (Ebashi et al., 1969; Katz, 1970). In general terms, muscle contraction involves the transduction of the chemical energy of adenosine

triphosphate (ATP) into mechanical energy through the sliding process of the thin filaments internally over the thick filaments — the A-band remains constant in length, whereas the I-band shortens (Huxley and Hanson, 1954). Myosin plays a paramount role in contraction, for not only is ATP hydrolyzed at active sites located in the myosin molecule but also the many cross-bridges which actually interact with the actin filaments and provide the driving force for the sliding movement originate from the thick filaments (Huxley and Brown, 1967).

Current Status of Cardiac Myosin

In the past two decades considerable information has been obtained with respect to the structure and enzymatic properties of myosin in vitro. The bulk of this information, however, concerns rabbit skeletal myosin; the added difficulty of purifying cardiac myosin, in conjunction with its tendency toward aggregation, has discouraged, somewhat, the extensive investigation of this important contractile protein (Katz, 1970). Due partly to the limited availability of fresh rabbit hearts in the past, most of the previous studies of cardiac myosin have dealt with myosin prepared from canine or bovine tissue. Consequently, little research has been directed towards rabbit cardiac myosin, and its complete characterization has not been carried out. Moreover, this situation has introduced an additional variable, that of species differences, to which consideration must be made when comparing the properties of cardiac myosin to rabbit skeletal myosin (Mueller et al., 1964). An excellent review of past and current developments with regard to the major contractile proteins of the myocardium, as well as the white skeletal muscle of rabbit, has been published by Katz (1970). While no attempt is made to

emulate this rather comprehensive survey of the literature, details pertinent to the background of the present study are briefly considered.

Comparative Features of the Cardiac and Skeletal Molecules. Morphologically, cardiac and skeletal myosin are thought to be very similar. Intrinsic estimates of the reduced viscosity and diffusion and sedimentation coefficients of canine cardiac myosin do not differ greatly from corresponding values determined for rabbit skeletal myosin (Brahms and Kay, 1963; Mueller et al., 1964). Furthermore, the marked concentration dependence exhibited by these hydrodynamic parameters indicates that the molecular structure of mysoin is highly asymmetric. The results of electron microscopic studies confirm this conclusion and reveal that the myosin molecule is essentially a narrow rod approximately 1.3×10^3 Å in length with two globular protrusions at one end (Mueller et al., 1964; Carney and Brown Jr., 1966; Slayter and Lowey, 1967). It has been shown that the rodlike portion of the molecules may be involved in the formation of the thick filaments (Harrington et al., 1973) and that the end globules possess the enzymatically active sites which interact with actin and hydrolyze ATP (Lowey et al., 1969). The results of comparative ultraviolet optical rotatory dispersion measurements with respect to canine cardiac and rabbit skeletal myosin are also in good agreement, reflecting the general similarity in their amino acid compositions and implying that the secondary structure of both proteins is very much alike (Brahms and Kay, 1963; Kay et al., 1964). The adenosinetriphosphatase (ATPase) activity of cardiac myosin, like that of skeletal myosin, is activated in the presence of calcium ions and inhibited with magnesium ions, shows a two mode effect with increasing concentrations of p-chloromercuribenzoate,

and does not display a definite pH maximum in the range 7 to 9 (Brahms and Kay, 1962; Mueller et al., 1964).

Perhaps the most elusive elementary property of cardiac myosin to be measured has been its monomer molecular weight. Although a value in the order of 5.0×10^5 has been considered for some time to be a reasonable estimate, general agreement with respect to the true intrinsic value has not been reached (Katz, 1970). Only fairly recently has a similar situation regarding skeletal myosin been satisfactorily resolved. Utilizing high-speed sedimentation equilibrium techniques and sophisticated computer analyses described by Roark and Yphantis (1969), Godfrey and Harrington (1970) have demonstrated that skeletal myosin exists in a monomer-dimer equilibrium in solvents of high ionic strength, and that the true molecular weight of the monomer at infinite dilution is close to 4.6×10^5. There are essentially two reasons why conflicting values were obtained in the early studies. Firstly, myosin solutions are non-ideal due to the semi-rigid, asymmetric shape of the molecules. Secondly, because of the strong tendency of myosin to aggregate, the resultant molecular weight estimate indirectly reflects the age of the myosin preparation (Brahms and Kay, 1962) and, to some extent, depends on the method of purification employed. With respect to the latter point, Vierling et al. (1968) have found that the apparent molecular weight of canine cardiac myosin purified by ammonium sulfate fractionation (5.4×10^5) is substantially higher than that of myosin not prepared with this salt but by the conventional dilution-precipitation method (4.8×10^5).

Despite the apparent homology in the molecular and physicochemical properties of cardiac and skeletal myosin, well defined differences between the two proteins are known to exist. The calcium ion-

activated ATPase activity of cardiac myosin, for example, is significantly lower, under identical experimental conditions, than that of skeletal myosin (Bailey, 1942; Brahms and Kay, 1962). Rabbit cardiac myosin possesses two distinct classes of light chains (low molecular weight protein components associated with the globular portion of the myosin molecule (Dreizen et al., 1967)), whereas skeletal myosin contains a total of three (Locker and Hagyard, 1967; Sarkar et al., 1971). Moreover, the light chains of ovine and bovine cardiac myosin yield two additional thiol peptides upon limited tryptic digestion, evidently not present in the light chains of ovine and rabbit skeletal myosin (Weeds and Pope, 1971). The amino acid sequence of corresponding thiol peptides and methylated and non-methylated histidine peptides from cardiac and skeletal myosin are found to be dissimilar (Weeds and Frank, 1973; Huszar and Elzinga, 1972). It is thus not surprising that differences between the immunological properties of the two myosin proteins are additionally observed (Finck, 1965). Finally, canine cardiac myosin is more resistant to proteolysis by trypsin than is rabbit skeletal myosin, perhaps also reflecting variations in their primary structures (Brahms and Kay, 1963; Theiner, 1963).

The Substructure of Myosin as Revealed by Proteolytic Studies.

A considerable proportion of the current knowledge pertaining to the structural properties of rabbit skeletal myosin has been derived through proteolytic fragmentation experiments and subsequent study of the purified subfragments. Early investigations showed that brief treatment of skeletal myosin with trypsin or chymotrypsin initially cleaves the molecule into two parts, designated with respect to their relative size, light and heavy meromyosin (Gergely, 1953; Mihalyi and Szent-Györgyi,

1953). Light meromyosin (LMM) is structurally a rigid protein of high α-helical content which originates from the rodlike region of the myosin molecule and displays the solubility characteristics of native myosin (Szent-Györgyi, Cohen, and Philpott, 1960). Heavy meromyosin (HMM), on the other hand, consists mainly of the globular portions of the native molecule plus a short segment of attached rod and retains the enzymatic properties of the parent molecule (Szent-Györgyi, 1953). Further tryptic digestion of heavy meromyosin releases yet smaller integral fragments: subfragment 1, the individual globules which retain the ability to hydrolyze ATP and bind actin (Mueller and Perry, 1962), and subfragment 2, the rodlike segment of HMM which is not enzymatically active (Lowey, Goldstein, and Luck, 1966). Likewise, a series of α-helical fragments (light meromyosin Fractions 1 to 3) are obtained by stepwise degradation of LMM (Bálint et al., 1968).

Depending on the duration of the proteolytic reaction, varying amounts of small peptides are concurrently liberated during the production of the major subfragments (Segal et al., 1967). This single fact represents the chief limitation of this approach to the study of the substructure of myosin — particularly in the preparation of undegraded subfragments 1 and 2 via tryptic digestion. Kominz et al. (1965) have discovered that an insoluble form of papain preferentially cleaves skeletal myosin in the attachment region of the globules, thus initially releasing subfragment 1 with relatively minor loss of non-protein nitrogen. Lowey et al. (1969), exploiting this finding, have established the following points: one, the action of papain on rabbit skeletal myosin; two, the conditions under which a wide variety of fragments may be produced; and three, the size and shape of these subfragments, as deduced from electron

micrographic, physicochemical, and enzymatic activity measurements.

The success of this experimental approach achieved with rabbit skeletal myosin has only been partially realized with respect to the cardiac system. It has been shown, for instance, that the meromyosins can be produced from canine cardiac myosin by limited tryptic digestion, although at higher trypsin to myosin ratios compared to that employed with skeletal myosin (Theiner, 1963). It was additionally suggested that the higher resistance of cardiac myosin than skeletal myosin to proteolysis was not solely attributable to the different tissues from which the proteins were isolated, but, to some extent, to the difference in animal species. More recently, Tada et al. (1969) have reported that active subfragment 1 can be obtained from bovine cardiac heavy meromyosin by short digestion with soluble papain. Furthermore, comparative pH-stat measurements indicated that bovine cardiac HMM was more resistant to proteolysis by papain, chymotrypsin, or trypsin than either rabbit skeletal HMM or myosin. However, the proteolytic degradation of native cardiac myosin with papain, analysis of the reaction, and characterization of the subfragments released are aspects of the cardiac system which have not been studied.

Aims of the Present Investigation

The ultimate purpose of this study has been the comprehensive characterization of rabbit cardiac myosin. With fresh rabbit hearts readily available in substantial quantities, comparison has been made with the rabbit skeletal system without the added variable of species differences. The experimental objectives of the present investigation were, therefore, as follows:

1) to prepare homogeneous rabbit cardiac myosin from frozen tissue;
2) to thoroughly examine its enzymatic, ultraviolet optical, amino acid, and physicochemical properties (in particular its molecular weight by advanced techniques);
3) to fragment native cardiac myosin by limited proteolysis with insolubilized papain and analyze the degradative process; and
4) to isolate, purify, and study the major subfragments thus produced and derive additional information with respect to the molecular structure of rabbit cardiac myosin.

CHAPTER 2

GENERAL MATERIALS AND METHODS

The physicochemical and enzymatic techniques employed in the characterization of cardiac myosin and the proteolytic subfragments, as well as mercuripapain, are extensively summarized in this chapter. Specific details and experimental conditions pertaining to a particular protein system are given in relevant sections of later chapters. Departing slightly from the precedent of including methods of protein preparation under a general heading of materials and methods, procedures for the isolation and purification of myosin, the subfragments, and mercuripapain are individually described in appropriate chapters with the intention of presenting the results of the entire investigation in a logical sequence and coherent manner.

Laboratory Materials and Procedures

The water which was used in the preparation of all protein and chemical solutions was distilled, redistilled in glass apparatus, and further deionized by passage through a demineralizer column (Crystalab). Disodium adenosine 5'-triphosphate (ATP), α-N-benzoyl-L-arginine etnyl ester HCl (BAEE), and p-chloromercuribenzoic acid (PCMB) were purchased in the highest purity available from the Sigma Chemical Company, St. Louis, Missouri; and dithiothreitol (DTT) was purchased from Calbiochem, Los Angeles, California. All were stored tightly sealed at

temperatures below 0°C. Potassium chloride, potassium phosphate (mono- and dibasic), sodium chloride, potassium hydroxide, and concentrated hydrochloric acid were 'Baker Analyzed' Reagent grade, obtained from the J.T. Baker Chemical Company through Canadian Laboratory Supplies Limited, Edmonton, Alberta. All other chemicals used in this study, unless otherwise specified, were certified A.C.S. grade, purchased from the Fisher Scientific Company, Ltd., Edmonton, Alberta.

Sephadex G-200 (40 to 120 μ particle size) was obtained from Pharmacia Fine Chemicals, Uppsala, Sweden, and the gel was prepared and poured in columns using procedures as described in the Pharmacia technical brochures. When not used, prepared Sephadex was suspended in double-distilled, deionized water and stored sealed at 10°C; a small amount of sodium azide was added to prevent possible bacterial growth.

Diethylaminoethyl (DEAE-) cellulose was purchased from the Fisher Scientific Company, and was thoroughly washed using the method as outlined by Peterson and Sober (1962) with the following modifications: 0.5 M potassium hydroxide was substituted for 1 M sodium hydroxide, the final treatment with alkali was eliminated, and double-distilled, deionized water was used throughout the rinsing procedures.

Measurements of pH were routinely made using a Radiometer pH-meter equipped with a variable temperature compensator and combination glass electrode (Radiometer Inc., Copenhagen, Denmark), frequently standardized with standard pH buffers in the neutral pH range (Fisher Scientific Company).

Buffers and chemical solutions, which were quantitatively prepared directly or indirectly from solid salts, were millipore filtered (0.22 or 0.45 μ pore size) during their preparation to remove dust

and fiber particles, and were adjusted with respect to pH prior to use.

All glassware and preparative centrifuge tubes and bottles were scrupulously cleaned with detergent and water, rinsed with hot water, distilled water, then double-distilled, deionized water, and were dried inverted in an air oven set at 100°C. Pipettes were briefly treated with freshly prepared chromic acid prior to the rinsing and drying procedures.

Enzymatic Activity and pH-Stat Measurements

Release of hydrogen ions during proteolysis and esterolysis was followed by recording the uptake of hydroxide ions required to maintain pH with pH-stat apparatus using established procedures (Jacobsen et al., 1957). The apparatus (Radiometer Inc., Copenhagen, Denmark) consisted of a pH-meter/titrator (type TTTlc) equipped with a variable temperature compensator and combination glass electrode (type K2321c), a titrigraph (type SBR2c) with syringe burette (type SBUla), and a 25 x 65 mm Pyrex reaction cell placed in a plexiglass water jacket. The temperature of the reaction vessel was maintained to ± 0.1°C with a Colora ultra-thermostat circulating water bath; for experiments below room temperature, an external cooling compressor was used in conjunction with the bath. Mixing of the cell contents was accomplished by fixing the position of the electrode in the reaction solution and rapidly turning the cell with the force of the circulating water. Carbon dioxide was excluded by gently passing a stream of nitrogen gas over the surface of the cell contents under a specifically designed hood. Titrant, 5×10^{-3} to 10^{-1} N potassium hydroxide, was freshly prepared, stored under paraffin oil in the titrant reservoir, and delivered by a glass syringe

through finely drawn-out plastic tubing, the tip of which was positioned below the surface of the reaction mixture. The delivery capacity of the glass syringe was calibrated by determining the volume delivered, from measurements of the plunger diameter and length of movement along the syringe barrel, associated with a recorder pen travel of 100 chart units. Prior to pH-stat measurements, the pH-meter was standardized, and the normality of the base was determined by titrating to an end point of pH 7.0 known volumes of dilute standard hydrochloric acid, standardized in turn using potassium hydrogen phthalate (Fisher Primary Standard). Specific volumes of freshly prepared substrate solutions were pipetted into clean reaction cells and allowed to equilibrate with respect to temperature. If necessary, the pH was adjusted to appropriate values with small volumes of potassium hydroxide or hydrochloric acid before the reaction was started by the addition of enzyme. A check for spontaneous release of hydrogen ions under the experimental conditions by substrate alone was conducted over the duration of a typical activity measurement (5 to 10 minutes). Enzymatic activity was calculated from the slope of the best straight line drawn through the pH-stat trace and expressed as moles substrate consumed or product released/min/mg enzyme.

UV Optical Property Measurements

Ultraviolet Absorption. Measurements of ultraviolet absorbance at selected wavelengths were routinely made with either a Beckman DU spectrophotometer (Beckman Instruments Inc., Fullerton, California) or a Gilford Model 240 spectrophotometer (Gilford Instrument Laboratories Inc., Oberlin, Ohio) using standard procedures with 1 cm pathlength, ultraviolet cells and dialysate as the blank. The ultraviolet absorption

spectra of dialyzed protein solutions were determined over a wavelength range of 240 to 340 nm with either a Beckman DB-G grating spectrophotometer or a Gilford Model 240 spectrophotometer. Spectral measurements were made at room temperature (23°C) utilizing 1 cm pathlength cuvettes, and dialysate was used to establish the solvent base line. Sample solutions with too high absorbance to be efficiently measured were accurately diluted using volumetric micropipettes. After use, cuvettes were thoroughly washed with detergent and distilled water, rinsed with double-distilled, deionized water then redistilled ethanol, and dried inverted in an air oven set at 100°C. Periodically the cuvettes were briefly treated with a solution of 3 N hydrochloric acid and 50% ethanol (1:1 by volume) prior to the rinsing and drying procedures.

Circular Dichroism. Ultraviolet circular dichroism (CD) measurements were made with a Cary Model 60 recording spectropolarimeter (Cary Instruments, Monrovia, California), with attached Cary Model 6001 CD accessory, using standard procedures. The instrument, equipped with a water cooled lamp housing maintained at 27°C, was calibrated with an aqueous solution of recrystallized d-10-camphor sulfonic acid (Eastman Organic Chemicals). Constant nitrogen flushing was employed over the examined wavelength range of 200 to 250 nm. All measurements were made with 0.5 mm pathlength cells held in a thermostated cell holder maintained at 13°C with a Lauda (type K2R) circulating water bath. Protein samples, 0.1 to 0.6 mg/ml, were dialyzed against the appropriate buffer at 4°C for at least 24 hours prior to use. Their concentrations were determined on the same day as the CD measurement, and dialysate was used to establish the solvent base line. The mean residue molecular ellipticity is given by the relationship:

$$[\theta] = \frac{\theta^\circ M}{100\ \ell c},$$

where θ° is the observed ellipticity in degrees, M the mean residue molecular weight (taken as 115), ℓ the cell pathlength in dm, and c the protein concentration in gm/cm^3. The units of $[\theta]$ are degrees·cm^2/decimole.

Protein Concentration Measurements

Protein concentration was routinely determined from ultraviolet absorption measurements (made at the appropriate wavelength of maximum absorption and corrected for turbidity by subtracting the absorbance at 320 nm) using extinction coefficients experimentally determined on the basis of at least two of the following methods: dry weight, micro-Kjeldahl, Lowry, and refractometry. Protein solutions were extensively dialyzed at 4°C, with several changes of external solvent, prior to analysis for the quantity of protein in solution.

Dry Weight Method. An aliquot of protein solution (8 to 40 mg protein) was measured and transferred with a calibrated pipette to each of four or five tared small volume beakers (previously marked, thoroughly cleaned, and dried at 110°C under vacuum to constant weight). The protein samples were dried first in an air oven at 80 to 100°C, then to constant weight at 110°C under vacuum. The dried samples were cooled under vacuum, singly removed and weighed on a Mettler S-6 semi-micro analytical balance. The average dried weight of the protein solution was corrected for the weight of salt by subtracting the average dried weight of duplicate aliquots of the dialysate obtained in the same manner.

Micro-Kjeldahl Method. Protein nitrogen was determined by the micro-Kjeldahl method using procedures essentially as outlined by Gurd (1950). A measured volume of dialysate or protein solution (2 to 5 mg protein) was transferred into a clean 100 ml Kjeldahl flask and digested by heating with 2.5 ml fuming sulfuric acid, 1.5 gm sodium sulfate, and a selenium-coated Henger boiling chip. At the completion of digestion, the mixture was cooled, diluted with 35 ml distilled water, and rendered alkaline by the addition of approximately 5 gm solid sodium hydroxide, whereupon a Kjeldahl trap and distillation apparatus were quickly connected. Ammonia in the alkaline mixture was released by steam distillation and collected in 10.0 ml of standard 0.02 N hydrochloric acid. The number of nitrogen equivalents was calculated after back titration of excess acid with standardized 0.02 N sodium hydroxide using a mixed indicator, 0.04% alcoholic bromocresol green plus 0.04% alcoholic methyl red (5:1 by volume), and titrating to a gray end point. Samples of dialysate and protein solution were analyzed in duplicate, and the equivalents of nitrogen determined in the dialysate was used to correct the corresponding solution estimate. Amount protein was subsequently calculated using literature values of the percent nitrogen content of the proteins analyzed. The overall method was tested using standard solutions of ammonium sulfate (Ultrapure grade, Schwarz/Mann Research Laboratories, Inc., New York) and the total error found to be approximately 3%.

Lowry Method. Amount protein was determined using the Folin-Ciocalteu phenol reagent as described by Lowry et al. (1951), adopting the modifications as proposed by Gellert et al. (1959). A major disadvantage in the use of the Folin-Ciocalteu reagent to estimate amount

protein, as reported by Lowry et al. (1951), is the varying amount of color developed with different proteins (in part reflecting the effect of different contents of certain amino acids). Since the amino acid composition of cardiac myosin was found to correspond much more closely to that of skeletal myosin than that of bovine serum albumin, and since methods were available by which skeletal myosin could be freshly prepared in pure form (from the same species of animal) and its solution concentration could be readily determined with a good degree of certainty, rabbit skeletal myosin was substituted for bovine serum albumin as the standard protein.

Rabbit skeletal myosin was prepared by essentially the method of Szent-Györgyi (1951). Its concentration was determined from ultraviolet absorbance measurements at 280 nm using an extinction coefficient, $E^{1\%}_{1\ cm}$, of 5.88 (Verpoorte and Kay, 1966). All standard samples had a 280/260 absorbance ratio equal to, or greater than, 1.7. The minimum time for stable color development and the wavelength range of maximum absorption for the colored complex were redetermined using skeletal myosin, and were found to be 20 minutes and 740 to 750 nm, respectively. On a standard plot, the absorbance of the colored complex was directly proportional to amount protein up to 200 µg skeletal myosin.

Duplicate samples of dialysate and protein solution were diluted to known volumes with 0.5 M sodium chloride to minimize interference due to potassium ion (Gellert et al., 1959). Aliquots were removed and mixed with appropriate volumes of freshly prepared Lowry reagents. The colored complex was allowed to develop for 25 minutes, whereupon its absorbance at 750 nm was measured with a Beckman DU spectrophotometer

type viscometers, with solvent flow times of approximately 195 seconds, were used for solutions of the proteolytic subfragments. Temperature was precisely maintained (± 0.02°C) with a thermostatically controlled viscosity water bath equipped with an internal microheater and external cooling system (Scientific Development Co., State College, Pennsylvania). Dialyzed stock solutions, clarified by high speed centrifugation and/or by millipore filtration (5 μ pore size), were quantitatively diluted to specific concentrations using filtered dialysate as the solvent. Prior to each series of viscosity measurements, viscometers were thoroughly cleaned and dried, then reproducibly positioned in the water bath, care taken to fix the capillary arm in a vertical position. After the viscometers were cooled for several minutes, aliquots of solvent or the diluted samples were carefully introduced to the bottom of the charging tube with a long, narrow pipette and allowed to equilibrate with respect to the low temperature. During cooling and temperature equilibration, the viscometers were sealed with Parafilm to minimize formation of condensation on the inside glass surfaces. Flow times were accurately measured, and remeasured, with Heuer-Leonidas precision stopwatches. Repeated values of the flow time were within 0.3 seconds, and the average value was used in subsequent calculations.

For capillary viscometers, derived in part from the Hagen-Poiseuille equation relating viscosity to flow time, the relative viscosity of solution to solvent can be written as

$$\frac{\eta}{\eta_o} = \frac{t\,\rho}{t_o\,\rho_o} \quad ,$$

where t and ρ are the solution flow time and density, respectively, and

t_o and ρ_o the corresponding parameters for the solvent (dialysate). Terms pertaining to instrument constants have been cancelled from the numerator and denominator since the same viscometer was used in an identical manner to measure the flow time of the solvent and each associated protein sample. Densities of the protein solutions and dialysate were determined at 5.0°C using pycnometric methods. For the greatest concentration examined viscometrically, approximately 7 mg/ml, the relative increase in density with respect to the density of the dialysate was found to be less than 0.2%. Therefore correction for solution density was not applied in calculating the relative viscosity. In addition, corrections for kinetic energy and capillary end effects were assumed to be negligibly small due to the appreciable flow times and the design of the viscometers (Bradbury, 1970). No extrapolation was made to zero shear stress. The specific viscosity, η_{sp}, equal to the relative viscosity minus one (Tanford, 1961) was thus calculated using the expression

$$\eta_{sp} = \frac{t}{t_o} - 1 \quad .$$

The weight intrinsic viscosity, $[\eta]$, is defined as

$$[\eta] \equiv \lim_{c \to o} (\eta_{sp}/c) \quad ,$$

where c is the protein concentration expressed in gm/dℓ (Tanford, 1961). The reduced viscosity, (η_{sp}/c), was plotted with respect to concentration, and the experimental points were analyzed in terms of the empirical equation (Huggins, 1942)

$$(\eta_{sp}/c) = [\eta] + k' [\eta]^2 c \quad .$$

In addition to the variables previously defined, k', a measure of the concentration dependence, is called the Huggins constant. The intrinsic viscosity was determined graphically as the ordinate intercept upon linear extrapolation to zero concentration.

Ultracentrifugation Studies

Sedimentation velocity, sedimentation equilibrium, and Archibald experiments were conducted with a Spinco Model E analytical ultracentrifuge (Beckman Instruments Inc., Palo Alto, California) using standard operating procedures. The ultracentrifuge was equipped with an electronic speed control unit, and an average value of the selected rotor speed was accurately determined on the basis of the revolution count over lengthy and measured intervals of time. The temperature of Model E operations was precisely maintained by the refrigeration and RTIC (Rotor Temperature Indicator and Control) units. Standard Analytical-D rotors were used for all studies. The schlieren/interference optical system (with a water-cooled, mercury-arc lamp light source, a Wratten A77 filter, and appropriate symmetrical masks) was aligned and focused following procedures as outlined in the instrument manual. Schlieren and interference patterns were measured with a Nikon Model 6C microcomparator (Nippon Kogaku K.K., Tokyo, Japan) equipped with precision digital micrometers (IKL Incorporated, Newport Beach, California). Protein solutions for ultracentrifugal analysis were extensively dialyzed at 4°C with several changes of the external buffer, and were considered as two-component systems comprised of protein and dilute buffers of low to moderate ionic strength. Precautions were

taken to minimize the possibility of solvent evaporation and denaturation of temperature sensitive proteins, thus precluding an erroneous assignment of concentration values (Richards et al., 1968). Diluted samples were temporarily stored in sealed, clean test tubes of minimal volume placed in crushed ice, and for experiments conducted at low temperature, rotors, assembled cells, and syringes were cooled in the refrigerator to the appropriate temperature prior to being used. Concentrations of protein solutions were determined spectrophotometrically shortly before the ultracentrifugal runs were conducted. Density of the phosphate buffer used as solvent in the study of myosin and its proteolytic subfragments was pycnometrically determined at 5°C. The densities of all other solvent buffers at various temperatures were obtained by reference to tables of physical constants (Svedberg and Pedersen, 1940).

Determination of Sedimentation Rates and Molecular Homogeneity. Sedimentation velocity runs were carried out at a set rotor speed of 60×10^3 rpm utilizing the schlieren optical system, quartz windows, and standard 12 mm, Kel F single-sector or valve-type synthetic boundary centerpieces. Appropriate bar angle and temperature were selected and maintained depending on the nature of the sample and the purpose of the run. Photographs of the schlieren patterns were routinely taken on Kodak metallographic plates at either 8 or 16 minute intervals. Boundary sedimentation rates were determined by procedures essentially as described by Schachman (1959). Distances from the maximum ordinate boundary position to the inner edge of either reference hole image were accurately measured in each photograph, corrected for magnification, and converted to true distances from the axis of rotation. It was explicitly assumed that the position of the maximum ordinate corresponded to the equivalent

boundary position and closely approximated the second moment of the gradient curve. The symmetrical shape and relative sharpness of the boundaries observed with the various protein solutions ultracentrifugally examined validated this assumption. For example, boundaries of even dilute myosin solutions observed at low bar angle were hypersharp due in part to the molecular shape of myosin. Thus, sedimentation coefficients derived from distance measurements using the maximum ordinate position were considered as reliable, if not more so, as sedimentation coefficients determined using second moments laboriously calculated for a steep gradient of small schlieren area.

The sedimentation coefficient, s, is defined as

$$s = \frac{dx/dt}{\omega^2 x}$$

and has the units seconds. Written in alternative form:

$$s = \frac{1}{\omega^2} \frac{d \ln x}{dt} ,$$

where x, in cm, is the distance of the average boundary position from the axis of rotation, t the time in seconds, and ω the angular velocity of the rotor in radians/sec, calculated using the relationship:

$$\omega = \frac{2\pi \text{ RPM}}{60} ,$$

RPM being the rotor speed in revolutions/min.

The natural logarithms of a series of corrected boundary positions were plotted with respect to time (in minutes). A straight line

was fitted through the data, and the observed sedimentation coefficient was evaluated from the slope of the line by converting the units of time to seconds and dividing by the appropriate value of ω^2. Because of the short radial distance traversed by the schlieren boundary during the time concerned in the determination of the sedimentation coefficients (due to the low sedimentation rates of the various proteins studied and the relative shortness of the overall time of the sedimentation velocity run), corrections for the effects of radial dilution were assumed to be negligibly small. In this regard, the apparently precise linearity of the experimental points in the plots of ln x versus t lent support to this assumption.

To facilitate comparison of sedimentation rates of various protein solutions experimentally determined with different solvent buffers and/or at different temperatures, the observed sedimentation coefficients were corrected to a standard reference solvent having the viscosity and density of water at 20°C using the following expression as introduced by Svedberg and Pedersen (1940):

$$s_{20,w} = s_{obs} \left(\frac{\eta_t}{\eta_{20}}\right)\left(\frac{\eta}{\eta_o}\right)\left(\frac{1 - \bar{v}\rho_{20,w}}{1 - \bar{v}\rho_t}\right),$$

where s_{obs} is the observed sedimentation coefficient, η_t/η_{20} the principal correction factor corresponding to the viscosity of water at a temperature of t°C relative to that at 20°C, η/η_o the relative viscosity of the solvent to that of water, $\bar{v}$ the apparent partial specific volume of the protein in question, and $\rho_{20,w}$ and ρ_t are the densities of water at 20°C and the solvent buffer at t°C, respectively (Schachman, 1959).

The relative viscosity of phosphate buffers at 5°C was determined viscometrically by procedures already described. Parameters of other solvent buffers at various temperatures were obtained by reference to tables of physical constants (Svedberg and Pedersen, 1940). Calculations of $s_{20,w}$ from a series of plate measurements were routinely performed using an IBM 360 computer and the APL program SDCF which incorporated the procedures and equations presented above. The program and a brief description of the pertinent features are given in Appendix 1.

Sedimentation velocity data from various experiments on a particular protein were combined and adequately described by the relationship:

$$s = s^\circ (1 - K_s c) \quad ,$$

where s°, the intrinsic sedimentation coefficient, is the value of the sedimentation coefficient at infinite dilution, K_s a constant expressing dependence of sedimentation coefficients on concentration, and s the sedimentation coefficient at the concentration c (Schachman, 1959). Corrected sedimentation coefficients, $s_{20,w}$, were plotted with respect to the corresponding concentration, and a straight line was fitted through the experimental points. The intrinsic sedimentation coefficient was determined graphically as the ordinate intercept upon extrapolation of the straight line to zero concentration, and the concentration-dependence constant, K_s, was evaluated from the slope.

Unlike ultracentrifugal runs conducted to determine sedimentation rates where the overall time concerned was minimized, runs to establish the degree of molecular homogeneity were carried out for a reasonable length of time to distinquish all resolvable components and

possible skewing of the main schlieren peak.

Molecular Weight Determination by Sedimentation Equilibrium. Conventional and meniscus depletion sedimentation equilibrium experiments were conducted using procedures essentially as described by Richards, Teller, and Schachman (1968) and Yphantis (1964), respectively. Sedimentation equilibrium runs were carried out at low temperatures (set in the vicinity of 5°C) utilizing the Rayleigh interference optical system, quartz windows, and standard 12 mm, charcoal-filled Epon, double-sector centerpieces. Assembled cells were routinely filled with 130 μℓ protein solution and a slightly greater volume of dialysate using Hamilton precision microsyringes, forming a column length of approximately 3 mm. Heavy oils, such as FC-43 fluorocarbon, were not used for the formation of an artifical cell bottom because of their potential protein denaturing effect (Adams, 1967). Initial values of the equilibrium rotor speed (for both conventional and meniscus depletion experiments) were estimated, knowing an approximate value of the molecular weight of the protein in question, either by solution of the appropriate equation of the two given below for ω, the angular velocity in radians/sec converted to speed in revolutions/min using the relationship RPM = $\omega(60/2\pi)$, or by reference to a Rotor Speed Selection Chart, which had been constructed by solving the same equations for typical conditions applying to proteins and plotting rotor speed versus molecular weight (Van Holde, 1967). For conventional or low-speed sedimentation equilibrium runs,

$$\omega^2 = \frac{\ln (c_b/c_m)}{(r_b^2 - r_m^2)} \frac{2RT}{M(1 - \bar{\nu}\rho)},$$

where r_m and r_b are the radial positions (in cm) of the meniscus and column bottom from the axis of rotation, respectively, c_b/c_m is the ratio of the solution concentration at the cell bottom to the meniscus concentration expected at equilibrium (taken to be 3 or 4), R the universal gas constant equal to 8.314×10^7 ergs/degree·mole, T the experimental temperature in °K, M the molecular weight, $\bar{\nu}$ the apparent partial specific volume, and ρ the solution density (Van Holde, 1967). For meniscus depletion or high-speed sedimentation equilibrium runs,

$$\omega^2 = \frac{5RT}{M\,(1 - \bar{\nu}\rho)} \quad ,$$

where the variables have a similar meaning as previously defined (Yphantis, 1964).

Rayleigh interference patterns were recorded on Kodak spectrographic plates, type II-G. Photographs of principal equilibrium pattern were periodically taken and measured after approximately 20 hours of centrifugation to ascertain conditions of equilibrium. The time taken to reach apparent equilibrium in conventional, low-speed experiments was substantially reduced by moderate overspeeding at 1.4 to 2 times the estimated equilibrium rotor speed for a brief length of time at the beginning of the run (Richards, Teller, and Schachman, 1968). In the majority of the runs, sedimentation equilibrium was attained in approximately 40 hours as inferred from the constancy of measured fringe positions.

To subsequently account for residual optical inequalities between the solution and solvent channels (Yphantis, 1964), two sets of solution base-line patterns were recorded: one, just after reaching the selected rotor speed before appreciable solute distribution had occurred,

and two, after the conclusion of the equilibrium run — the rotor was removed from the chamber, gently shaken (without removing the cell or disturbing its orientation in the rotor) to destroy the solute concentration gradient, and returned to the operating rotor speed, whereupon the base-line pattern was photographed (Richards, Teller, and Schachman, 1968). In addition, solvent blank runs were carried out under identical conditions of the equilibrium run as outlined by Godfrey and Harrington (1970). After completion of the equilibrium experiment proper (that is, including solution base lines), without disassembling the cell, the solution sector of the centerpiece was rinsed out several times and refilled with dialysate to the level of the adjacent solvent column. The loaded cell was carefully repositioned in the rotor, taken up to the particular equilibrium speed, and the interference pattern of the solvent blank was photographed.

Before fringes of the solution base-line, solvent blank, and equilibrium patterns were examined in detail, a check was made to see whether a significant leak from either sector of the centerpiece had occurred by comparing measured values of the column length in the two solution base-line patterns. If a loss of material was detected, the particular experiment was disregarded. Recorded interference patterns on developed plates were aligned in the microcomparator such that the horizontal movement of the comparator stage (and thus the plate) was parallel to the central fringe of the reference fringes produced by the counterbalance. The vertical displacement of a dark fringe in the equilibrium pattern was measured, with reference to a meniscus zero level, five times, and an average value calculated, at each of at least thirty selected x-coordinate positions, the latter number depending directly on

the steepness of the concentration gradient. Similarly, fringe displacements of the two solution base lines and the solvent blank were determined once at approximately fifteen x-coordinate positions, chosen at regular intervals; an average value was usually calculated for each set of associated displacements. The average and variance values of the equilibrium and base-line comparator readings were determined using an Olivetti Programma 101 desk computer. The reciprocal of the variance was used as an initial weighting factor of the corresponding average value in subsequent calculations. Horizontal distances were measured from the inner edge of the outer reference hole fringes, corrected for magnification, and converted to true radial distances from the axis of rotation.

Although interference fringes when identified in absolute terms are directly proportional to the refraction increment and thus to concentration on a scale of mass/unit volume, observed values of fringe displacement denote only differences in solute concentration relative to the concentration at the meniscus position (Van Holde and Baldwin, 1958). Fringe displacements, corrected for base-line distortion, were calibrated in absolute terms with respect to concentration by the following methods. In meniscus depletion equilibrium experiments the rotor speed was chosen sufficiently high that, at equilibrium, the solute concentration at the meniscus was effectively zero, and thus the actual concentration (in fringes) at any radial position along the column was directly given by the measured fringe displacement (Yphantis, 1964). In conventional sedimentation equilibrium experiments a low rotor speed was employed, and as a consequence, at equilibrium, the solute concentration at the meniscus was appreciable. Explicitly assuming that no loss of solute had occurred during the run, the meniscus concentration, denoted by c_m, was

determined in fringes using the expression, derived on the basis of conservation of mass (Van Holde, 1967),

$$c_m = c_o - \frac{r_b^2 (c_b - c_m) - \int_{r_m}^{r_b} r^2 \, dc}{r_b^2 - r_m^2} .$$

The quantity $(c_b - c_m)$ is the total fringe shift measured from the radial meniscus position, r_m, to the radial position of the column bottom, r_b, and c_o is the initial concentration of the sample solution ultracentrifugally calibrated in terms of fringes. The integral was evaluated by trapezoidal approximation (r being the radial distance at a given point along the column from the axis of rotation). The ancillary c_o run was carried out using the equilibrium sample, dialysate as the solvent, and a 12 mm, double-sector, capillary-type synthetic boundary centerpiece at a rotor speed of approximately 11 x 10^3 rpm and the corresponding equilibrium run temperature (Van Holde, 1967; Richards, Teller, and Schachman, 1968). Three interference patterns were routinely recorded and utilized in the determination of c_o: one, at the completion of solvent layering (to evaluate the fractional fringe); two, at the resolution of the boundary fringes (to establish the whole fringe number); and three, at the termination of the run after redistributing the cell contents by gently tilting the rotor (to correct the fractional fringe value for base-line distortion). The concentration, in absolute terms, at any radial position along the equilibrium column in conventional experiments was subsequently calculated by adding the appropriate fringe displacement to the computed value of c_m.

Apparent weight-average molecular weights were determined from

interferential concentration and radial distance data using computational methods as described by Yphantis (1964) and Richards, Teller, and Schachman (1968) in conjunction with the fundamental expression, derived on a thermodynamic basis (Williams et al., 1958) and written in differential logarithmic form with respect to concentration,

$$\frac{d \ln c}{d(r^2/2)} = \frac{\overline{M}_{app}(1 - \bar{\nu}\rho)\omega^2}{RT} .$$

In addition to the previous definitions of R, T, $\bar{\nu}$, ρ, and ω, $\overline{M}_{app}$ is the apparent weight-average molecular weight of a single, homogeneous solute of a two-component system experimentally observed at the finite concentration c, at a position along the equilibrium column a radial distance r from the axis of rotation (Yphantis, 1964). The natural logarithms of computed concentration values were plotted against the corresponding values of $r^2/2$, and a line was fitted through the experimental points by the method of polynomial least squares — the degree of the polynomial equation was directly dependent on the shape of the equilibrium concentration gradient. The apparent weight-average molecular weight was subsequently determined at each radial position by multiplying the first derivative of the polynomial equation, $d \ln c/d(r^2/2)$, evaluated at each point by the appropriate value of the constant term, $RT/(1 - \bar{\nu}\rho)\omega^2$.

Using the procedures and relationships derived by Roark and Yphantis (1969), the apparent number, z-, and y_2-average, point molecular weights were additionally calculated if the corresponding concentration and derivative data showed internal consistency and low statistical noise.

In the determination of all the molecular weight moments, it

was explicitly assumed that the pressure and concentration dependence of the buoyancy term, $(1 - \bar{v}\rho)$, was neglibly small (Yphantis, 1964).

The computations involved in the evaluation of point molecular weights from the average comparator readings were carried out using an IBM 360 computer and programs written in APL based on a Fortran IV high-speed sedimentation equilibrium computer program by Roark and Yphantis (1969). A copy of the latter was kindly provided by Michael Johnston for Dr. Yphantis. The APL programs HSDQM and LSDQM (for the determination of weight-average molecular weights from, respectively, high- and low-speed experimental data) were written incorportating not only the basic procedures and equations given above but also the following features: the correction of the equilibrium fringe data for base-line distortion by the method of interpolation; the refinement and subsequent evaluation of the zero meniscus level (in HSDQM); the smoothing of the ln c versus $r^2/2$ plots by a weighted, sliding least squares technique, with reassignment of each weighting factor based upon the deviation of the experimental points from the previous fit; and the estimation of the propagated error in the derived molecular weight values. These programs, together with the APL program MNZY2 (for the calculation of number, z-, and y_2-average molecular weights) and the ancillary, polynomial least squares program, LSPFIT, are presented and briefly described in Appendix 2.

From various experiments for a given protein, the concentration dependence of the apparent molecular weight was analyzed, in part, by plotting the reciprocal values of the apparent point molecular weights against the corresponding values of concentration. A value for the intrinsic molecular weight was determined graphically as the ordinate intercept upon appropriate extrapolation to zero concentration of the line

fitted through the experimental points (Van Holde, 1967). A measure of the extent of the concentration dependence was derived from the slope and shape of the fitted line.

Molecular Weight Determination by the Archibald Method.

Approach to sedimentation equilibrium experiments, based on the theoretical development of Archibald (1947), were conducted using procedures as described by Mueller (1964). Archibald runs were carried out at a temperature of 5°C utilizing the schlieren optical system, quartz windows, and a standard 12 mm, Kel F single-sector centerpiece. During the course of centrifugation, a series of selected rotor speeds was employed (Mueller, 1964), set in successive stages of approximately 1000 rpm from an initial speed slightly lower than the value calculated for a corresponding conventional sedimentation equilibrium run to a final speed three to four times higher, causing the solution boundary to pull completely away from the meniscus. Photographs were taken on Kodak metallographic plates at suitable time intervals after each speed change.

Selected gradient patterns were aligned in the microcomparator with respect to the inner edge of the inner reference hole image, enlarged ten times, and traced on graph paper (ruled in 1 mm squares) for subsequent measurement, taking as the meniscus position a line one-third of the width of the "central shadow" towards the solution side (Erlander and Babcock, 1961). Values of the concentration gradient, in terms of the vertical distance between the traced gradient line and the level of the plateau region, were measured at 1 mm intervals along the pattern from the position of the meniscus to a position in the plateau region where the concentration gradient was first equal to zero. Horizontal distances were measured from the inner edge of the inner reference hole

image, corrected for magnification, and converted to true radial distances (in cm) from the axis of rotation.

Apparent weight-average molecular weights were calculated with respect to the meniscus using the expression derived by Archibald (1947):

$$\bar{M}_{app} = \frac{RT}{(1 - \bar{\nu}\rho)\omega^2} \frac{1}{r_m c_m} \left(\frac{dc}{dr}\right)_m ,$$

in which $\bar{M}_{app}$, R, T, $\bar{\nu}$, and ρ are as previously defined, ω is the particular angular velocity of the rotor associated with the selected pattern analyzed, and $(dc/dr)_m$ is the extrapolated value of the concentration gradient at the meniscus position, r_m. The meniscus solute concentration, c_m, was computed using the following relationship as formulated by Klainer and Kegeles (1955):

$$c_m = c_o - \frac{1}{r_m^2} \int_{r_m}^{r_p} r^2 \left(\frac{dc}{dr}\right) dr ,$$

where (dc/dr) is the value of the concentration gradient at a given point a radial distance r along the pattern measured from the meniscus position, r_m, to a position in the plateau region, r_p, and c_o is the initial concentration of the sample solution ultracentrifugally calibrated in arbitrary units. The integral was evaluated by rectangular summation. The c_o run was carried out at a rotor speed of approximately 13×10^3 rpm and at the corresponding gradient-run bar angle and temperature using a value-type synthetic boundary centerpiece, the sample solution from the gradient run, and dialysate as the solvent. The schlieren pattern of the synthetic boundary peak was enlarged ten times and

carefully traced on graph paper. The area of the peak was measured at least five times with a planimeter, and the average value, corrected for magnification, was used for c_o.

The series of c_m and apparent molecular weight calculations involved with Mueller-type Archibald experiments were performed using an IBM 360 computer and an APL program, ARCH, written incorporating the mathematical expressions presented above. The program ARCH and the ancillary rounding program, RND, are given and briefly described in Appendix 3.

The concentration dependence of the apparent molecular weights was graphically analyzed using procedures as described in the previous section on sedimentation equilibrium with one difference: here, the reciprocal values of the apparent molecular weights were plotted against corresponding values of c_m (Mueller, 1964).

CHAPTER 3

NATIVE CARDIAC MYOSIN

Although results of recent physical, chemical, and enzymatic investigations of cardiac myosin are generally in agreement (Katz, 1970), a number of significant differences exist (for example, with respect to the value of the molecular weight) attributed, in part, to species differences (Mueller et al., 1964), to diverse methods of preparation (Vierling et al., 1968), and to the apparent instability of cardiac myosin solutions (Katz, 1970). In consideration of this, several molecular properties of native cardiac myosin were reexamined in detail not only to be useful in attempting to resolve existing discrepancies but also, perhaps more importantly, to form a necessary basis upon which conclusions pertaining to molecular structure could validly be made from the results of proteolytic subfragment studies. Procedures for the isolation and purification of rabbit cardiac myosin and the experimental results of associated enzymatic, ultraviolet optical, amino acid, and physicochemical studies are delineated in this chapter.

Preparation of Rabbit Cardiac Myosin

Myosin was isolated and purified from rabbit cardiac tissue using essentially the method described by Mueller et al. (1964) — fundamentally the dilution-precipitation method of Szent-Györgyi (1951) with minor modifications. Hearts of mature rabbits of mixed sex and breed were obtained individually frozen and shipped via air express in

insulated, dry-iced containers from Pel-Freez Biologicals, Inc., Rogers, Arkansas and Calgary Rabbit Processors Ltd., Calgary, Alberta. Hearts were received frozen usually 24 to 72 hours after being processed. All preparative procedures were carried out at a low temperature, 0 to 4°C; glassware, plasticware, and stainless-steel apparatus were thoroughly cooled before being used. Immediately upon delivery, the frozen hearts were completely thawed in several changes of cold, double-distilled, deionized water. Pericardia, aortae, other major blood vessels, and fat were quickly excised with scissors and discarded. The remaining tissue (mainly ventricles) was cut into small pieces, washed twice with cold, double-distilled, deionized water to remove excess blood, and minced slowly in a stainless-steel grinder. The muscle mince was extracted with a freshly prepared solution of 0.3 M KCl, 0.075 M KH_2PO_4, 0.075 M K_2HPO_4, 0.5 mM ATP, pH 6.6 at a volume of 3 ml/gm wet weight of mince for 15 minutes with constant stirring (the short time of extraction and low pH minimizes inclusion of actomyosin (Mueller et al., 1964)). Extraction was terminated by the addition of an equal volume of cold, double-distilled, deionized water (actomyosin is partially eliminated by differential precipitation upon decreasing the ionic strength to approximately 0.15 (Mueller et al., 1964)). The residue and precipitated material were removed by straining the diluted mixture through several layers of cheesecloth and by subsequent centrifugation at 2.3×10^3 rpm for 30 minutes. The extract solution was further clarified (mainly of large fat particles) by straining the supernatant through cheesecloth into a clean graduated cylinder. Myosin was precipitated by adding the strained solution to six volumes of cold,

double-distilled, deionized water and allowed to settle for 2 to 3 hours, whereupon the red supernatant was carefully siphoned off and discarded. The precipitate was collected by centrifugation at 2.3×10^3 rpm for 40 minutes and dissolved by the addition of double-distilled, deionized water, concentrated buffer, and solid ATP to make a final volume of 360 ml of 0.5 M KCl, 0.05 M phosphate, 0.5 mM ATP, pH 7.0. The dilute myosin solution was centrifuged in a Spinco Model L preparative centrifuge (Beckman Instruments, Inc., Palo Alto, California) at 40×10^3 rpm for 4 hours to effect the quantitative removal of actomyosin by differential centrifugation (Mueller et al., 1964). The resulting supernatant was filtered through Whatman 541 filter paper, and myosin was precipitated by adding the filtrate to ten volumes of cold, double-distilled, deionized water. The precipitate was collected by centrifugation at 2.3×10^3 rpm for 30 minutes, dissolved in 0.2 M KCl, pH 7, to a final volume of 360 ml, and treated batchwise with freshly prepared DEAE-cellulose equilibrated with respect to 0.2 M KCl, pH 7 (to remove aggregates of myosin, which apparently are selectively adsorbed at this ionic strength (Asai, 1963), as well as associated polyribonucleotides (Perry, 1960)). Approximately 10 gm of prepared cellulose were stirred into the myosin solution and allowed to thoroughly mix for at least 10 minutes, whereupon the suspension was filtered through several layers of cheesecloth, and the pulp squeezed out by hand. This procedure was repeated with an equal amount of fresh cellulose, and the final filtrate was centrifuged at 20×10^3 rpm for 30 minutes to remove fine cellulose particles. The supernatant was filtered through Whatman 541 filter paper, and myosin was again precipitated by adding the filtrate to six

volumes of cold, double-distilled, deionized water. The white, flocculent precipitate was collected by centrifugation and taken up in a minimum volume of buffer, usually 0.5 M KCl, 0.05 M phosphate, pH 7.0. The final solution was clarified of fat, insoluble aggregates and particulate matter by centrifugation at 50 x 10^3 rpm for 3 hours, and was subsequently dialyzed against the appropriate buffer at 4°C. The resulting solution was clear and colorless with a 280/260 absorbance ratio of 1.7 to 1.8. Generally, the yield of cardiac myosin was approximately 500 mg from 300 gm of muscle mince.

Results

The effectiveness of DEAE-cellulose treatment in the additional purification of cardiac myosin preparations was evidenced in schlieren patterns of final myosin solutions routinely observed during sedimentation velocity (typical patterns are presented in Figure 1). A leading hypersharp peak was usually evident in untreated preparations (for example, the upper series of patterns in Figure 1) presumably representing some actomyosin (as suggested by Mueller et al., 1964) and possibly low n-mers of myosin (attributable to the inherent tendency of myosin to aggregate (Stracher and Dreizen, 1966; Katz, 1970) and to the lack of immediate freshness of the rabbit hearts). The 280/260 absorbance ratios of untreated preparations were invariably low, 1.3 to 1.5, indicative of associated nucleotide. In contrast, myosin preparations treated with DEAE-cellulose prior to the final precipitation of myosin resulted in seemingly homogeneous material as inferred from the single, hypersharp peak observed in the ultracentrifuge (for example, the lower series of patterns in Figure 1).

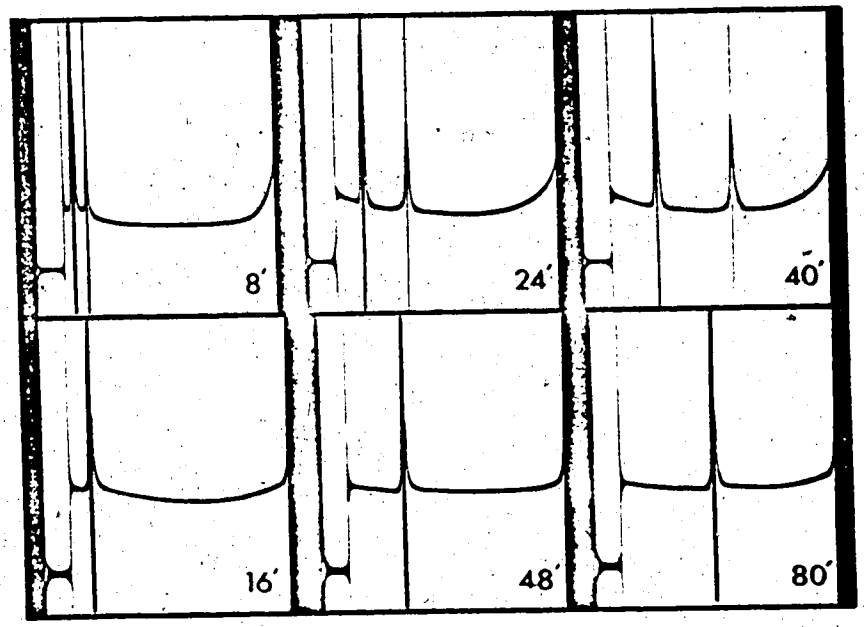

Figure 1. Schlieren patterns of cardiac myosin in 0.5 M KCl, 0.05 M phosphate buffer, pH 7.0, treated and not treated with DEAE-cellulose. Upper series: an untreated preparation (7 mg/ml) observed in the ultracentrifuge at 15°C, 60 x 10^3 rpm, and a bar angle of 65°. Lower series: a treated preparation (5 mg/ml) observed at 8°C, 60 x 10^3 rpm, and a bar angle of 50°. Photographs of the patterns were taken at the times indicated after reaching speed.

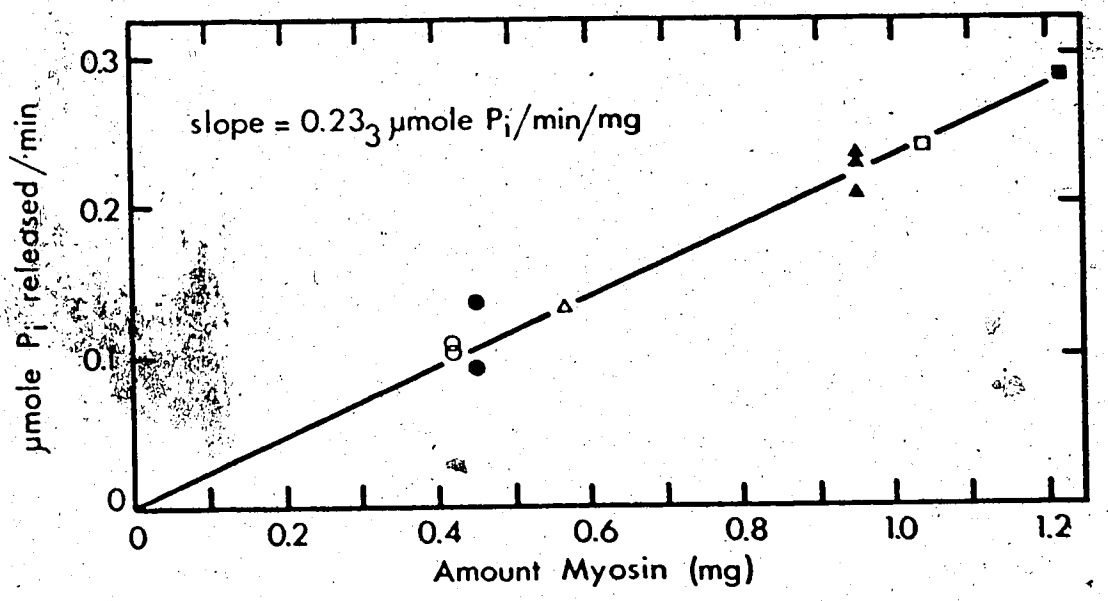

Figure 2. The Ca^{++} ion-activated ATPase activity of cardiac myosin (µmoles P_i/min) as a function of amount myosin (mg) at 25°C in 0.4 M KCl, 5 mM ATP, 10 mM $CaCl_2$, pH 8.2. The various point styles represent the results of experiments using different preparations of cardiac myosin.

Studies with respect to cardiac myosin were conducted using only preparations less than one week old (Brahms and Kay, 1962) and generally in phosphate buffers at neutral pH and low temperature to minimize particle aggregation (Lowey and Holtzer, 1959).

Adenosinetriphosphatase Activity. Cardiac myosin, prepared as outlined above, was enzymatically active, catalyzing the hydrolysis of ATP. Adenosinetriphosphatase (ATPase) activity measurements were carried out at a temperature of 25°C with substrate solutions of 0.4 M KCl, 5 mM ATP, 10 mM $CaCl_2$ at pH 8.2 (unless otherwise specified) utilizing the pH-stat as described in Chapter 2 in accordance with the following reaction scheme: $ATP^{4-} + HOH \rightarrow ADP^{3-} + HPO_4^{2-} + H^+$. The specific activity was expressed as μmoles P_i released per minute per mg myosin even though inorganic phosphate was not directly analyzed. Stock substrate solutions of ATP were freshly prepared by volumetrically diluting accurately weighed amounts of solid ATP. The reliability of this method was confirmed by periodically checking the resulting concentration spectrophotometrically at 259 nm using a value of $15.4 \times 10^3\ M^{-1}$ (at pH 7) for the molar extinction coefficient (Morell and Bock, 1954).

Preliminary experiments were conducted to determine the reproducibility and the enzyme concentration dependence of myosin ATPase activity. The rate of ATP hydrolysis was measured with respect to various amounts of myosin (0.4 to 1.2 mg). The combined results using different preparations of cardiac myosin are graphically summarized in Figure 2. The reaction rate was found to be linearly related to the amount of myosin over the range examined. Slight variations in activity were observed between the different preparations as well as in repeated

measurements with a given amount of myosin within a single preparation. The average specific ATPase activity (equal to the slope of the straight line) was 0.23_3 μmole P_i/min/mg (note: substrate solutions contained 10 mM $CaCl_2$).

The effect of calcium ions on the catalytic activity of myosin was examined over a $CaCl_2$ concentration range of 0 to 20 mM. As evident in Figure 3, the ATPase activity of cardiac myosin was activated in the presence of calcium ions, and reached a maximum value of 0.23_5 μmole P_i/min/mg at an optimal $CaCl_2$ concentration of 8 to 10 mM. Correspondingly, the effect of magnesium ions was examined under similar experimental conditions over a $MgCl_2$ concentration range of 0 to 0.5 mM. Magnesium ions were found to cause a pronounced inhibition (Figure 4), and at much lower concentrations of $MgCl_2$ in relation to the levels of $CaCl_2$ necessary for minimal activation. The specific activity of cardiac myosin, measured in the absence of divalent cations, was 0.090 μmole P_i/min/mg.

Activity measurements were carried out at various concentrations of ATP (0 to 5 mM), in the absence and presence of calcium ions, to investigate the substrate concentration dependence of the enzymatic activity of myosin. The final results are presented in Figure 5. The activating effect of calcium ions was evident in a parallel manner at all the ATP concentrations examined. As determined from the plateau region of both hyperbolic curves, the specific activity appeared to be zero order with respect to ATP at minimal substrate concentrations of 4 to 5 mM. The substrate curves were assumed to follow the Michaelis-Menten equation, and kinetic parameters were evaluated using the graphical method of Lineweaver and Burk (Figure 6). The apparent linearity of the experimental points in the double-reciprocal plots supported the

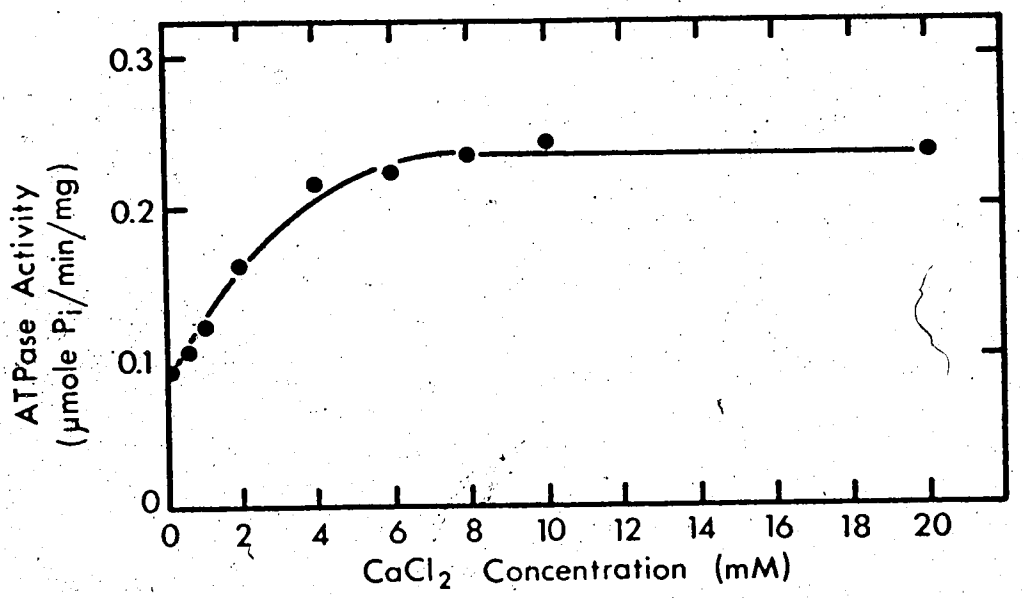

Figure 3. The effect of varying $CaCl_2$ concentration on the specific ATPase activity of cardiac myosin as measured at 25°C in 0.4 M KCl, 5 mM ATP, pH 8.2, using 0.95 mg myosin.

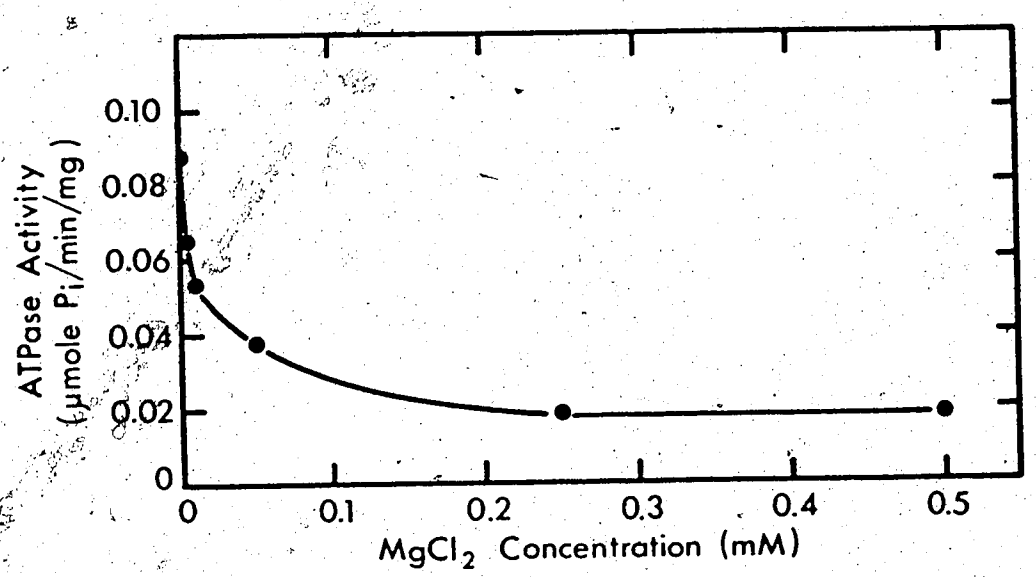

Figure 4. The effect of varying $MgCl_2$ concentration on the specific ATPase activity of cardiac myosin as determined at 25°C in 0.4 M KCl, 4 mM ATP, pH 8.2, using 0.95 mg myosin.

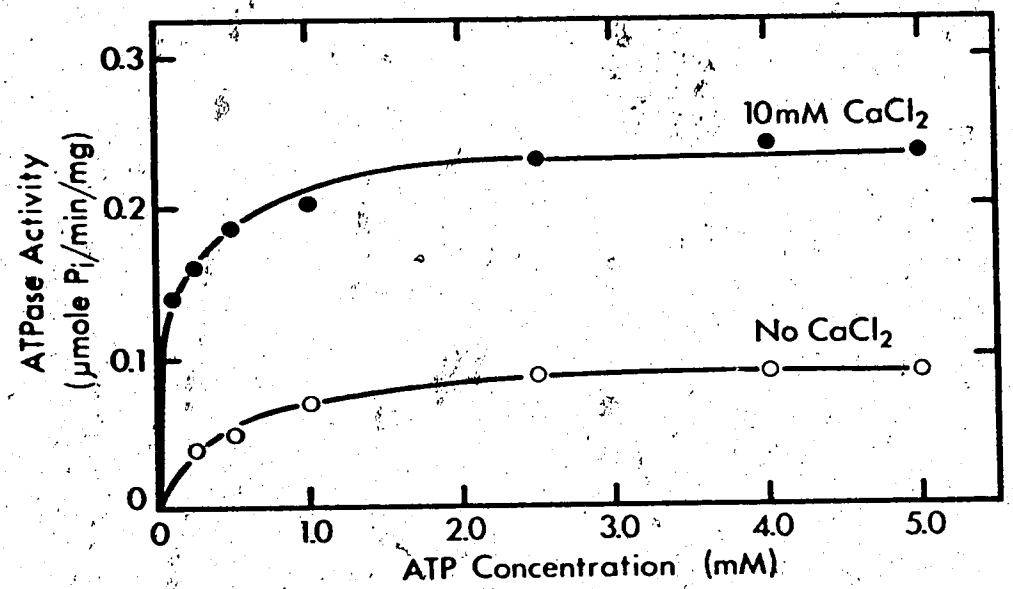

Figure 5. The effect of varying ATP concentration, in the absence and presence of $CaCl_2$, on the specific ATPase activity of cardiac myosin in 0.4 M KCl, pH 8.2, at 25°C (using 1.0 mg enzyme).

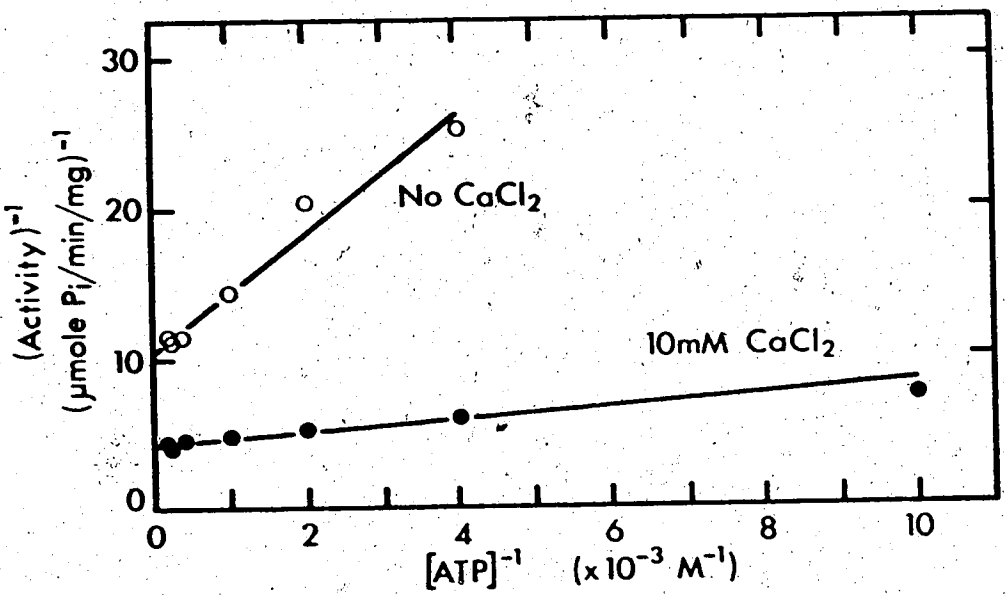

Figure 6. Double-reciprocal plot of inverse specific ATPase activity against inverse varying ATP concentration, in the absence and presence of $CaCl_2$, derived from the data presented in Figure 5.

assumption made concerning the mathematical description of the original curves. Derived values of the maximum velocity (the reciprocal of the ordinate intercept) and the apparent Michaelis constant (calculated from the slope of the straight line) were, respectively, 0.094 μmole P_i/min/mg and 3.6×10^{-4} M (in the absence of added calcium ions) and 0.235 μmole P_i/min/mg and 0.96×10^{-4} M (in substrate solutions containing 10 mM $CaCl_2$).

The effect of pH on myosin ATPase activity was examined over the alkaline pH range 7.1 to 9.3. Measurements were made in random order with respect to pH, and were repeated with a separate preparation of cardiac myosin. From an apparent minimum in the vicinity of pH 7.2, the resulting pH curve was found to gradually increase with higher pH, reaching a plateau around pH 9 (Figure 7). Though scatter of the experimental points was inherently evident, the results from the two preparations of myosin were in general agreement.

Experiments were also conducted to study the effect of p-chloromercuribenzoate on the catalytic activity of cardiac myosin. The concentration of stock solutions of PCMB in 0.4 M KCl, pH 7, was measured spectrophotometrically at 233 nm using a value of 1.599×10^4 M^{-1} for the molar extinction coefficient (both the wavelength of maximum absorbance and the value of the molar extinction coefficient were precisely determined from auxiliary experiments). Representative results are plotted in Figure 8. Cardiac myosin ATPase activity was stimulated at low concentrations of PCMB and inhibited at higher PCMB/myosin ratios. Maximum activation occurred at approximately 4 moles of PCMB per 10^5 gm myosin.

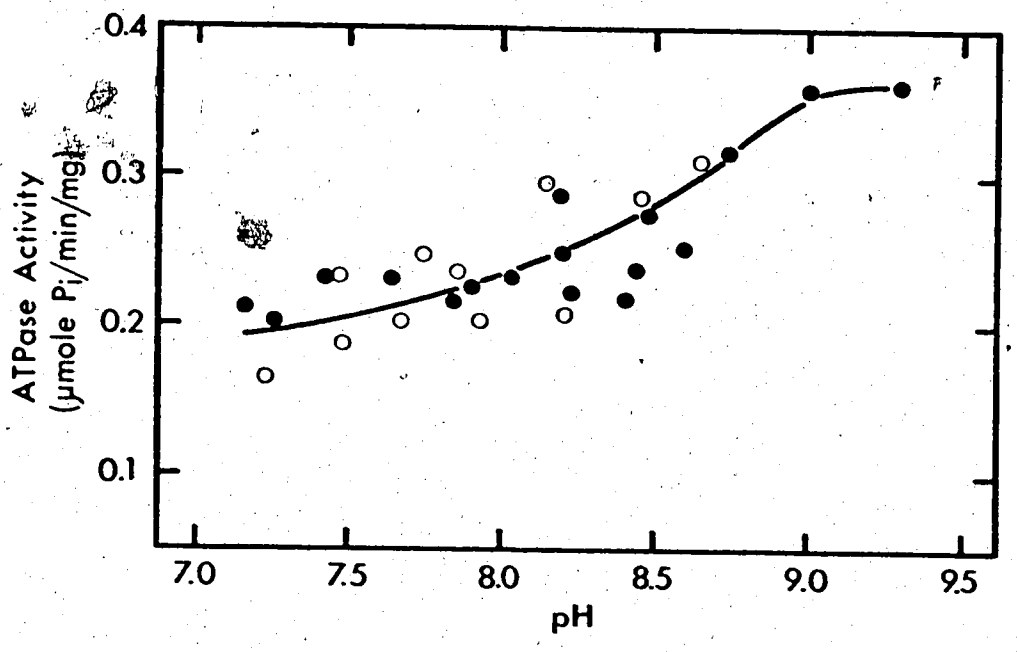

Figure 7. The pH profile of the Ca^{++} ion-activated specific ATPase activity of cardiac myosin as determined in 0.4 M KCl, 5 mM ATP, 10 mM $CaCl_2$, at 25°C, using 0.45 mg myosin prep.#1 (○—○) and 0.95 mg myosin prep.#12 (●—●).

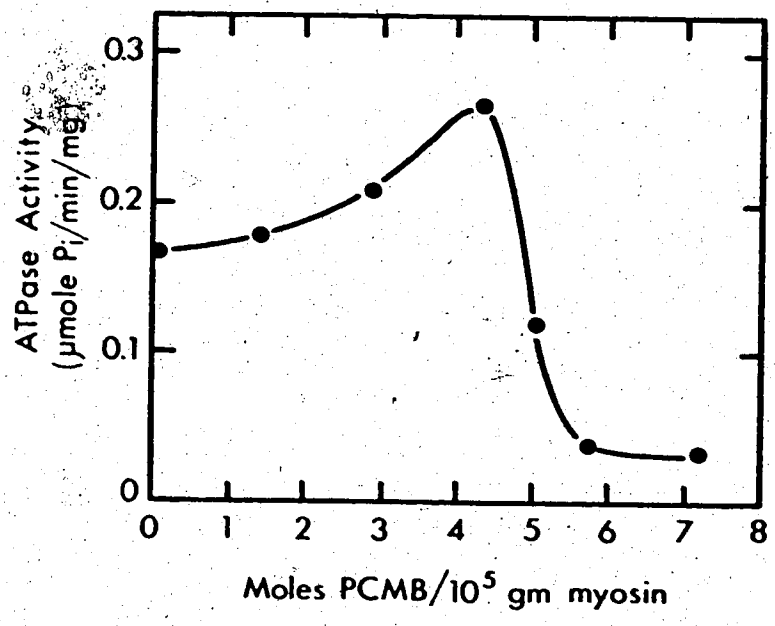

Figure 8. The effect of varying ratios of p-chloromercuribenzoic acid to protein on the Ca^{++} ion-activated specific ATPase activity of cardiac myosin as measured at 25°C in 0.4 M KCl, 3 mM ATP, 10 mM $CaCl_2$, pH 8.2, using 0.7 mg myosin.

Ultraviolet Optical Properties. The ultraviolet absorption spectrum of rabbit cardiac myosin, as determined in 0.5 M KCl, 0.05 M phosphate buffer at pH 7.0, was typical of ultraviolet spectra of most proteins, with maximum absorbance observed at a wavelength of 280 nm (Figure 9). The extinction coefficient of cardiac myosin was determined correspondingly at 280 nm, in the same solvent system, using different preparations of myosin. The average value of $E^{1\%}_{1\ cm}$, derived from 18 sets of data, was 6.06 ± 0.06. Values of the protein concentration used in the calculation of the extinction coefficient were standardized by three methods: dry weight, Lowry (the major method), and micro-Kjeldahl (using a nitrogen factor of 6.25 (Mueller et al., 1964)).

The ultraviolet circular dichroism (CD) of cardiac myosin was measured in 0.5 M KCl, 0.05 M phosphate buffer, pH 7.0, over the wavelength range 250 to 200 nm. A representative CD spectrum is shown in Figure 10. Myosin solutions exhibited negative dichroic bands at 221 and 209 nm, with respective mean residue ellipticity values of $^{-}2.69 \times 10^4$ and $^{-}2.56 \times 10^4$ degree·cm^2/dmole. Though CD measurements were not extended into the far ultraviolet (that is, to wavelengths shorter than 200 nm), a positive trend was evident at the lower end of the wavelength range examined, with the crossover point of the spectrum occurring at 201 nm. No significant changes in the shape of the curve, the position of the minima, and the ellipticity values at the minima were detected, by comparison with control scans, in circular dichroism spectra of myosin determined at 23°C at pH 7, 8, and 9.5, or in the presence of 1 mM ATP and 10 mM $CaCl_2$ (or 10 mM $MgCl_2$) at pH 7. However, variations in ellipticity values up to approximately 5% were observed between different preparations of cardiac myosin. Due to the disparity in

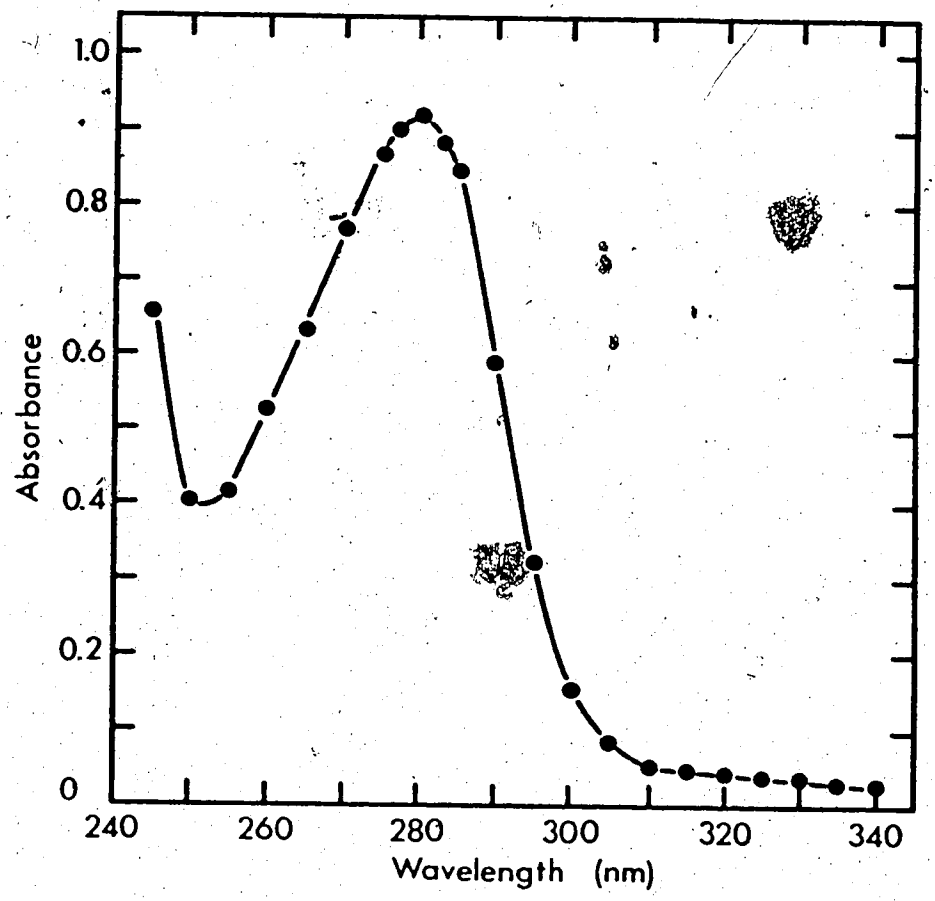

Figure 9. Ultraviolet absorption spectrum of cardiac myosin in 0.5 M KCl, 0.05 M phosphate buffer, pH 7.0, at a protein concentration of 1.5 mg/ml, using a 1 cm path length cuvette and dialysate as the blank.

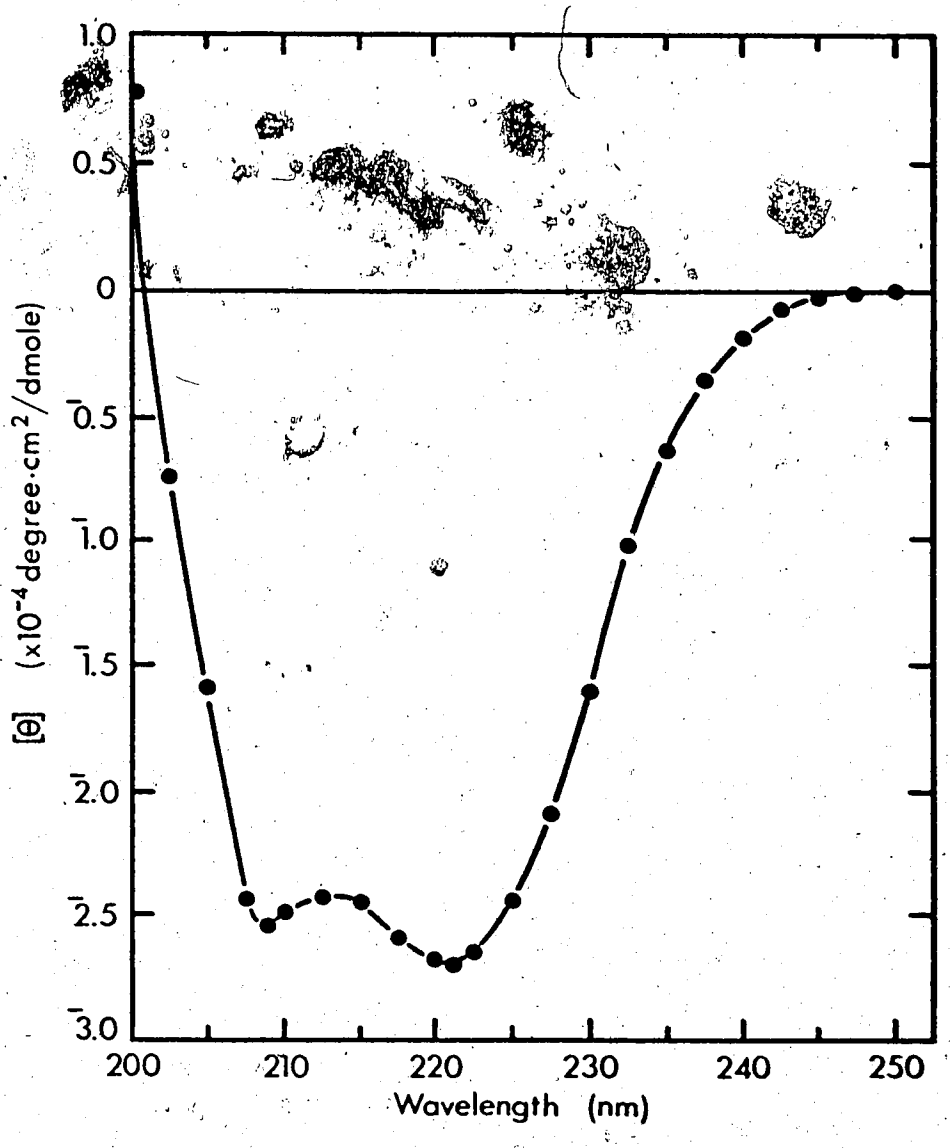

Figure 10. Ultraviolet circular dichroic spectrum of cardiac myosin in 0.5 M KCl, 0.05 M phosphate buffer, pH 7.0, as determined at 13.5°C and a protein concentration of 0.36 mg/ml, using a 0.0502 cm path length optical cell and dialysate for the base line.

reported standard ellipticity values, the helical content of myosin was not directly estimated from the circular dichroism data with reference to the optical rotatory properties of helical polyamino acids (Oikawa et al., 1968).

Amino Acid Composition. The amino acid composition of rabbit cardiac myosin was analyzed as described in Chapter 2. Corrected values of the labile residues, threonine, serine, and tyrosine, were obtained by linear extrapolation to zero hydrolysis time. Average values of duplicate 12-, 24-, 48-, and 72-hour hydrolysate results were calculated for the remaining amino acids. The recovery of all amino acids was determined relative to 76 residues of alanine per 10^5 gm protein. The final results, expressed as moles per 10^5 gm myosin, are presented in Table I. Included in the table for comparison are the reported amino acid analyses of myosin prepared from rabbit, bovine, and canine cardiac tissue. The major features of the present analysis are briefly summarized as follows: The average values of lysine, aspartic acid, alanine, leucine, and particularly glutamic acid were notably high. Threonine, serine, glycine, valine, isoleucine, and phenylalanine were found in similar and intermediate amounts. The total cysteine and half cystine content, determined and expressed as cysteic acid, was 7 moles per 10^5 gm myosin. In addition to the residues histidine and tyrosine, the average amount of proline was relatively low. The results of this study were in agreement with those of Bárány et al. (1964) for rabbit cardiac myosin, though prepared in an alternative manner, and to a large extent closely resembled the amino acid composition of bovine and canine cardiac myosin.

TABLE I

AMINO ACID COMPOSITION OF CARDIAC MYOSIN

(moles/10^5 gm myosin)

Amino Acid	Present Study	Rabbit Cardiac Bárány et al. (1964)	Bovine Cardiac Tada et al. (1969)	Canine Cardiac Iyengar & Olson (1965)*
Lys	85	84	91	82
His	15	16	15	14
Arg	47.5	47	47	47
Asp	82	87	92	81
Thr	42	41	44	38
Ser	40	41	40	36
Glu	163	150	169	147
Pro	23	22	23	24
Gly	39	43	38	37
Ala	76	76	77	71
Cya	6.8	7	7.4	8
Val	40	42	38	33
Met	22.5	22	23	20
Ile	38	40	37	28
Leu	92	85	93	80
Tyr	18	18	16	15
Phe	29	27	31	26
Try	--	6.2	3.5	3

*Standard hydrolysis time was 72 hours; no corrections were applied for the loss of labile residues.

Viscosity. Diluted samples of cardiac myosin (in 0.5 M KCl, 0.05 M phosphate buffer, pH 7.0) were examined in the ultracentrifuge prior to viscometric analysis: all were observed to exhibit a single schlieren peak. Graphs of reduced viscosity, (η_{sp}/c), versus concentration were found to be linear over the concentration range investigated (1 to 7 mg/ml). The final results of one set of viscosity measurements are presented in Figure 11. The equation of the straight line fitted through the experimental points by the method of least squares was

$$(\eta_{sp}/c) = 2.06 + 1.91\ c\ ,$$

and derived values of the intrinsic viscosity and Huggins constant were 2.06 dℓ/gm and 0.45, respectively. Viscometric experiments were repeated with different preparations of cardiac myosin and yielded similar results. From three such series of measurements, the average value of the intrinsic viscosity was 2.04 ± 0.08 dℓ/gm, and the average value of the Huggins constant was 0.46 ± 0.09.

Sedimentation Velocity. The schlieren patterns of myosin samples (in 0.5 M KCl, 0.05 M phosphate buffer, pH 7.0) were characterized by a single, hypersharp peak at all concentrations (similar to the representative patterns shown in the lower series of Figure 1). In subsequent comparator measurement of radial distances, the center of the concentration line, evident even at low bar angle, was assumed to correspond to the maximum ordinate position. A value of 0.721 ml/gm was taken for the apparent partial specific volume of myosin in 0.5 M KCl, 0.05 M phosphate buffer, pH 7.0 at 5 to 6°C (Kay, 1960; Godfrey and Harrington, 1970). The density of the solvent buffer was determined at 5.0°C using pycnometric methods and was equal to 1.0309 ± 0.0001 gm/cm^3

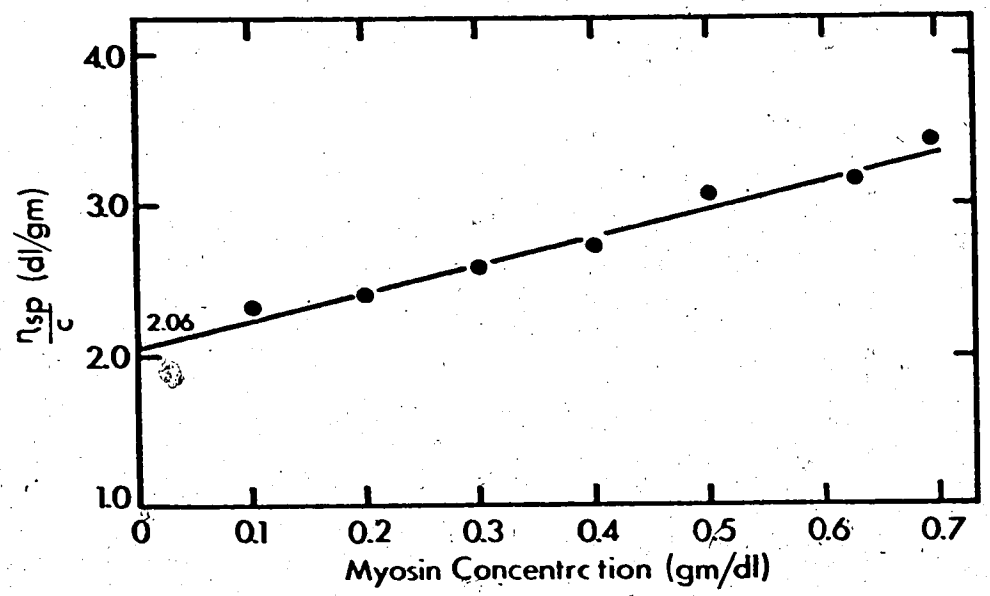

Figure 11. Concentration dependence of the reduced specific viscosity of cardiac myosin at 5.0°C in 0.5 M KCl, 0.05 M phosphate buffer, pH 7.0.

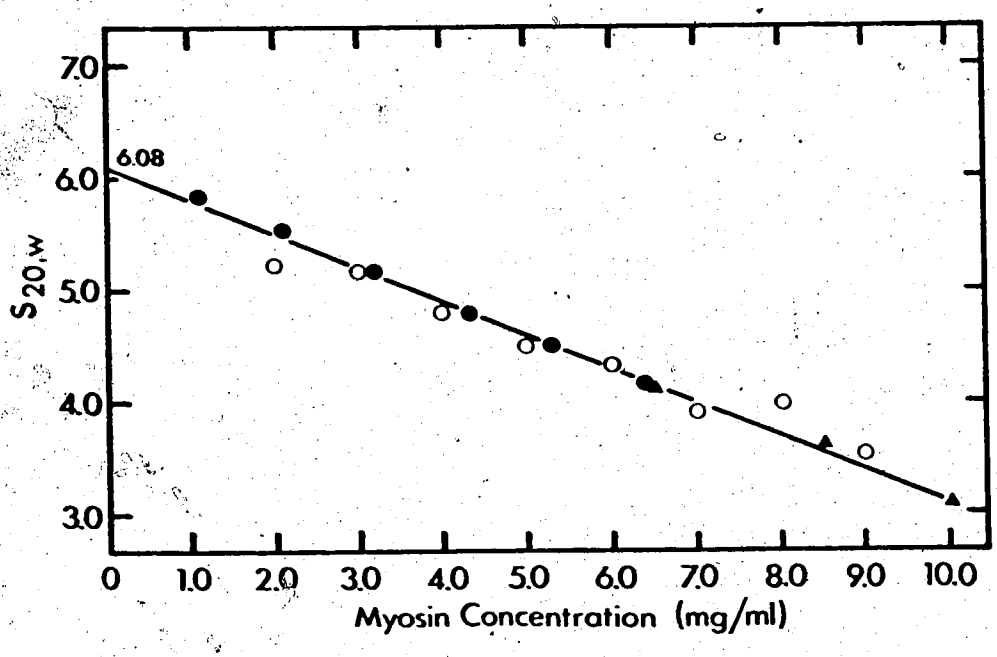

Figure 12. Concentration dependence of the corrected sedimentation velocity of cardiac myosin in 0.5 M KCl, 0.05 M phosphate buffer, pH 7.0. The various point styles represent results from experiments conducted at low temperatures (3 to 7°C) and a set rotor speed of 60 x 10^3 rpm using different preparations of cardiac myosin.

(average of seven trials). The combined results of sedimentation velocity studies, carried out at 3 to 7°C with several preparations of cardiac myosin, are plotted in Figure 12. The sedimentation rate of myosin, corrected to standard conditions, was found to vary inversely with respect to concentration. The equation of the straight line drawn in Figure 12, fitted by the method of least squares, was

$$s_{20,w} = 6.08 - 0.30\ c \quad .$$

From the least squares analysis, the intrinsic sedimentation coefficient, $s^{\circ}_{20,w}$, of cardiac myosin was 6.08 ± 0.06 S, and the concentration-dependence constant, K_s, was 0.049 ± 0.002 ml/mg.

Molecular Weight. Apparent molecular weight moments of rabbit cardiac myosin (in 0.5 M KCl, 0.05 M phosphate buffer, pH 7.0) were determined at low temperatures by three ultracentrifugal techniques: Archibald (Mueller, 1964), low-speed sedimentation equilibrium (Richards, Teller, and Schachman, 1968), and high-speed sedimentation equilibrium (Yphantis, 1964). Pertinent theory and the procedures employed have been described in Chapter 2. The values of the apparent partial specific volume and the solvent density that were used in the molecular weight calculations have been given in the previous section concerning sedimentation velocity.

The final results of a representative, multispeed Archibald experiment are shown in Figure 13. Molecular weight analysis was applied only at the upper meniscus postion. Myosin, at an initial concentration of 13 mg/ml, was examined in conjunction with eight, successively set rotor speeds from 3.0×10^3 to 11.0×10^3 rpm, yielding weight-average

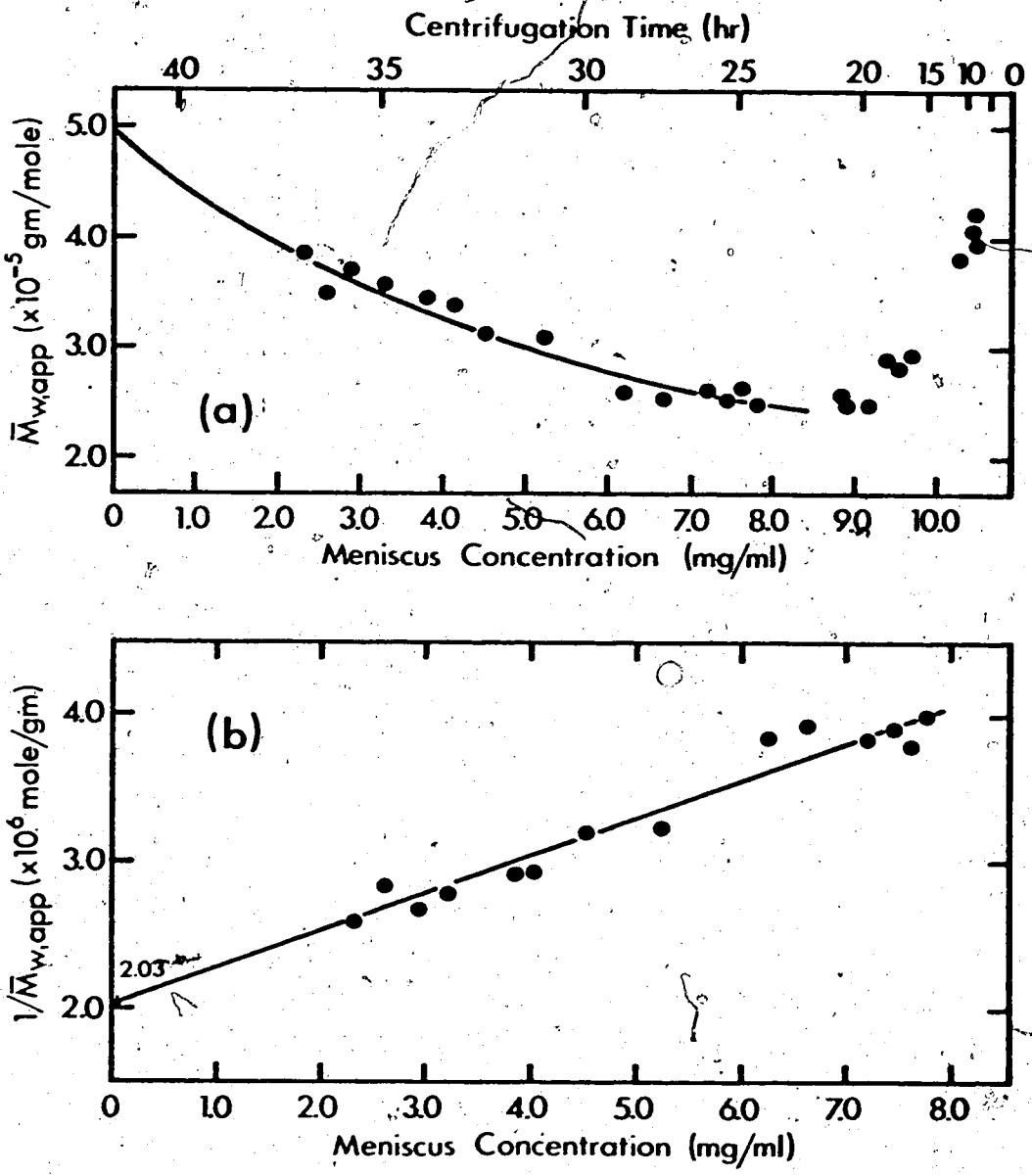

Figure 13. Molecular weight study of cardiac myosin in 0.5 M KCl, 0.05 M phosphate buffer, pH 7.0, by the Archibald method. (a) The apparent weight-average molecular weight of myosin determined at the meniscus as a function of the time of centrifugation or meniscus concentration employing increasing speeds of rotation. (b) Concentration dependence of the reciprocal apparent weight-average molecular weight.

molecular weight estimates ($\overline{M}_{w,app}$ values) over a meniscus concentration range of 2.3 to 10.4 mg/ml. Values of $\overline{M}_{w,app}$ were plotted with respect to the centrifugation time during the course of the run (increasing from right to left, upper X-axis of Figure 13a) and corresponding values of the meniscus concentration (lower X-axis of Figure 13a). As was evident from the relatively higher values of $\overline{M}_{w,app}$ and the downward trend observed during the early part of the Archibald run at high meniscus concentration, a significant amount of heavy material was initially present in cardiac myosin preparations. With increasing time of centrifugation, this material was progressively removed from the meniscus region, and the apparent molecular weight of the resulting myosin solution exhibited a pronounced, non-linear concentration dependence with respect to the meniscus concentration, characteristic of nonideality (Figure 13a). Upon plotting the reciprocal of $\overline{M}_{w,app}$ values, derived after approximately 22 hours of centrifugation, against values of the meniscus concentration (Figure 13b), the experimental data was found to be adequately described by a linear relationship of the form (Mueller, 1964):

$$\frac{1}{\overline{M}_{w,app}} = \frac{1}{\overline{M}_w} + 2Bc \quad .$$

From analysis by the method of least squares (the straight line drawn in Figure 13b and the corresponding curve in Figure 13a), the weight-average molecular weight ($\overline{M}_w$) of cardiac myosin, as determined at infinite dilution, was $4.93 \pm 0.24 \times 10^5$ gm/mole, and the value of the second virial coefficient, calculated from the slope, was $1.28 \pm 0.09 \times 10^{-4}$ mole·ml/gm^2.

A limitation of the Archibald method, attributable in this instance to the utilization of the schlieren optical system rather than the technique itself, was the inability to derive information at protein concentrations less than approximately 2 mg/ml, necessitating extended extrapolation to infinite dilution from data at high concentrations. Seven low-speed sedimentation equilibrium experiments were conducted at 5°C, with different preparations of cardiac myosin over a range of set rotor speeds of 3.0×10^3 to 3.9×10^3 rpm and initial cell-loading concentrations of 3 to 14.2 fringes (0.75 to 3.58 mg/ml), as determined by c_o measurements. In almost every case examined (including high-speed sedimentation equilibrium experiments), corresponding fringe displacements of the solution base lines and the solvent blank were found to be in excellent agreement, lending support to the practice of using an average of the three for base-line corrections. The maximum average base-line deviation observed was of the order of 50 μ. A graph of the natural logarithm of corrected fringe displacements plotted with respect to the square of the radial distances of one low-speed run (c_o of 5.8 fringes, 3.0×10^3 rpm, for approximately 45 hours after over speeding) is presented in Figure 14a. Plots of ln dy versus r^2 derived from all the low-speed runs were sigmoidal in shape with upward curvature evident at the high concentration end, indicative of the presence of heavy molecular weight components. It seemed unlikely that the sigmoidal nature of these curves was artifactual as a result of short equilibrium times, since runs carried out for up to 67 hours after initial overspeeding produced similar shaped ln dy versus r^2 plots. With reference to the results of the multispeed Archibald experiment, the apparent decrease in the slope from the low concentration end to the inflection

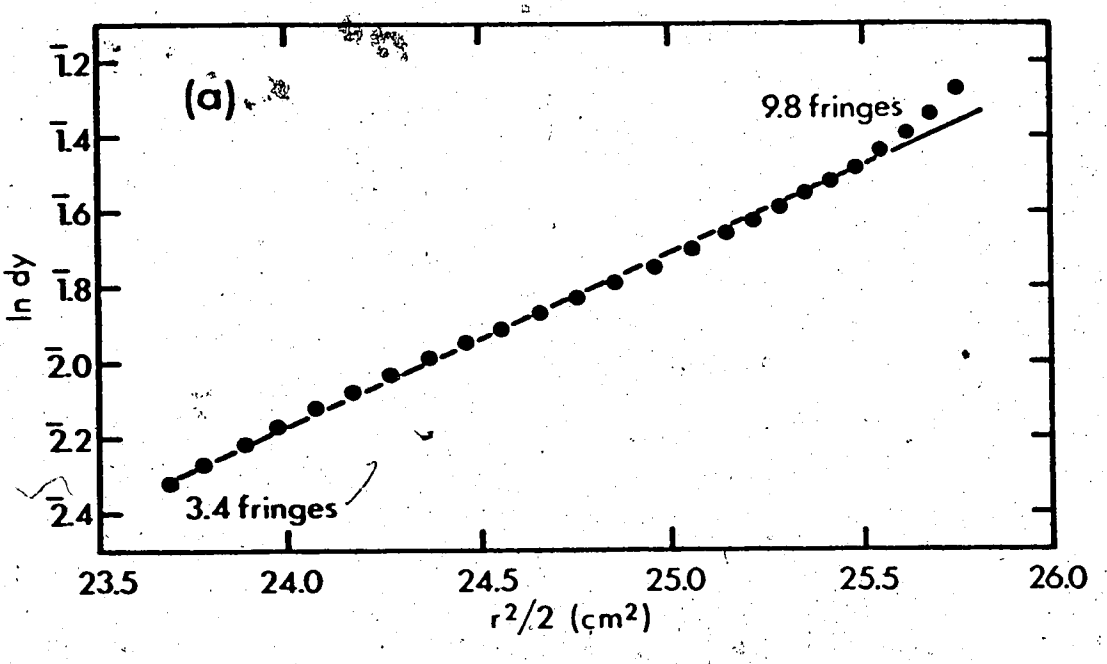

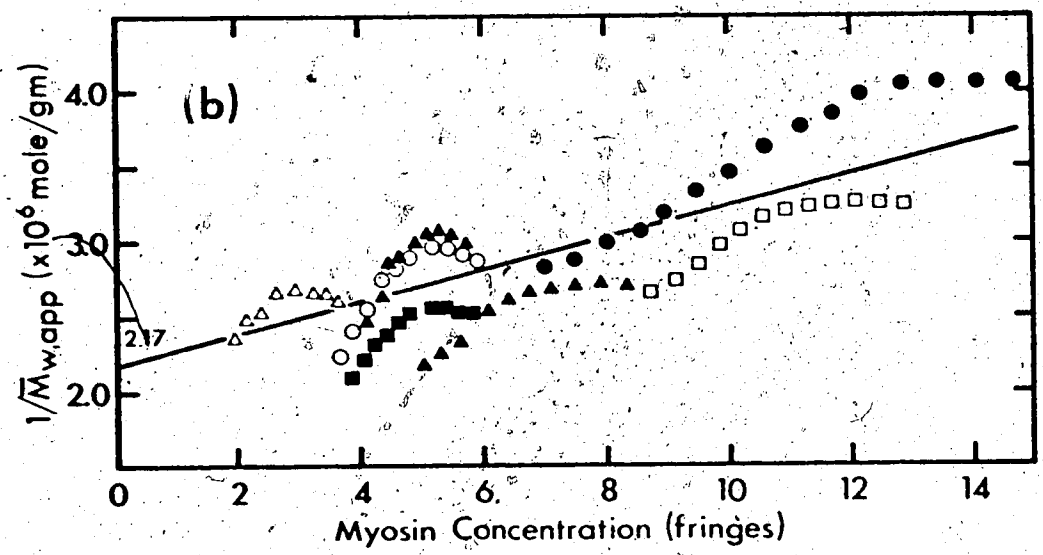

Figure 14. Molecular weight study of cardiac myosin in 0.5 M KCl, 0.05 M phosphate buffer, pH 7.0, by low-speed sedimentation equilibrium. (a) Representative plot of ln dy versus $r^2/2$ derived from a run carried out at 5°C and 3.0×10^3 rpm with c_o equal to 5.8 fringes. A value of 4.22×10^5 gm/mole for the apparent weight-average molecular weight of myosin was calculated from the slope of the straight line shown. (b) Concentration dependence of reciprocal point weight-average molecular weight values from seven low-speed sedimentation equilibrium experiments (see text for detailed explanation).

point more likely reflected the marked nonideality of cardiac myosin, observable in this region due to transport of the heavy material toward the column bottom during the course of centrifugation. Furthermore, accumulation of such material in the lower region of the solution column would in turn be reflected by noticeable upward curvature in the latter part of ln dy versus r^2 plots as seen in Figure 14a. The value of $\overline{M}_{w,app}$ calculated from the slope of the straight line drawn in Figure 14a was 4.22×10^5 gm/mole.

The combined results of the seven low-speed sedimentation equilibrium experiments are graphically summarized in Figure 14b, where the reciprocal of $\overline{M}_{w,app}$ values, determined at each measured radial position (derivative data), has been plotted against computed values of the protein concentration, expressed in fringes. Data associated with the lower end of the solution column (that is, corresponding to the upward curvature observed in ln dy versus r^2 plots), though used in the derivative calculations, was not included in the final analysis of $\overline{M}_{w,app}$ and subsequently is not shown in Figure 14b. The general overlap of the resulting curves was reasonably good; the extent to which the curves did not superimpose confirmed the conclusion that the preparations of rabbit cardiac myosin were slightly polydisperse. The concentration dependence of the apparent molecular weight of myosin was graphically analyzed in terms of the linear relationship used in conjunction with the analysis of the Archibald data, that is:

$$\frac{1}{\overline{M}_{w,app}} = \frac{1}{\overline{M}_w} + 2Bc \quad .$$

A straight line was fitted by the method of least squares through values of $1/\overline{M}_{w,app}$ and concentration at the hinge point of each set of results (Figure 14b). The position of the hinge point was evaluated using the following expression derived by Richards, Teller, and Schachman (1968):

$$r_o^2 = r_b^2 - (r_b^2 - r_m^2) \frac{\ln \frac{c_b}{c_o}}{\ln \frac{c_b}{c_m}} .$$

Experimental values associated with the column bottom were used in these computations. Since the calculated position of r_o^2 did not happen to correspond exactly to any radial position initially measured, values of $1/\overline{M}_{w,app}$ and concentration at the hinge point were determined by linear interpolation of the derivative data at adjacent points. The close agreement of the estimated value of the concentration at the hinge point and c_o substantiated the assumption of conservation of mass. As can be seen in Figure 14b, the resulting straight line fitted the entire data remarkably well, although deviations of the experimental points from the line were relatively large. From the results of the least squares analysis, the weight-average molecular weight of cardiac myosin, as evaluated from the ordinate intercept at zero concentration, was equal to $4.61 \pm 0.34 \times 10^5$ gm/mole, and the value of the second virial coefficient, derived from the slope term, was $2.09 \pm 0.59 \times 10^{-4}$ mole·ml/gm^2.

To minimize the effects of heterogeneity and nonideality on the determination of molecular weight, a series of high-speed sedimentation equilibrium experiments were carried out using dilute solutions

of cardiac myosin. Lengthy centrifugation at high speeds would selectively remove the heavy molecular weight components, and low initial loading concentrations would result in the possible resolution of molecular weight distributions at concentrations less than 1 mg/ml (Yphantis, 1964).

Seven meniscus depletion experiments were conducted at 5°C over a range of set rotor speeds of 8.0×10^3 to 11.0×10^3 rpm in conjunction with three different preparations of cardiac myosin at initial concentrations from approximately 0.5 to 2.0 mg/ml. In nearly all of the runs, the meniscus concentration was effectively reduced to zero as deduced by preliminary examination of the concentration gradient at the meniscus region, subsequently confirmed by computer analysis. Estimated values of the zero level were equal to 2 μ of fringe displacement or less. The final results of a representative high-speed run (at 10×10^3 rpm and an initial loading concentration of 0.85 mg/ml) are graphically illustrated in Figure 15. As was generally noted, plots of ln dy versus r^2 appeared linear throughout most of their length: no significant upward curvature was evident at the higher concentration end (Figure 15a). Slight upward deflection of the initial points, associated with the low concentration region of the solution column, was observed, however, in data from several runs. In all experiments but one, reciprocal values of the point molecular weight moments, plotted with respect to myosin concentration (expressed in fringes), exhibited a definite upward trend and apparent convergence approaching zero concentration. Minima in the reciprocal weight- and z-average molecular weight distributions were observed at low concentrations of approximately 0.3 mg/ml. In addition,

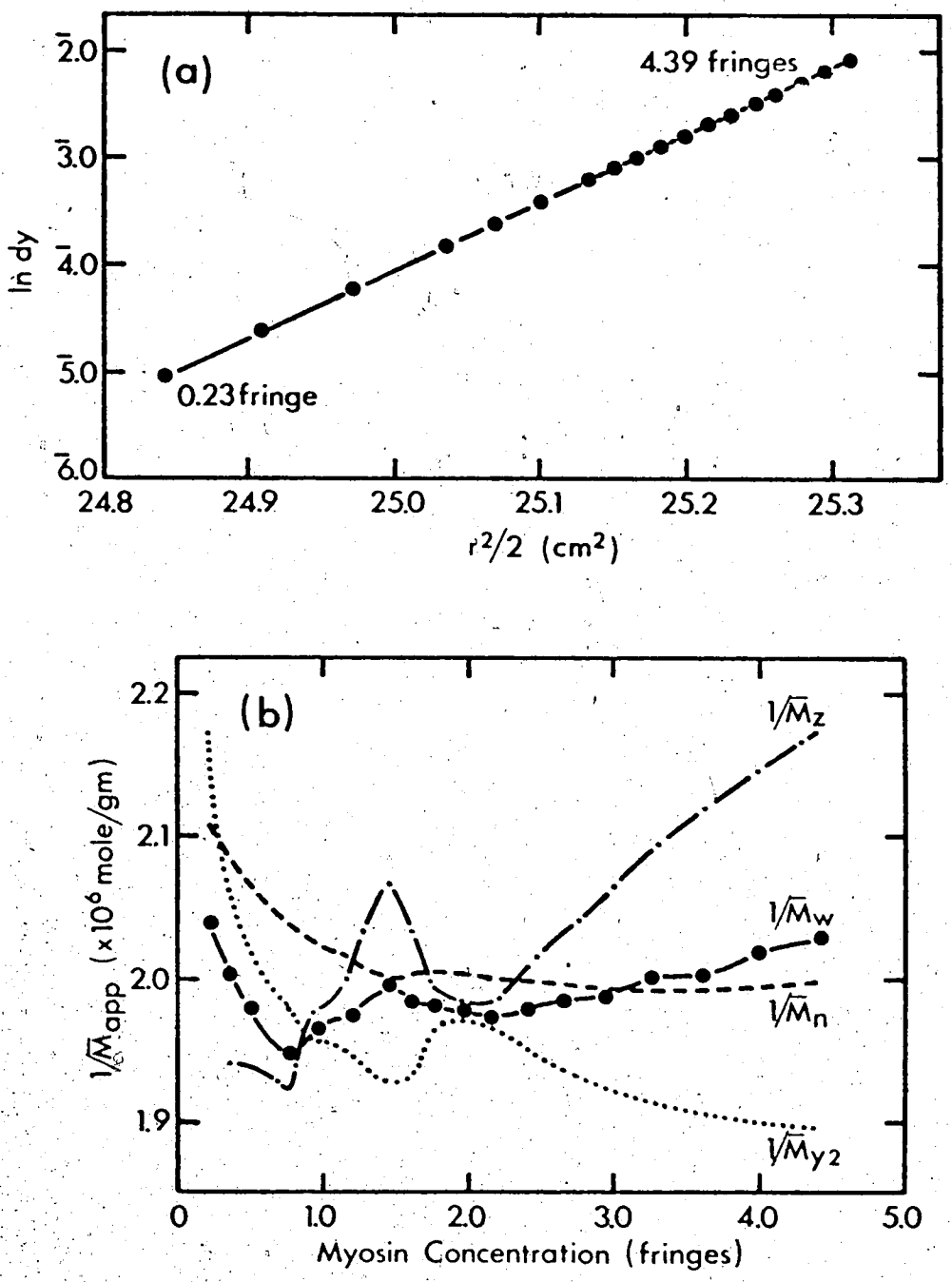

Figure 15. Molecular weight study of cardiac myosin in 0.5 M KCl, 0.05 M phosphate buffer, pH 7.0, by high-speed sedimentation equilibrium. (a) Representative plot of ln dy versus $r^2/2$ resulting from a run conducted at 5°C and 10 x 10^3 rpm with an initial concentration of 0.85 mg/ml (3.4 fringes). The apparent weight-average molecular weight of myosin, as evaluated from the slope of the straight line drawn, was 5.06 x 10^5 gm/mole. (b) Concentration dependence of reciprocal point number-, weight-, z-, and y_2-average molecular weight moments derived from computer analysis of the high-speed data.

perturbation in the $1/\overline{M}_{w,app}$, $1/\overline{M}_{z,app}$, and $1/\overline{M}_{y_2}$ curves was evident at a higher protein concentration (0.5 to 0.6 mg/ml). The resulting graph derived from the data presented in Figure 15a is shown in Figure 15b.

Due to the limited amount of data and, partly, to the large relative errors inherently associated with fringe displacements of less than 100 μ (Yphantis, 1964), the variations observed in corresponding experimental values of the reciprocal moments from the different runs were great enough to preclude a quantitative analysis of the association properties of cardiac myosin with any degree of confidence in the derived parameters. However, by analogy with the results reported by Godfrey and Harrington (1970) concerning the self-association behavior of skeletal myosin in dilute solutions, qualitative conclusions could be drawn. An association reaction of a similar type appeared to exist in dilute solutions of cardiac myosin as evidenced by the parallel trend of the molecular weight moments toward lower values, with the appearance of a distinct minimum in the reciprocal weight- and z-average weight distributions at very low protein concentrations. Although inclusion of light molecular weight components could not be directly discounted because only seven runs were conducted, this effect was assumed to be small since the molecular weight distribution resulting from runs carried out at high speeds and initial loading concentrations was not that greatly different or displaced from that produced at lower speeds and initial concentrations (Godfrey and Harrington, 1970). The presence of higher n-mers of cardiac myosin in significant amounts (that noted in the results of the Archibald and low-speed experiments) was reflected by the perturbation of the molecular weight curves observed at higher

concentrations and the steady decrease in $1/\overline{M}_{y2}$ in the reciprocal graphs (Godfrey and Harrington, 1970). The molecular weight moment, $\overline{M}_{y2}$, is mathematically independent of the second virial coefficient, though not of the higher virial terms (Roark and Yphantis, 1969), and thus provides additional information under conditions of expressed nonideality (which in the high-speed runs was found to prevail in the lower region of the solution column (Figure 15b)).

Analysis of the meniscus depletion data from regions of higher concentration yielded estimates of the number-, weight-, and z-average molecular weights of cardiac myosin associated with protein concentrations of approximately 1 mg/ml or less. For example, the value of $\overline{M}_{w,app}$ obtained from the slope of the least squares line drawn in Figure 15a was equal to 5.06×10^5 gm/mole. These results, and the corresponding initial loading concentrations and rotor speeds employed, are presented in Table II. Values of $\overline{M}_{z,app}$, calculated using the relationship of Lansing and Kraemer (1935)

$$\overline{M}_{z,app} = \frac{c_b \overline{M}_{w,b} - c_m \overline{M}_{w,m}}{c_b - c_m},$$

with extrapolated values of the variables from the computer analysis of the derivative data, were in good agreement with those shown in the table. The average value of $\overline{M}_{w,app}$ for cardiac myosin as estimated from high-speed sedimentation equilibrium experiments (4.77×10^5 gm/mole) was consistent with the values determined by the previous techniques.

TABLE II

MOLECULAR WEIGHT OF CARDIAC MYOSIN AS DETERMINED BY HIGH-SPEED SEDIMENTATION EQUILIBRIUM

(0.5 M KCl, 0.05 M phosphate buffer, pH 7.0, at 5°C)

Initial Concentration (mg/ml)	Rotor Speed (rpm)	Apparent Molecular Weight ($\times 10^{-5}$)*		
		$\bar{M}_n$	$\bar{M}_w$	$\bar{M}_z$
0.85	10091	5.00	5.06	5.01
0.53	9090	4.94	4.88	5.03
1.92	11112	4.63	4.69	5.18
1.17	11113	4.37	4.78	5.04
1.92	8990	4.12	4.55	4.72
1.45	8952	4.30	4.66	4.81
Average ± Std. Dev.		4.56 ± 0.36	4.77 ± 0.18	4.96 ± 0.17

*$\bar{M}_n$ are the limiting values from computer analysis of the derivative data; $\bar{M}_w$ are derived from the slope of the linear least squares fit of ln y versus $r^2/2$ data; and $\bar{M}_z$ are values taken at $(c_m + c_b)/2$ from computer analysis of the derivative data.

Discussion

The preparation of cardiac myosin samples totally devoid of myosin aggregates, actomyosin, and associated contaminants (such as RNA and 5'-adenylic deaminase) has been reported to be relatively difficult (Vierling et al., 1968; Katz, 1970). The isolation procedures employed in the present study appeared adequate in yielding consistent material from frozen tissue suitable for enzymatic and physicochemical investigation — although final yields were invariably low reflecting, in part, the difficulty of extracting myosin from cardiac muscle (Mueller, 1964; Katz, 1970). Whether the minor degree of heterogeneity detected in cardiac myosin samples was a result of the inherent tendency of myosin to aggregate (Katz, 1970), or a result of the preparative methods (Stracher and Dreizen, 1966) and frozen starting material, cannot be distinguished: both reasons are likely correct. Certainly, as was pointed out by Godfrey and Harrington (1970) with respect to skeletal myosin, the initial presence of aggregated material in myosin solutions was a separate manifestation (though perhaps related) to the possible association reaction evident at very low protein concentration.

As noted from enzymatic analysis, the Ca^{++} ion-activated ATPase activity of rabbit cardiac myosin, V_{max} of 0.23 μmole P_i/min/mg, was approximately one-third that reported for rabbit skeletal myosin as measured under simialr conditions, V_{max} of 0.5 to 0.6 μmole P_i/min/mg (Lowey et al., 1969; McCubbin et al., 1973). This finding is consistent with the observations originally made by Bailey (1942) and with the results later reported by Bárány et al. (1964). The value of the apparent Michaelis constant derived for rabbit cardiac myosin in the presence of

calcium ions (0.96×10^{-4} M) is higher compared to published values fo skeletal myosin (1.4×10^{-5} M, Ouellet et al., 1952; 1.09×10^{-6} M, Eisenberg and Moos, 1970; 8.8×10^{-5} M, McCubbin et al., 1973). This may indicate a relatively lower affinity of cardiac myosin for substrate, possibly reflecting a structural difference of the active site (Katz, 1970).

Recent investigations have established that native myosin is comprised of two heavy polypeptide chains, each approximately 2.0×10^5 in molecular weight, and a small number of light chains with an average molecular weight of about 2.0×10^4 (Brahms and Kay, 1963; Gershman et al., 1969; Lowey et al., 1969; Gazith et al., 1970). The interaction of light and heavy chains has been shown to be essential for the hydrolysis of ATP by myosin (Stracher, 1969; Dreizen and Gershman, 1970). Results of hybridization experiments with preparations of myosin from different muscle tissues suggest that the nature of the associated light chains, to a great extent, determines the level of ATPase activity (Dreizen and Richards, 1973). In this regard, significant physical and chemical differences have been observed between skeletal and cardiac light chains. Rabbit skeletal myosin yields three distinct classes of light chains upon SDS-polyacrylamide gel electrophoresis with estimated molecular weights of 2.5×10^4, 1.8×10^4, and 1.6×10^4 in an apparent stoichiometry, of 1:2:1, respectively, as determined from densitometry of the acrylamide gels (Weeds and Lowey, 1971; Lowey and Risby, 1971; Sarkar, 1973). On the other hand, rabbit cardiac myosin shows only two distinct classes, having slightly different electrophoretic mobilities as compared to the skeletal light chains, with estimated molecular weights of 2.7×10^4 and 1.8×10^4 in a molar ratio of 2:1 (Mani and Kay, 1973).

These observations closely agree with the results of comparative experiments conducted with skeletal, red, and cardiac myosins (Locker and Hagyard, 1967; Sarkar et al., 1971). Furthermore, as shown by Weeds and Pope (1971), the light chains of bovine and ovine cardiac myosin possess two additional thiol peptide sequences evidently not present in ovine and rabbit skeletal light chains. These authors have also noted that treatment with the sulfhydryl reagent 5,5'-dithiobis-(2-nitrobenzoic acid), which dissociates approximately 6% of the total amount of rabbit skeletal myosin, has little effect on the light chains of cardiac myosin. Finally, comparison of two-dimensional, tryptic peptide maps of bovine cardiac and rabbit skeletal light chains (screened for histidine, arginine, tyrosine, and CM-cysteine containing peptides) show no overall similarities (Weeds and Frank, 1973).

Evidence for the contribution of the heavy chains to the quantitative difference observed between cardiac and skeletal myosin ATPase activity is, however, scant and indirect (Dreizen and Richards, 1973). For example, Huszar and Elzinga (1972) have reported variations in the amino acid sequence of homologous methylated and non-methylated histidine peptides from rabbit cardiac and skeletal myosin, and concluded that the two proteins are synthesized under the control of separate genes. Extrapolating further, significant differences may thus exist in regions of the heavy chains directly associated with the active site and partly determine the level of enzymatic activity in combination with the light chains.

Measured values of the ATPase activity of rabbit cardiac myosin, although comparable, appeared to be consistently greater than corresponding values reported for myosin obtained from canine (Mueller

et al., 1964), bovine (Tada et al., 1969) and rabbit (Bárány et al., 1964) cardiac tissue. Three reasons may account for this observation: difference in the preparative methods employed (though Vierling et al. (1968) found that the Ca^{++} ion-activated ATPase activity of canine cardiac myosin, measured at pH 9, was unaffected by the method of preparation); species differences of the muscle source (Mueller et al., 1964); and the apparent activation of myosin ATPase activity after purification from DEAE-cellulose (Asai, 1963; Richards et al., 1967). With regard to the latter point, preparations of cardiac myosin resulting in lower 280/260 absorbance ratios (indicative of ineffective treatment with DEAE-cellulose) were found to exhibit lower activity.

The effect of Ca^{++} and Mg^{++} ions on the catalytic activity of cardiac myosin (in the presence of potassium chloride) is consistent with documented observations concerning both the optimal levels of the respective salts required to produce a maximal effect (8 to 10 mM $CaCl_2$ or 0.5 mM $MgCl_2$) and the relatively higher potency of $MgCl_2$ to $CaCl_2$ (Katz, 1970).

The pH dependence of rabbit cardiac myosin ATPase activity is similar to that found for canine cardiac myosin by Brahms and Kay (1962): that is, from approximately pH 7.5, activation with increasing pH and subsequent reduction in the hydrolysis rate at pH 9 (Figure 7). However, these findings are in disagreement with the results reported by Bárány et al. (1964) also carried out with rabbit cardiac myosin, though prepared by an alternate method. The resolution of this discrepancy apparently is related to the order and time in which the components of the enzyme assay were added together. As shown by Sreter et al. (1966) and later by Seidel (1967), the enzymatic activity of cardiac myosin is

labile under mild alkaline conditions and is quickly lost at pH values greater than 9. Moreover, no increase in activity is observable over the alkaline pH range if myosin is preincubated for a short period of time in the absence of ATP (Sreter et al., 1966). This was the procedure adopted by Bárány et al. (1964), who initiated their enzyme assays by the addition of ATP. In the investigation of Brahms and Kay (1962), as well as in the present study, the addition of myosin to substrate solutions was used to start the enzymatic reaction. The inactivating effect of preincubation at alkaline pH may also explain why rates of activity as reported by Bárány et al. (1964) were lower relative to values measured in this study.

The observed bimodal effect of PCMB on the enzymatic activity of rabbit cardiac myosin is similar to the results of Brahms and Kay (1962) and Mueller et al. (1964) derived with canine cardiac myosin. As was initially noted by Kielley and Bradley (1956) with rabbit skeletal myosin, increasing concentrations of PCMB (in the presence of Ca^{++} ions) elevated the ATPase activity until approximately one-half of the total number of sulfhydryl groups were titrated (in this case, approximately 4 residues/10^5 gm protein of a total number of 7 residues/10^5 gm protein determined by amino acid analysis). Further increasing amounts of PCMB caused progressively increasing inhibition. The present results concur with the interpretation that two types of sulfhydryl groups are present at, or associated with, the active site, one inherently essential for ATPase activity (Kielley and Bradley, 1956).

The amino acid composition of rabbit cardiac myosin and recently reported values for rabbit skeletal myosin are compared in Table III. The slightly higher values of glutamic acid and leucine

TABLE III

COMPARISON OF THE AMINO ACID COMPOSITION OF RABBIT CARDIAC AND SKELETAL MYOSIN

(moles/10^5 gm myosin)

Amino Acid	Cardiac Myosin This Study	Skeletal Myosin		
		Kominz et al. (1954)	Lowey & Cohen (1962)	Bárány et al. (1964)
Lys	85	85	92	89
His	15	15	16	16
Arg	47.5	41	43	43
Asp	82	85	85	85
Thr	42	41	44	41
Ser	40	41	39	36
Glu	163	155	157	155
Pro	23	22	22	22
Gly	39	39	40	43
Ala	76	78	78	75
Cya	6.8	9	8.8	8.8
Val	40	42	43	47
Met	22.5	22	23	23
Ile	38	42	42	43
Leu	92	79	81	78
Tyr	18	18	20	19
Phe	29	27	29	27
Try	-	4	-	6.7

evidently present in cardiac myosin are the only major differences found; otherwise, within the variation shown among the analyses of skeletal myosin presented in the table, the amino acid compositions of rabbit cardiac and skeletal myosin are very similar. This represents a major factor supporting the practice of having used skeletal myosin as the standard in the determination of amount protein by the Lowry method. This is not to conclude, however, that the two proteins are identical because significant differences in certain regions of the primary structure have been reported (for example, as was discussed earlier, the thiol peptide sequences (Weeds and Pope, 1971; Weeds and Fra[illegible] 1973) and the methylated and non-methylated histidine peptide sequences (Huszar and Elzinga, 1972)). Immunological dissimilarities observed between cardiac and skeletal myosin additionally suggest that the amino acid sequences at least at the antigen recognition sites must also be different (Finck, 1965).

The similarity in amino acid content was also reflected by the similarities in the ultraviolet optical properties. The value of $E^{1\%}_{1cm,\ 280\ nm}$ equal to 6.06 found for rabbit cardiac myosin in phosphate buffer at neutral pH is not greatly different from that reported for skeletal myosin: 5.43 (Woods et al., 1963), 5.88 (Verpoorte and Kay, 1966), 6.7 (Schliselfeld and Bárány, 1968), and 5.6 (Gershman et al., 1969). In addition, the ultraviolet absorbance and circular dichroic spectra of cardiac myosin appear analogous with spectra observed with skeletal myosin (Finck, 1965; Mommaerts, 1966; and Oikawa et al., 1968). As far as the author is aware, the CD properties of rabbit cardiac myosin have not been previously published; however, from the similarity of the mean residue ellipticity values of cardiac myosin at 221 and

209 nm ($\bar{}2.69 \times 10^4$ and $\bar{}2.56 \times 10^4$ degree·cm^2/dmole, respectively) and the corresponding values for skeletal myosin ($\bar{}2.33 \times 10^4$ and $\bar{}2.28 \times 10^4$ degree·cm^2/dmole, respectively, (Oikawa et al., 1968)), the secondary structure of the two proteins is undoubtedly very much alike. It is then not surprising that conformational changes in cardiac myosin were not observed by CD measurements at different pH or in the presence of ATP since neither similar optical rotatory dispersion experiments (Kay et al., 1964; McCubbin et al., 1967) nor ultraviolet absorbance studies (Gratzer and Lowey, 1969) with skeletal myosin have detected significant changes.

The viscometric and sedimentation velocity results obtained with rabbit cardiac myosin, $[\eta]$ equal to 2.04 dℓ/gm and $s^\circ_{20,w}$ equal to 6.08 S, are within the range of published values for both the cardiac and skeletal system (Katz, 1970). Furthermore, the derived parameters associated with a quantitative description of the concentration dependence of these hydrodynamic properties (that is, Huggins constant and K_s) are also similar to accepted values for skeletal myosin (Creeth and Knight, 1965; Harrington and Burke, 1972), and support the conclusion that rabbit cardiac myosin is highly asymmetric (Katz, 1970).

The effect of polydispersity on the determination of molecular weight of cardiac myosin was minimized by using ultracentrifugal techniques. As pointed out by Mueller (1964), one advantage of the multi-speed Archibald method is the selective removal of heavy aggregates from the meniscus region during the course of centrifugation. Obviously, any method which involves centrifugation for a lengthy period of time will do the same. The pronounced nonideality of cardiac myosin solutions, as evident in the viscometric and sedimentation velocity studies, was also

reflected by a marked concentration dependence of the molecular weight, particularly at protein concentrations greater than about 1 mg/ml. Estimated values of the second virial coefficient are slightly higher than corresponding values determined for canine cardiac myosin (Mueller et al., 1964) and for skeletal myosin (Mueller, 1964; Tonomura et al., 1966), though the relatively large standard deviations observed, due partly to polydispersity, may account for a greater part of this difference. The measured values of the weight-average molecular weight of rabbit cardiac myosin are, in general, lower than most reported values for cardiac myosin (Mueller et al., 1964; Conway and Roberts, 1965; Luchi et al., 1965), but are similar to molecular weight values recently determined for skeletal myosin (Tonomura et al., 1966; Gershman et al., 1969; Godfrey and Harrington, 1970). Furthermore, the results of the high-speed sedimentation equilibrium experiments indicate the presence of a possible association reaction at very low protein concentrations analogous to that seen with skeletal myosin (Godfrey and Harrington, 1970). The average value of the number-average molecular weight, though more variable than the other molecular weight moments, agrees with the value of 4.7×10^5 as determined by osmometry (Tonomura et al., 1966). The difference, and the direction of the difference, observed between the average values of the number-, weight-, and z-average molecular weight additionally suggests that cardiac myosin solutions were slightly heterogeneous, though the overall agreement would also indicate that the effects of nonideality and polydispersity had been substantially reduced by using low initial loading concentrations and high rotor speeds.

Further discussion of cardiac myosin, in light of the results of the proteolytic fragmentation study, is presented in Chapter 6.

CHAPTER 4

PROTEOLYTIC FRAGMENTATION OF CARDIAC MYOSIN WITH PAPAIN

Previous studies involving the enzymatic degradation of skeletal myosin with an insolubilized form of papain have shown that limited fragmentation and subsequent investigation of the purified subfragments are very useful approaches for the analysis of the molecular structure of myosin (Kominz et al., 1965; Nihei and Kay, 1968; Lowey et al., 1969). This method was thus adopted for the study of rabbit cardiac myosin and applied, to a great extent, in a parallel manner. Significant modifications were introduced with respect to the immobilized derivative employed and the temperature at which the proteolytic digestion was carried out. Papain was initially insolubilized by coupling crystalline enzyme (obtained commercially) to diazotized p-aminobenzyl (PAB-) cellulose as described by Lowey et al. (1969). However, from subsequent examination of the protein binding capacity and enzymatic activity of these insoluble complexes, as well as attempts to establish standard experimental conditions for fragmentation, it became apparent that papain-PAB-cellulose had several negative features. For example, the amount of papain bound per unit weight of PAB-cellulose, as determined from amino acid analysis, was very low (4 to 9 mg/gm of PAB-cellulose) and varied somewhat, as did the resulting esterase activity, with different preparations of the insoluble complex. (This was discovered to be partly attributable to the use of aged papain suspensions). Corresponding observations have been

reported by Nihei and Kay (1968), Lowey et al. (1969), and Goldstein et al. (1970). In addition, as was similarly noted by the latter investigators, PAB-cellulose in aqueous solutions was found to release varying amounts of colored material possessing optical absorption at ultraviolet wavelengths. For these reasons, an alternative supporting matrix was chosen, (dialdehyde)-starch-methylenedianiline (S-MDA) resin, and papain was freshly prepared and stabilized by conversion to mercuripapain. Based on the findings of Tada et al. (1969) that the apparent yield of subfragment 1, obtained from bovine cardiac heavy meromyosin by digestion with soluble papain, was greater at lower temperatures, the proteolytic fragmentation of rabbit cardiac myosin was conducted at approximately 0°C. Procedures for the preparation of mercuripapain, S-MDA resin, and insolubilized mercuripapain are briefly described prior to presenting the physicochemical and kinetic results of the enzymatic digestion of cardiac myosin. The results of background studies concerning pertinent properties of the S-MDA resin and S-MDA-mercuripapain are also considered in this chapter.

Preparative Methods and Procedures

Mercuripapain. Native papain was isolated and purified from dried papaya latex employing essentially the method of Kimmel and Smith (1958). Granular latex powder (200 gm Crude, Type I, Sigma Chemical Company) was mixed with 100 gm Celite (an inert filtering aid) and 150 gm washed sea sand. Crude enzyme was extracted at room temperature (23°C) by grinding this mixture thoroughly in a mortar with one liter of freshly prepared 0.04 M cysteine, pH 5.7. The aqueous extract was filtered at

4°C through a centimeter-thick layer of Hyflo Super-Cel on Whatman 541 filter paper under very weak vacuum using a large diameter Büchner funnel. The pH of the cold filtrate was slowly increased to 9.0 with 1 N sodium hydroxide, and the fine, gray precipitate that formed was removed by filtration as described above. The volume of the filtrate was measured, and papain was selectively precipitated at 4°C by the addition of solid ammonium sulfate to 40% saturation. The suspension was allowed to stand for approximately 2 hours, whereupon the precipitate was collected by centrifugation at 2°C and 2.5×10^3 rpm for 1 hour, washed once with 400 ml of a cold 40% saturated ammonium sulfate solution, and recollected by centrifugation. The solid material was dissolved in 600 ml of cold 0.02 M cysteine, pH 7, and the resulting solution clarified by millipore filtration (5 or 8 μ pore size). Papain was salted out at 4°C by the gradual addition of 60 gm solid sodium chloride and gentle stirring for approximately 1 hour. The white precipitate was collected by centrifugation and resuspended at room temperature in 400 ml of 0.02 M cysteine maintained at pH 6.5. The suspension was incubated at room temperature for 30 minutes, then cooled to 4°C — the enzyme crystallized over a period of approximately 12 hours. The light crystals were collected by centrifugation at 2°C and 2.5×10^3 rpm for 5 hours, and dissolved in a minimal amount of double-distilled, deionized water at room temperature. The protein solution was millipore filtered, and papain recrystallized by the very slow addition of a saturated solution of sodium chloride (1 ml per 30 ml papain solution). To promote complete crystallization, this suspension was cooled and kept overnight at 4°C. The purified enzyme was subsequently collected by centrifugation at 2°C and 20×10^3 rpm for 15 to 30 minutes. Recrystallization of papain was additionally repeated

once. The protein concentration of papain solutions was determined spectrophotometrically using an extinction coefficient, $E^{1\%}_{1\ cm,\ 278\ nm}$, equal to 25.0 (Glazer and Smith, 1961). Approximately 300 mg of twice recrystallized papain with a specific esterase activity of 20 to 28 μmole BAEE/min/mg was usually obtained from 100 gm granular powder. Enzymatic activity measurements were conducted at 20°C and pH 6.5 with substrate solutions of 0.05 M BAEE, 2 mM EDTA, 5 mM cysteine utilizing pH-stat techniques.

Native papain was routinely converted to mercuripapain using the modified method of Goldstein et al. (1970). Crystalline papain was dissolved in 2 mM EDTA, 5 mM cysteine, pH 7.0 to a final concentration of approximately 1 mg/ml and incubated at room temperature for 20 minutes. The pH of the resulting solution was slowly reduced to 5.5 with 0.1 N hydrochloric acid. A 3.3% solution of mercuric chloride (in distilled water or 0.01 M sodium acetate buffer) was adjusted to pH 5.5, and 1 ml per 10 ml of protein solution was then added dropwise with continuous stirring. The reaction mixture was transferred to prepared dialysis tubing and dialyzed against 0.01 M acetate buffer, pH 5.5, at 4°C for 7 to 10 days. Final mercuripapain solutions were clarified of insoluble material, which had precipitated during the course of dialysis, by centrifugation at 2°C and 20×10^3 rpm for 30 minutes, and they were subsequently stored sealed at 10°C. The concentration of mercuripapain was determined from ultraviolet absorbance measurements at 280 nm using a value of $E^{1\%}_{1\ cm}$ equal to 24.6 (Whitaker and Bender, 1965). From 100 gm of initial latex powder, the overall yield was approximately 250 mg of mercuripapain with a specific esterase activity of 18 to 21 μmole BAEE/min/mg at 20°C. Prior to measurement of enzymatic activity, both papain

and mercuripapain were activated by overnight dialysis at 4°C against 2 mM EDTA, 5 mM cysteine, pH 6.5.

S-MDA Resin. Synthesis of the water-insoluble polymer was carried out closely following the method outlined by Goldstein et al. (1970), the pertinent reactions of which are schematically illustrated in Figure 16. Unless otherwise stated, all preparative procedures were conducted at room temperature (23°C). A fine, aqueous slurry of dialdehyde starch (Sumstar-190, generously donated by Miles Laboratories Inc., Elkhart, Indiana) was made by suspending 10.0 gm in 200 ml of double-distilled, deionized water and stirring for 15 minutes. The suspension was rendered alkaline by the addition of 40 ml, 2 M sodium carbonate, pH 10.5, and slowly poured into 300 ml of a vigorously stirred, 10% methanolic solution of 4, 4'-diaminodiphenylmethane. The reaction mixture was loosely covered and continuously stirred for 3 days. The insoluble material was then collected by filtration (on a Büchner funnel with Whatman 541 filter paper), washed thoroughly with methanol, and resuspended in 300 ml double-distilled, deionized water. Reduction of the polymeric Schiff's base was effected by the addition of 40 gm sodium borohydride and gentle stirring for 18 hours. The pH of the resulting mixture was adjusted to neutrality with concentrated acetic acid. S-MDA resin was collected by filtration, washed with double-distilled, deionized water then methanol, and refluxed with four, 300 ml changes of methanol to remove contaminant aromatic amines. The refluxed material was filtered, spread thinly in a large diameter petri dish, and air dried. The final weight of dry S-MDA resin was 12.7 gm.

S-MDA-mercuripapain. Immobilized papain derivatives were

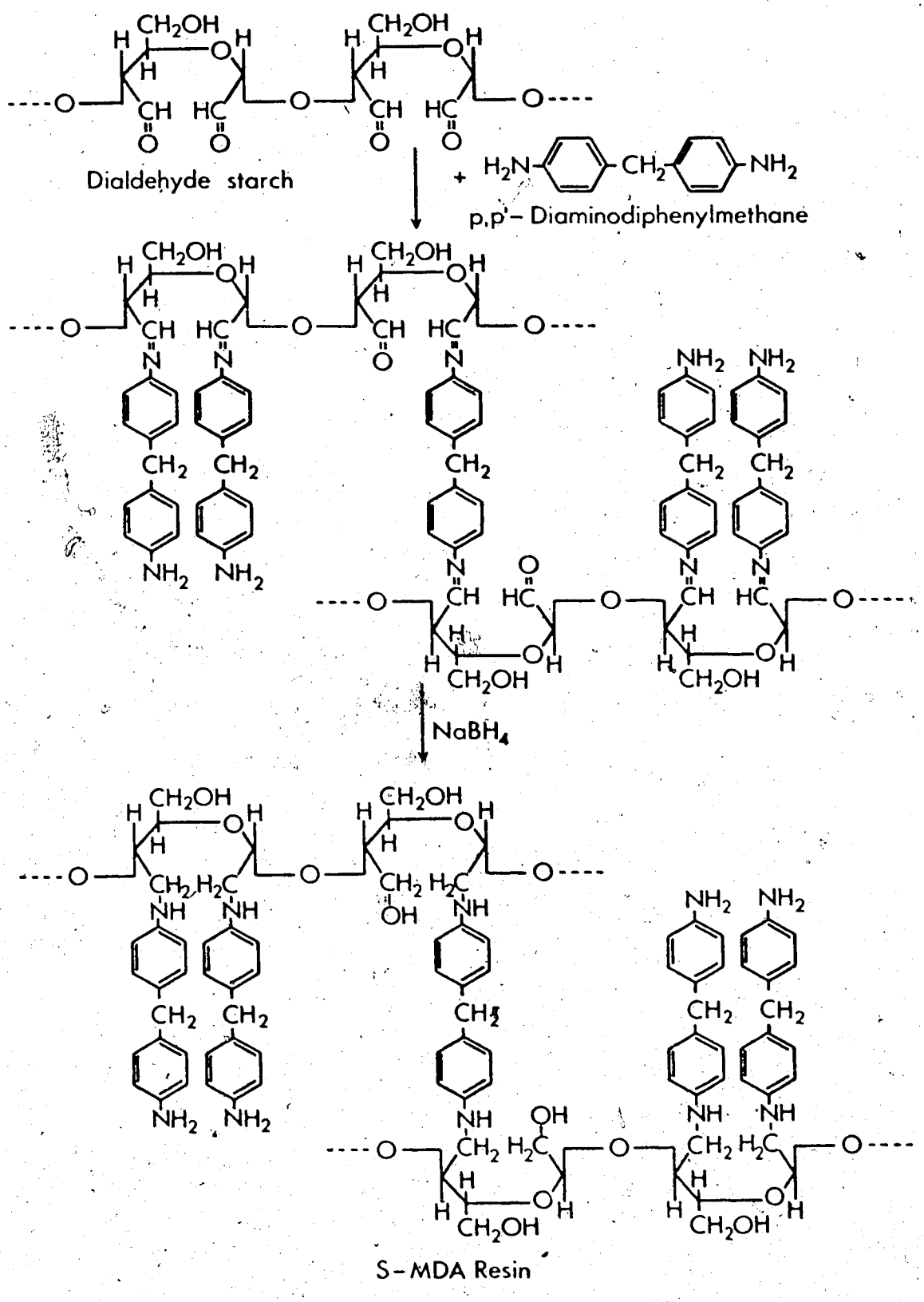

Figure 16. Schematic representation of the principal reaction steps in the synthesis of S-MDA resin (from Goldstein et al., 1970).

prepared by covalently linking mercuripapain to diazotized S-MDA resin as described by Goldstein et al. (1970). Diazotization of the free amino groups of S-MDA resin was routinely carried out in the following manner: 100 mg S-MDA resin was suspended in 8 ml of 50% acetic acid and stirred for 1 hour in a bath of crushed ice and water, whereupon 1 ml of a cold, freshly prepared 2% solution of sodium nitrite was added dropwise. The diazotization mixture was loosely covered and gently stirred for an additional hour at 0°C. The pH of the chilled suspension was then slowly raised to approximately 8.5 by the dropwise addition of 5 N sodium hydroxide — pieces of crushed ice were added periodically to maintain the low temperature. The dark brown, lumpy precipitate formed was collected by millipore filtration (8 μ pore size) and thoroughly washed with cold 0.2 M phosphate buffer, pH 7.6. The water-insoluble enzyme complex was subsequently prepared as follows: the wet polydiazonium salt was transferred into a clean 25 ml Erlenmeyer flask and resuspended in 10.0 ml of cold 0.2 M phosphate buffer, pH 7.6. A desired aliquot of mercuripapain solution was added dropwise to the stirred suspension. The flask was sealed, and coupling effected with continuous stirring at 4°C for 20 to 24 hours. The enzyme conjugate was collected by millipore filtration and washed with 200 ml of cold 1 M potassium chloride, then with 100 ml of cold double-distilled, deionized water to remove any protein simply adsorbed to the resin. S-MDA-mercuripapain was resuspended in 10.0 ml double-distilled, deionized water and stored sealed at 10°C until activated, as with papain and mercuripapain, by overnight dialysis at 4°C against 2 mM EDTA, 5 mM cysteine, pH 6.5.

Results

Studies of S-MDA Resin and S-MDA-mercuripapain. Several relevant properties of the S-MDA resin and the immobilized derivative of mercuripapain were examined prior to investigating the salient characteristics of the proteolytic digestion of cardiac myosin. Throughout these studies, the amount of enzyme covalently bound to the matrix was determined from quantitative amino acid analysis based on the recovery of glycine, alanine, valine, and leucine. This set of calculations was carried out assuming papain has a molecular weight of 23,406 and contains per mole, 28 glycine, 14 alanine, 18 valine, and 11 leucine (Mitchel, Chaiken, and Smith, 1970).

The protein binding capacity of the resin was estimated by preparing a series of insoluble-enzyme complexes involving the addition of various quantities of mercuripapain (5 to 40 mg) to 100 mg diazotized S-MDA resin. Final data was graphically analyzed by plotting the amount protein covalently fixed to the water-insoluble polymer against the corresponding quantity of mercuripapain added to the coupling reaction mixture (both expressed as mg/100 mg resin). From the horizontal portion of the resulting binding curve (shown in Figure 17), the present preparation of S-MDA resin was found to maximally bind approximately 23.5 mg mercuripapain per 100 mg dry weight of resin.

The results of a study conducted to establish the minimum time necessary for completion of the coupling reaction are depicted in Figure 18. The binding of 16 mg mercuripapain to 100 mg diazotized resin at 4°C appeared to follow a hyperbolic relationship with respect to the time of the reaction. The initial rate of coupling was relatively fast: approximately 80% of the total amount of enzyme that could be potentially

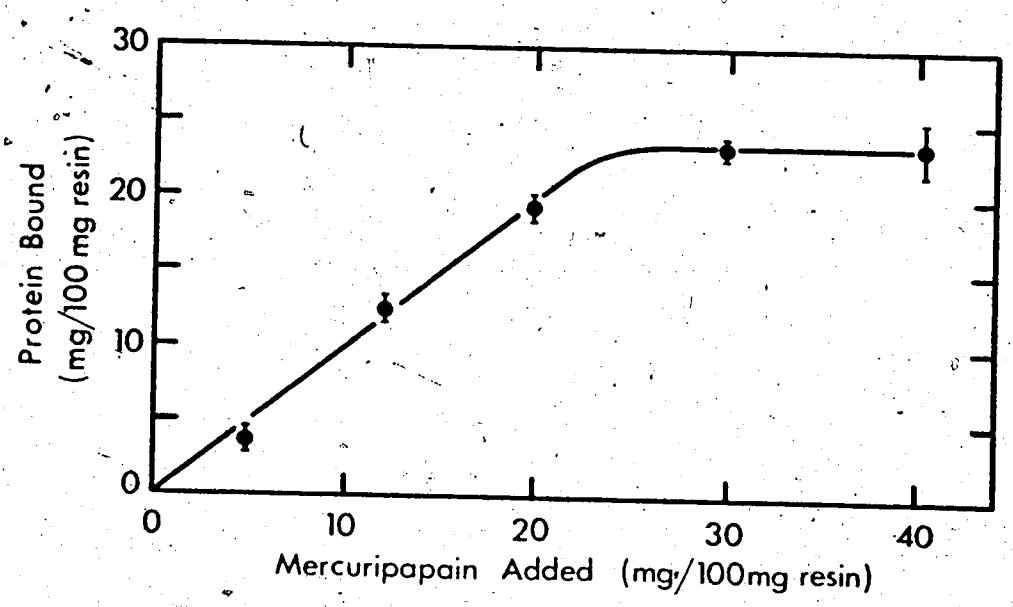

Figure 17. Protein binding curve for S-MDA resin. Varying amounts of mercuripapain were added to 100 mg (initial dry weight) diazotized S-MDA resin in suspension at 4°C and allowed to react for 24 hours. The quantity of protein bound was estimated from amino acid analyses, and the bars in the figure represent a variation of ±1 S.D. from the mean, the point plotted.

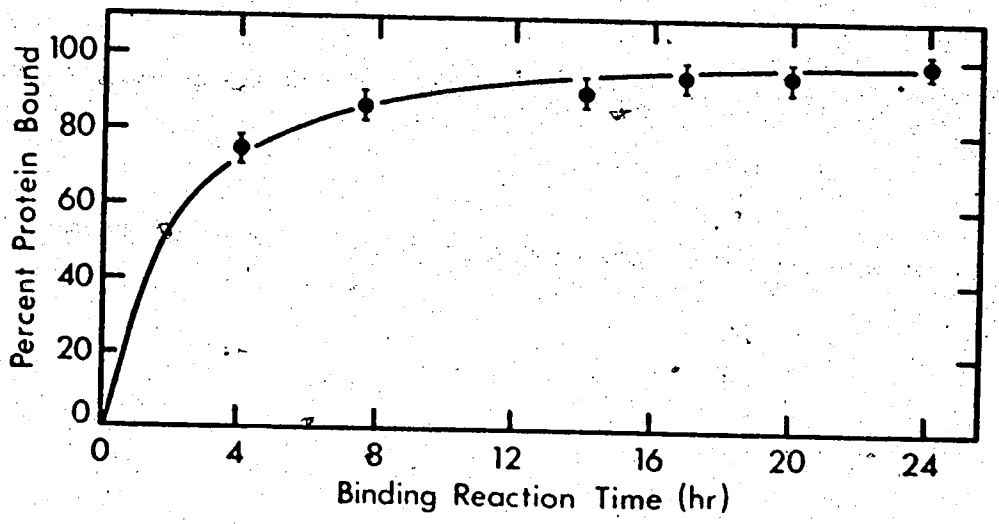

Figure 18. Time course of binding of mercuripapain to diazotized S-MDA resin at 4°C and a mercuripapain/resin ratio of 16:100 (mg/mg dry resin). The amount protein bound was estimated from amino acid analyses, and the bars represent a variation of ±1 S.D. from the mean, the point plotted.

bound was covalently fixed in the first 8 hours. The subsequent reaction rate progressively decreased, and the extent of binding asymptotically approached 100%. Total coupling was essentially completed in 24 hours.

Because of the unstable nature of aryl diazonium salts even in ice-cold solutions (Morrison and Boyd, 1966), additional experiments were carried out to determine the extent of this degradation in diazotized S-MDA resin over the duration of the coupling reaction and the resulting effect on the protein binding capacity. Weighed samples of S-MDA resin were diazotized and allowed to stand with continuous stirring at 4°C for 0 (the control), 8, 16, and 24 hours prior to the addition of known aliquots of mercuripapain. The preparation of the insolubilized enzyme derivatives and subsequent analyses were completed in the regular manner. As seen in Figure 19, the potential binding capacity of the resin gradually decreased to approximately 75% over the course of 24 hours, reflecting an apparent loss of diazonium groups available for binding protein. The significant portion of this degradation occurred, however, during the latter 12 hours, and with regard to the time course of the coupling reaction, well after over 90% of the capacity amount of mercuripapain was already covalently linked (see for example Figure 18).

Both mercuripapain (dissolved in 0.01 M acetate buffer, pH 5.5) and S-MDA-mercuripapain (suspended in double-distilled, deionized water) were found to retain high levels of esterase activity when stored at 10°C over lengthy periods of time (Figure 20). Mercuripapain was by far the more stable, losing less than 10% of its initial enzymatic activity when stored for up to 140 days. On the other hand, marked and progressive deterioration of the immobilized derivatives of mercuripapain was observed to occur after approximately 60 days storage (Figure 20). Only fresh

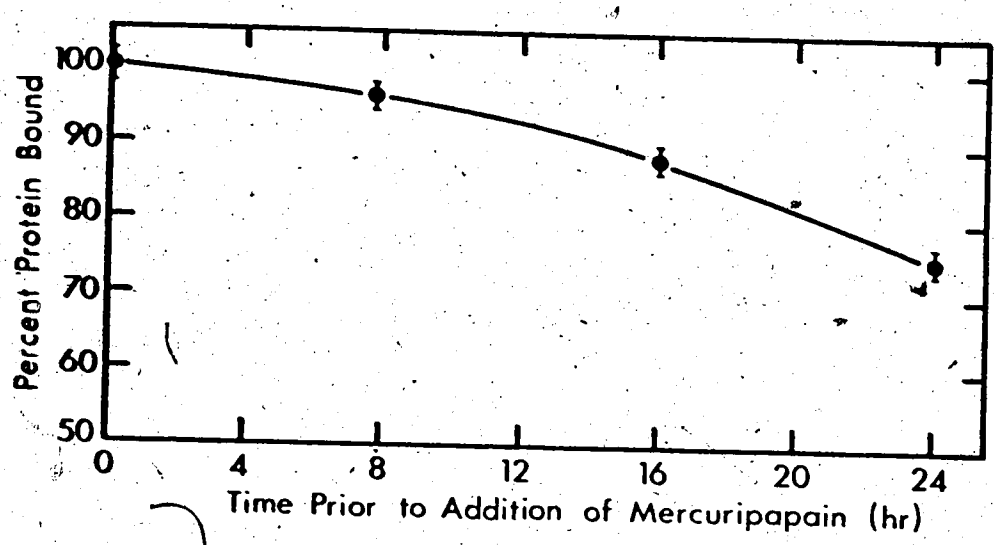

Figure 19. Apparent loss of protein binding capacity of diazotized S-MDA resin with time of standing prior to the addition of mercuripapain. The binding reaction was carried out at 4°C for 24 hours with a mercuripapain/resin ratio of 32:100 (mg/mg dry resin). The amount protein bound was estimated from amino acid analyses, and the bars represent a variation of ±1 S.D. from the mean, the point plotted.

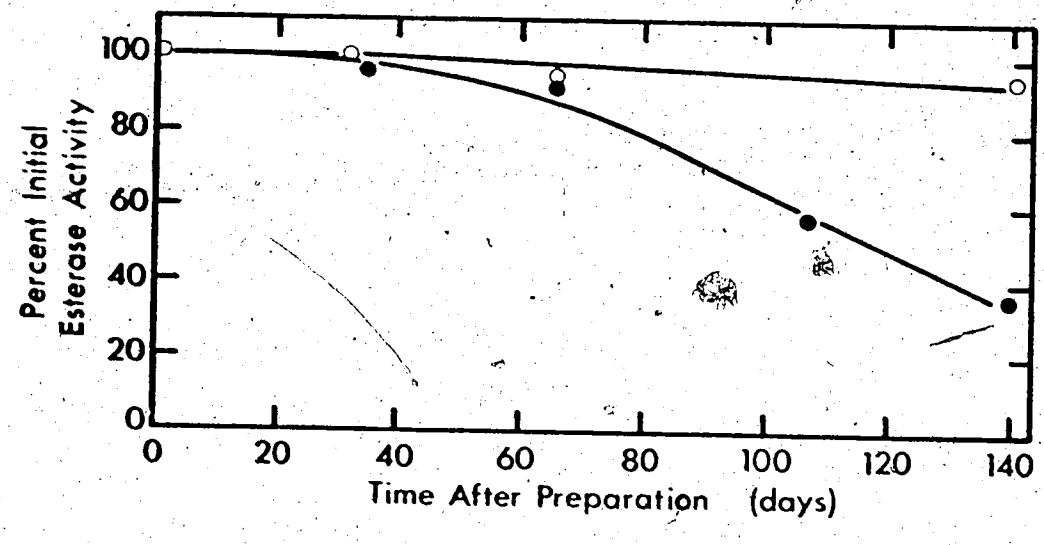

Figure 20. The effect of storage time on the enzymatic stability of mercuripapain, refrigerated at 10°C in 0.01 M sodium acetate buffer, pH 5.5 (○—○), and S-MDA-mercuripapain, suspended in double-distilled, deionized water at 10°C (●—●). Esterase activity measurements were conducted at 20°C and pH 6.5 with substrate solutions consisting of 0.05 M BAEE, 5 mM cysteine, 2 mM EDTA.

preparations of S-MDA-mercuripapain, stored for less than 40 days, were subsequently used in the proteolytic fragmentation of cardiac myosin.

The specific esterase activity recovered in preparations of S-MDA-mercuripapain was consistently 60 to 70% of that measured for the original mercuripapain. In an attempt to account for this difference, kinetic studies were conducted in the manner of Whitaker and Bender (1965) assuming the same Michaelis-Menten reaction scheme applied to both the soluble and immobilized enzyme. Activity measurements were carried out at 25°C with substrate solutions containing 7 to 50 mM BAEE, 2 mM EDTA, 5 mM cysteine, pH 6.5 employing pH-stat techniques as outlined in Chapter 2. A separate series of measurements was additionally performed at approximately 0°C to examine the general effect of low temperature on the enzymatic action of both mercuripapain and S-MDA-mercuripapain. The kinetic data was cast in a similar form as presented by Whitaker and Bender (1965) and analyzed by the graphical method of Lineweaver and Burk. Values of E/v (the particular amount of enzyme added divided by the measured velocity) were plotted with respect to reciprocal values of the corresponding substrate (BAEE) concentrations, and a straight line was fitted through the experimental points by the method of least squares (Figures 21b and 22b). The kinetic rate constant, k_{cat}, was evaluated from the ordinate intercept, and the apparent Michaelis constant calculated from the slope. From preliminary studies with saturating substrate concentrations, the velocity of ester hydrolysis at 25°C was found to be directly and linearly related to the amount of soluble or insolubilized enzyme added up to 0.25 mg (Figures 21a and 22a). The average specific activities of mercuripapain and S-MDA-mercuripapain so determined were 25.4 and 17.6 µmole BAEE/min/mg, respectively.

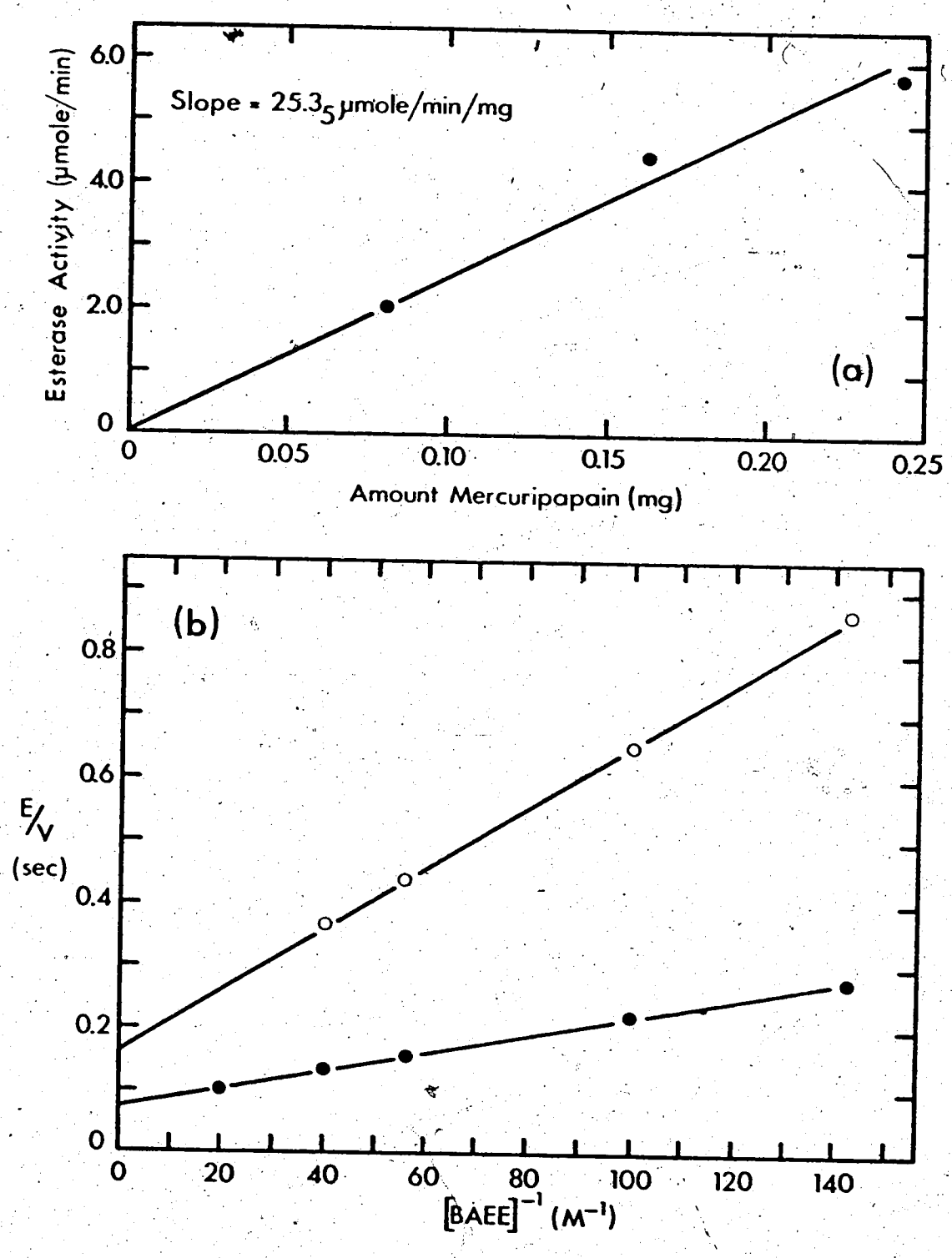

Figure 21. Kinetic study of mercuripapain. (a) The esterase activity of mercuripapain as a function of amount enzyme, measured at 25°C in 0.05 M BAEE, 5 mM cysteine, 2 mM EDTA, pH 6.5. (b) Double-reciprocal plot of inverse reduced esterase activity against inverse varying BAEE concentrations at 25°C (●—●) and 0.8°C (○—○). In addition to BAEE, the substrate solutions contained 5 mM cysteine, 2 mM EDTA, and were maintained at pH 6.5.

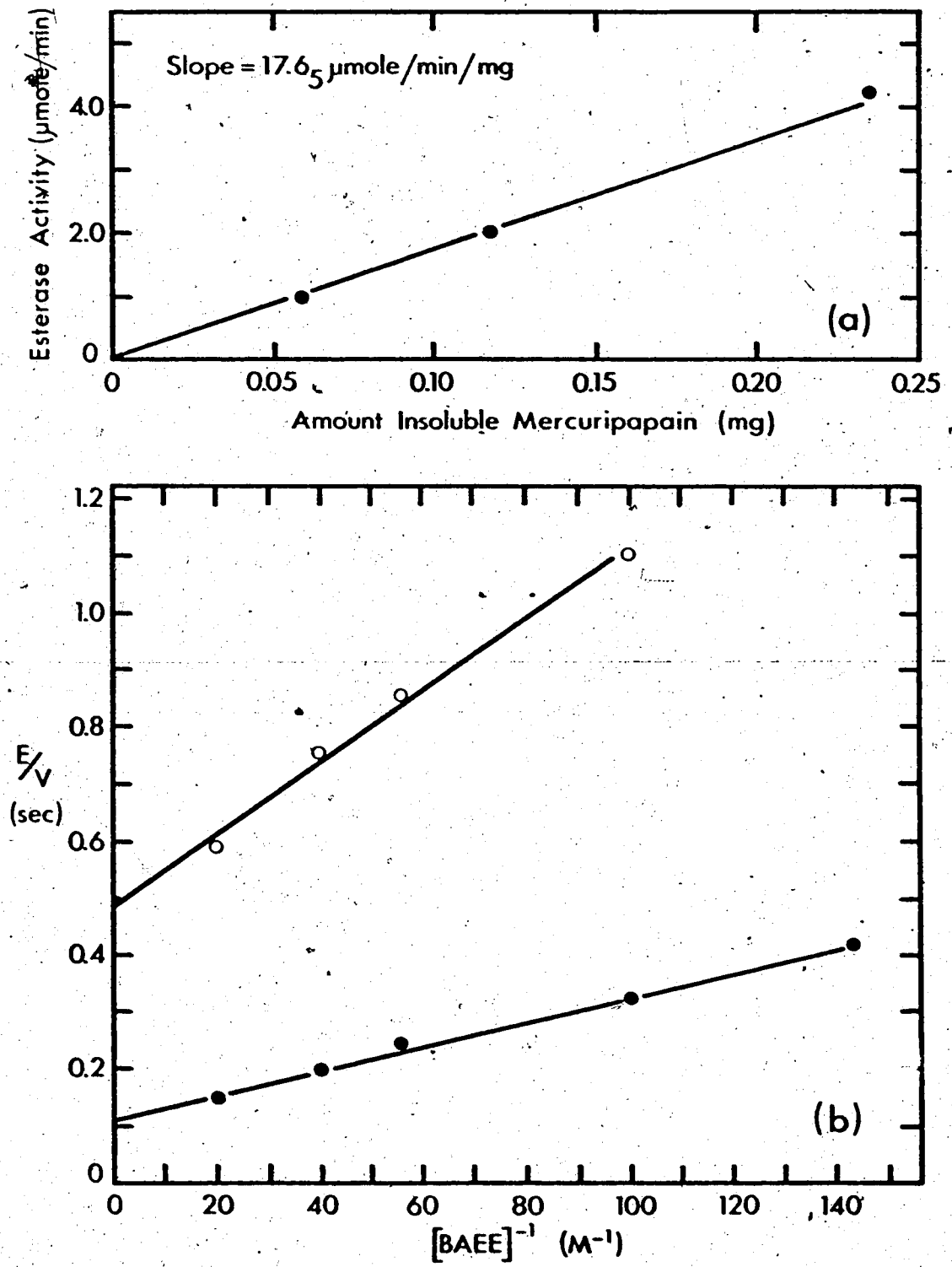

Figure 22. Kinetic study of S-MDA-mercuripapain. (a) The esterase activity of mercuripapain as a function of amount insolubilized enzyme present in varying volumes of resin-complex suspension, measured at 25°C in 0.05 M BAEE, 5 mM cysteine, 2 mM EDTA, pH 6.5. (b) Double-reciprocal plot of inverse reduced esterase activity against inverse varying BAEE concentrations at 25°C (●—●) and 0.8°C (○—○). In addition to BAEE, the substrate solutions contained 5 mM cysteine, 2 mM EDTA, and were maintained at pH 6.5.

TABLE IV

APPARENT KINETIC CONSTANTS ASSOCIATED WITH THE ESTERASE ACTIVITY OF MERCURIPAPAIN AND S-MDA-MERCURIPAPAIN*

Sample	Temperature (°C)	k_{cat} (sec^{-1})	K_{mapp} ($\times 10^2$ M)
Mercuripapain	25.0	13.2	1.87
	0.8	6.1	2.99
S-MDA-Mercuripapain	25.0	8.8	1.88
	0.8	2.1	1.31

*The kinetic data were analyzed in the manner of Whitaker and Bender (1965) – see text for details.

The associated values of the kinetic parameters derived from the double reciprocal plots are given in Table IV. Although a marked decrease in k_{cat} was observed upon immobilizing the enzyme and/or reducing the reaction temperature, essentially no change was found in the apparent Michaelis constant.

The final aspect of the insolubilized enzyme complex to be examined was that of amino acid content of its acid hydrolysates. The amino acid composition of S-MDA-mercuripapain and freshly prepared mercuripapain was determined as described in Chapter 2. Comparison was made with the amino acid composition of papain reported by Mitchel, Chaiken, and Smith (1970) to verify the assumptions associated with the calculation of the amount enzyme bound and to possibly determine which amino acid residues were covalently linked to the polymer. These results are presented in Table V. The amino acid composition of soluble mercuripapain was essentially identical with that reported for native papain — taking into account that no corrections had been applied for hydrolytic losses of threonine and serine. The coupled samples of mercuripapain also yielded similar results except for significantly lower recoveries of arginine and tyrosine residues. These missing amino acids are thought to have been covalently linked to the resin and not regenerated upon acid hydrolysis (Goldstein et al., 1970). The recovered numbers of glycine, alanine, valine, and leucine residues in analyses of S-MDA-mercuripapain were equivalent to theoretical values, lending support to the practice of using these amino acids as standards in the determination of amount protein bound.

General Method of Proteolysis. The experimental conditions and procedures routinely used for the proteolytic fragmentation of rabbit

TABLE V

AMINO ACID COMPOSITION OF PAPAIN, MERCURIPAPAIN, AND S-MDA-MERCURIPAPAIN

(moles/mole enzyme)

Amino Acid	Papain Mitchel et al. (1970)	Mercuripapain This Study*	S-MDA-Mercuripapain This Study*
Lys	10	10.6	9.1
His	2	1.7	2.1
Arg	12	12.1	4.7
Asp	19	19.6	18.3
Thr	8	7.7	7.4
Ser	13	11.3	11.3
Glu	20	21.4	19.6
Pro	10	10.8	10.3
Gly	28	29.1	28.4
Ala	14	14.6	14.3
Val	18	18.0	17.9
Ile	12	11.5	10.7
Leu	11	12.0	10.9
Tyr	19	19.3	10.8
Phe	4	3.8	4.0

*Average values of 24 hour hydrolysate results.

cardiac myosin with insolubilized mercuripapain were established based on the sedimentation velocity results of trial digests testing various ratios of enzyme to myosin and different lengths of the reaction time. Myosin samples to be digested were initially dialyzed for at least 24 hours at 4°C against a solution consisting of: 0.5 M KCl, 0.05 M phosphate, 2 mM EDTA, 5 mM cysteine, pH 7.0. The protein concentration of the dialysate was determined spectrophotometrically prior to the addition of activated S-MDA-mercuripapain (in suspension). Limited proteolysis was regularly carried out at 0°C (in a bath of crushed ice and water) for 30 minutes with an enzyme to myosin ratio of 1 to 50 (by weight of protein). The pH of the reaction was precisely maintained with pH-stat apparatus. Digestion was terminated by physically removing the water-insoluble enzyme complex via millipore filtration (5 μ pore size).

Observations of the Fragmentation Process. Representative schlieren patterns illustrating successive stages in the limited fragmentation of cardiac myosin are shown in Figure 23. The many peaks ultracentrifugally observed in the various digest mixtures were tentatively identified with reference to measured sedimentation rates and to analogous results published for the skeletal system (Lowey et al., 1969). Initial solutions of native cardiac myosin exhibited a single, hypersharp peak as seen in Figure 23a. During the early phase of the proteolytic reaction, four distinct peaks were evident in the schlieren patterns of the digestion mixtures. For example in Figure 23b, the larger, centrally located peak was found to correspond to a modified form of myosin present in significant amounts. This component presumably consisted of myosin molecules which had lost one of the two globular heads

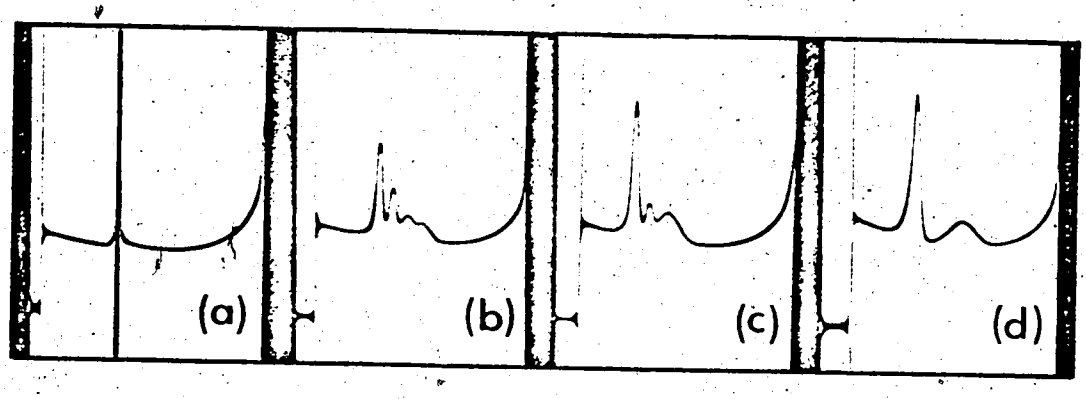

Figure 23. Schlieren patterns of trial digestion mixtures of cardiac myosin fragmented with insolubilized papain. Ultracentrifugation was carried out at 10 to 20°C and at a speed of 60 x 10^3 rpm. The solvent in each case was 0.5 M KCl, 0.05 M phosphate buffer, pH 7.0, and the bar angle 50 to 55°. Photographs of the patterns presented were taken 64 minutes after reaching speed. (a) Native cardiac myosin (5.1 mg/ml). (b) Digest of 5 minutes at 2°C using a myosin/enzyme ratio of 47:1 (w/w). (c) Digest of 20 minutes at 2°C and myosin/enzyme ratio of 93:1 (w/w). (d) Digest of 30 minutes at 4°C with a myosin/enzyme ratio of 50:1 (w/w).

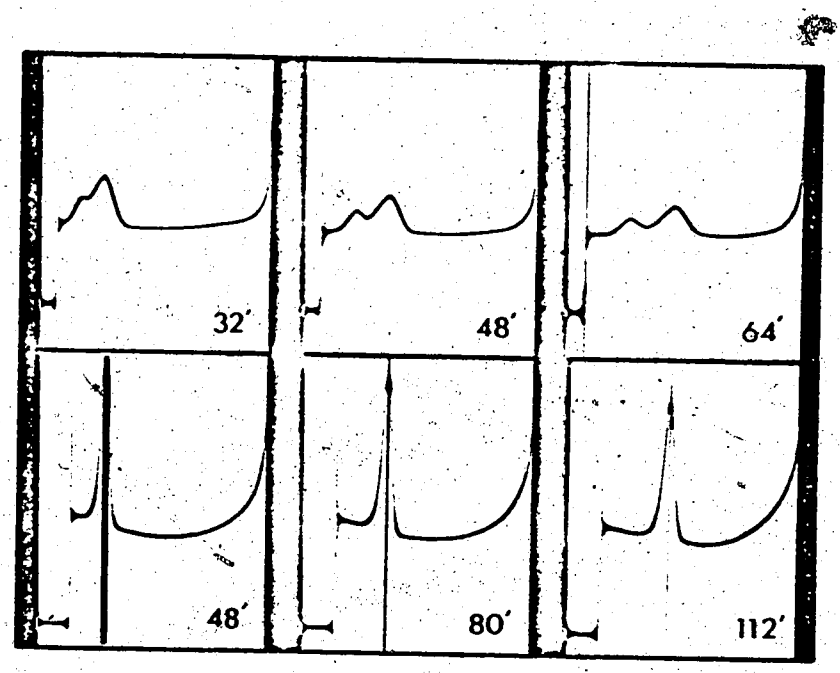

Figure 24. Schlieren patterns of the water-soluble fraction in 0.05 M KCl, 0.005 M phosphate buffer, pH 7 (upper series) and the water-insoluble fraction in 0.5 M KCl, 0.05 M phosphate buffer, pH 7 (lower series) of a routine papain digest of cardiac myosin. Sedimentation velocity runs were conducted at 20°C and 60 x 10^3 rpm, and observations made at a bar angle of 50°. Photographs were taken at the times indicated after reaching speed.

(Lowey et al., 1969). The tiny peak migrating slightly faster reflected the small proportion of native myosin remaining intact at this stage. Additionally, the trailing and leading peaks (3 and 5 S, respectively) were found to be associated with the final reaction products, analogous to the 3 and 6 S components observed in the skeletal system (Lowey et al., 1969). With further digestion, the myosin peak was no longer discerned; that corresponding to the modified form of myosin diminished in size with a concurrent increase in the relative proportions of the 3 and 5 S components (Figure 23c). Final digestion mixtures routinely exhibited only two schlieren peaks, that of the 3 and 5 S components, as illustrated in Figure 23d.

Preliminary separation of the reaction products (to simplify further delineation of the fragmentation process and to facilitate subsequent isolation of the constituent components) was accomplished by dialyzing the final millipore filtrate against either 10 volumes double-distilled, deionized water or a large volume of 0.05 M KCl, 5 mM phosphate buffer, pH 7.0, for up to 48 hours at 4°C. Material insoluble at low ionic strength precipitated during the course of dialysis (desic nated the water-insoluble fraction) and was effectively removed fron the supernatant (the water-soluble fraction) by centrifugation. Typical schlieren patterns of the water-soluble and water-insoluble fractions (the latter redissolved in 0.5 M KCl, 0.05 M phosphate buffer, pH 7.0) are presented in Figure 24. Two distinct peaks were exhibited by the water-soluble fraction (upper series in Figure 24): a leading component (5.6 S) similar to HMM-S1 and a trailing component (2.0 S) similar to HMM-S2, both produced by limited digestion of skeletal myosin with papain (Lowey et al., 1969). On the other hand, only a single peak (2.2 S)

was observed with the water-insoluble fraction (lower series in Figure 24) which from subsequent studies was established to be associated with LMM and LMM-like fragments. Comparison of the results shown in Figures 23d and 24 revealed that the 3 S component evident in the final digestion mixture included the fragments insoluble at low ionic strength plus the slower sedimenting material of the water-soluble fraction, whereas the 5 S component corresponded entirely to the faster sedimenting material of the water-soluble fraction.

Differences inherent between the components of the water-soluble and water-insoluble fractions were also reflected in their elution profiles upon gel filtration with Sephadex G-200 (Figure 25). The major proportion of the digestion products in each fraction eluted as a single peak, though at a distinctly separate eluant volume. The peak of the water-insoluble fraction occurred immediately after one void volume (Figure 25b) and that of the water-soluble fraction at approximately two void volumes (Figure 25c). Moreover, the separation of the peaks was clearly evident in the elution profile of the total digest, as can be seen in Figure 25a. These results would suggest that the proteolytic fragments insoluble at low ionic strength were relatively larger in apparent size than the water-soluble components. However, this could not be attributed solely to a greater molecular weight since the sedimentation rate of the water-insoluble material (3 S) previously observed was significantly lower than that of the major component of the water-soluble fraction (5 S). Obviously, a higher degree of asymmetry with respect to shape of the water-insoluble fragments was also a relevant factor. The third peak which was evident in the elution profile of the total digest at a position of approximately three void volumes (Figure 25a) and which

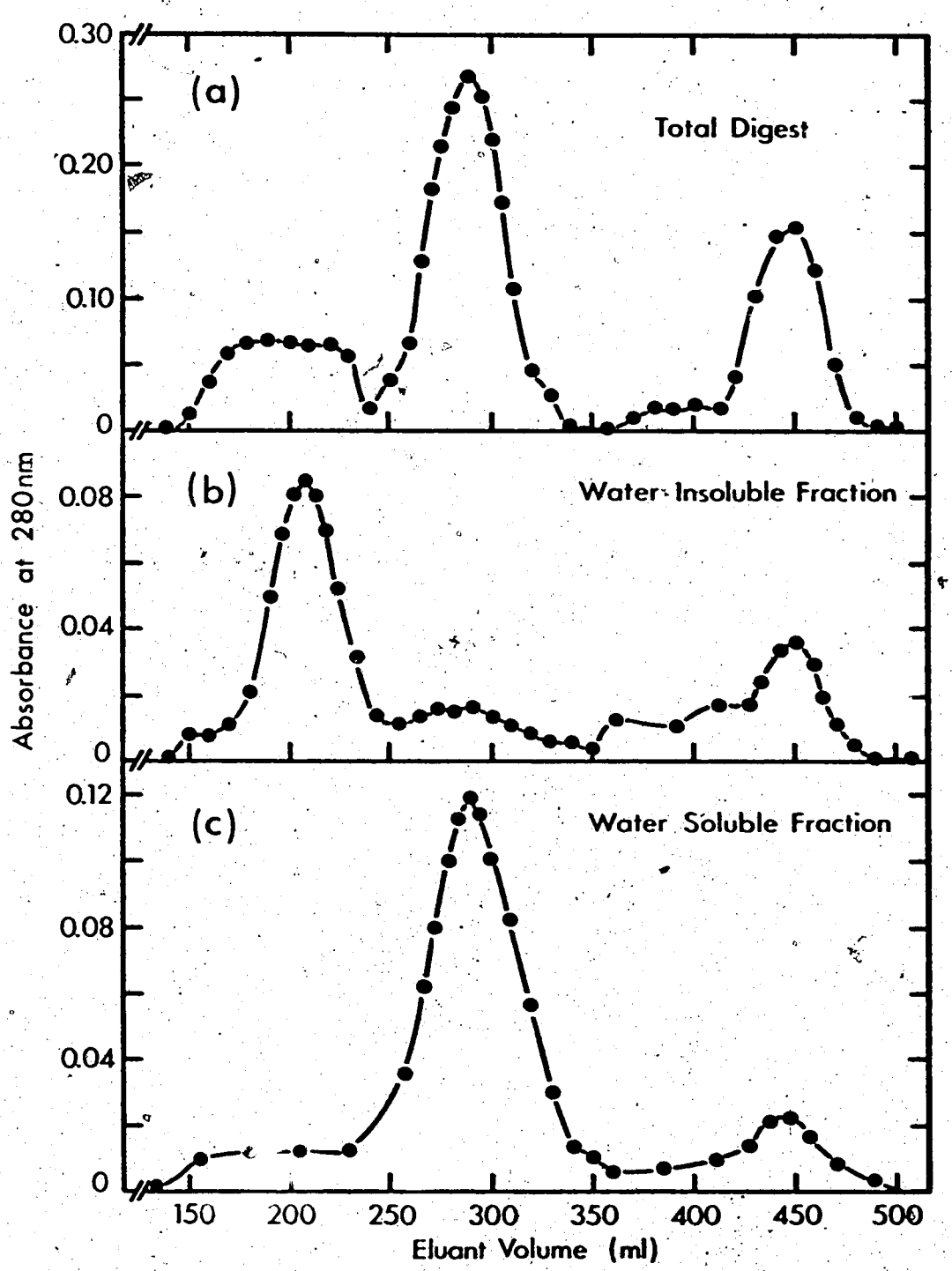

Figure 25. Elution profiles, upon gel filtration, of the water-soluble and water-insoluble fractions in relation to that of the total digest. Samples (7.6 ml total digest, 5 ml water-insoluble fraction, and 2 ml water-soluble fraction) were applied to a 2.5 x 90 cm Sephadex G-200 column (void volume ~145 ml) and eluted by ascending flow with 0.5 M KCl, 0.05 M phosphate buffer, pH 7.0, containing 1 mM DTT, at 4°C and a rate of approximately 10 ml/hr for the fractions, 5 ml/hr for the total digest. The eluant was collected over 30 minute time intervals, and the eluting protein monitored by absorbance measurements at 280 nm.

consisted of minor components of each fraction was found to correspond to small proteolytic peptides.

An experiment was conducted to delineate the order in which the water-soluble components were released. A 1.2% solution of rabbit cardiac myosin was digested with S-MDA-mercuripapain (ratio of 1 to 38 by weight of protein) in a manner as described earlier. Immediately after the addition of the enzyme complex and at 5 minute intervals thereafter, an aliquot of the digestion mixture was removed, millipore filtered (5 μ pore size), and placed to dialyze against buffer of low ionic strength to effect separation of the water-soluble and water-insoluble fractions. Precipitated material was subsequently removed by centrifugation, and the supernatant of each sample was examined in the ultracentrifuge. Illustrating the principal results derived from all the samples, representative schlieren patterns of the water-soluble fraction after 1, 15, and 30 minute digestion times are given in Figure 26. A burst of material which corresponded entirely to the faster sedimenting component was generated during the first minute of the fragmentation reaction (Figure 26a). The trailing 3 S component was initially discerned in sedimentation velocity patterns of the sample withdrawn at 5 minutes. With further digestion, the apparent quantity of the leading component appeared to remain the same or slightly decreased, whereas that of the trailing component progressively increased (Figures 26b and 26c). The latter observations were augmented by area measurements of the schlieren peaks associated with each sample. Individual patterns which had been recorded after similar times of centrifugation were enlarged ten fold, traced onto graph paper, and measured with a planimeter. The resulting values of the peak areas were corrected for magnification (but not for

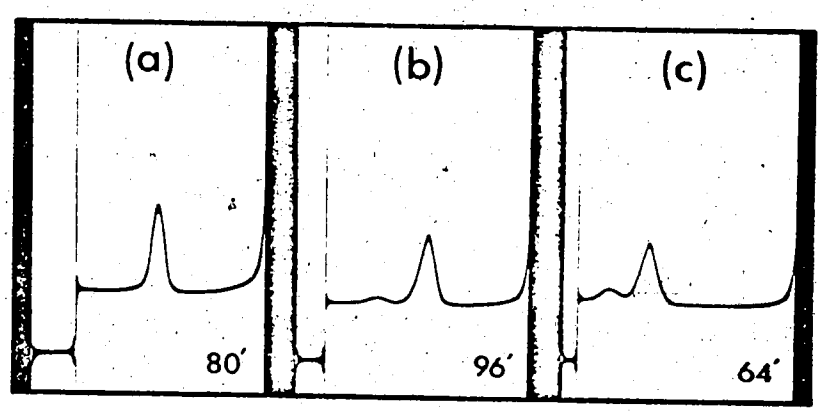

Figure 26. Schlieren patterns of the water-soluble fraction as observed in the ultracentrifuge after 1, 15, and 30 minute times of digestion (see text for full experimental details). Sedimentation velocity runs were conducted at 5°C, 60 x 10^3 rpm, and a bar angle of 60°. Photographs were taken at the times indicated after reaching speed.

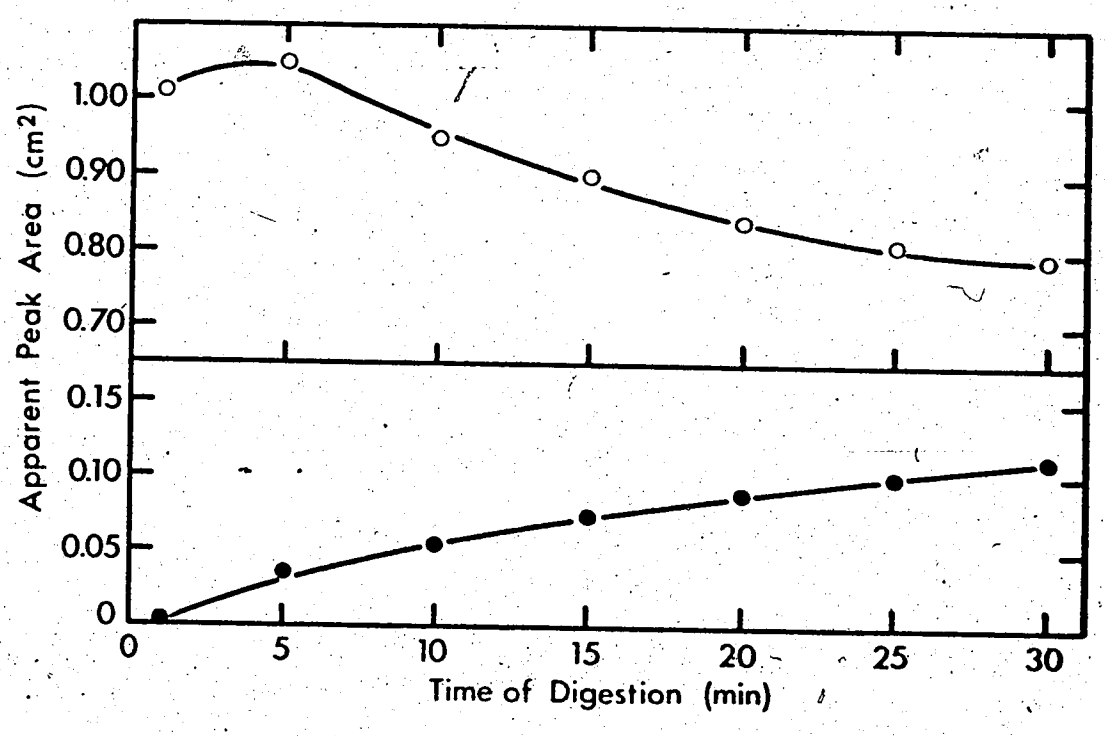

Figure 27. Apparent area of the schlieren peaks, ultracentrifugally evident in the water-soluble fraction, plotted as a function of digestion time: (○—○) faster sedimenting component, (●—●) slower sedimenting component. No corrections have been made for radial dilution or the Johnston-Ogston effect.

radial dilution or the Johnston-Ogston effect) and subsequently plotted with respect to the time at which the original samples were withdrawn from the reaction mixture. The general trends previously inferred from examination of the sedimentation velocity patterns were clearly demonstrated in this plot (presented in Figure 27). Over the course of the fragmentation process, the evident amount of the faster sedimenting component initially increased, reached an apparent maximum after approximately 5 minutes of digestion, and then gradually decreased with a progressively slowing rate (upper curve in Figure 27). Concurrently, the accumulation of the trailing component was observed to proceed in a seemingly hyperbolic manner, asymptotically approaching a maximum at the end of 30 minutes (lower curve in Figure 27).

The quantity and amino acid composition of the low molecular weight material released during the digestion process were additionally examined. The major proteolytic fragments in aliquots of the final millipore filtrate were precipitated by the addition of cold 15% trichloroacetic acid (TCA) and subsequently removed by centrifugation. The amount non-protein nitrogen present in the supernatant (an estimate of the extent of degradation) was measured by the micro-Kjeldahl method, applying the appropriate blank correction. Approximately 20% of the total protein nitrogen in untreated samples of the final digestion mixture was not precipitable with TCA. The amino acid composition of this material, determined following the procedures described in Chapter 2, was generally similar to that of native cardiac myosin except for notable differences in the yields of glutamic acid, leucine, and proline. Expressed as moles residue per 10^5 gm protein, the quantities of glutamic acid and leucine present in the small proteolytic peptides were lower than in

myosin by 33 and 21 residues, respectively, while the proline content was greater by 14 residues. The protein concentration of the supernatant was evaluated on the basis of micro-Kjeldahl analysis using a value of 6.2 for the nitrogen factor (Lowey et al., 1969).

Kinetic Analysis. Kinetic studies of the limited proteolysis of cardiac myosin with S-MDA-mercuripapain were carried out employing pH-stat techniques and the general reaction conditions previously described. Corrections for the uptake of hydrogen ions by the α-amino groups released upon the hydrolysis of peptide bonds at pH 7.0 were applied with respect to the recorded amount of titrant expended during the reaction. A value of 7.85 was used for the mean pK of the liberated α-amino groups (Mihalyi and Harrington, 1959). The final results of a representative experiment are depicted in Figure 28. Adjusted values of the amount of base consumed, derived from a continuous pH-stat trace at a number of discrete points and expressed as moles hydroxide ions per 10^5 gm myosin initially present, were plotted against time. A smooth curve was fitted through the experimental points by the method of polynomial least squares (the line drawn in Figure 28). The instantaneous rate of the reaction associated with each point was estimated by evaluating the corresponding first derivative of the polynomial curve. The kinetic data were graphically analyzed in terms of the following relationship derived from a combination of the first-order rate equation with its integrated form (Leonis, 1948; Mihalyi and Harrington, 1959):

$$\ln \frac{dA}{dt} = \ln (-kA_o) - kt \quad .$$

Here dA/dt is the rate of peptide bond hydrolysis at a reaction time of

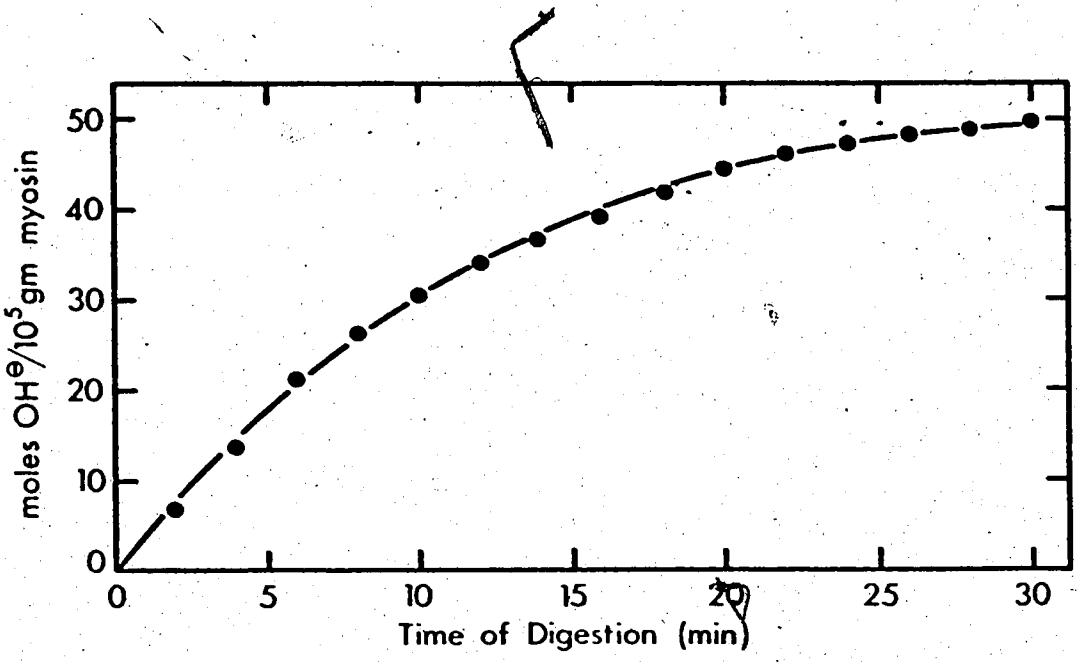

Figure 28. Uptake of hydroxide ions during the proteolytic digestion of cardiac myosin with insolubilized papain. Digestion was conducted at 1°C and pH 7.0 using a myosin/enzyme ratio of 41:1 (w/w). The points plotted represent the results at 2 minute intervals of a continuous pH-stat record. Corrections have been applied for the incorporation of hydrogen ions by the liberated α-amino groups.

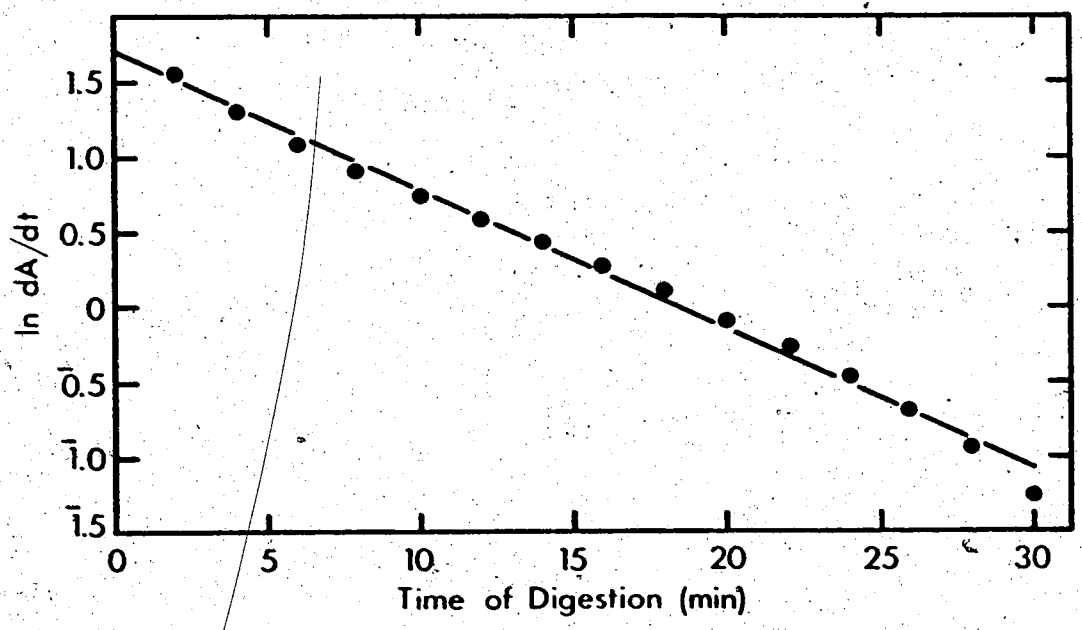

Figure 29. Graphical analysis of the adjusted pH-stat data derived from papain digestion of cardiac myosin as presented in Figure 28. The natural logarithms of the point rates of digestion were plotted with respect to time. See text for theoretical details.

t, A_o the total concentration of bonds in a given reaction class, and k the apparent first-order rate constant. The natural logarithms of the point rates of digestion were plotted with respect to time. The apparent rate constant, k, was determined from the slope of a straight line best fitting the experimental points, and A_o was calculated from the ordinate intercept upon extrapolation of the line to zero time. The resultant graph from such analysis of the data summarized in Figure 28 is presented in Figure 29. The estimated values of A_o and k were 60 bonds/10^5 gm myosin and 0.09 min^{-1}, respectively. As was observed in similar analyses of repeated kinetic experiments, the plot of ln dA/dt versus time was essentially a single straight line. Calculated from four sets of results, the average values of A_o and the apparent first-order rate constant were equal to 62 ± 14 bonds cleaved/10^5 gm myosin, and 0.08 ± 0.03 min^{-1}, respectively.

Discussion

The combination of S-MDA resin and mercuripapain proved to be satisfactory in the limited fragmentation of rabbit cardiac myosin. Not only were the protein binding capacity of the resin and the recovery and stability of the enzymatic activity of the immobilized derivative relatively high (at least as compared to papain complexes with PAB-cellulose) but also preparations of S-MDA-mercuripapain were reproducible. A major factor contributing to this reproducibility was the use of fresh preparations of mercuripapain, which in themselves were found to be consistent based on ultraviolet absorption, sedimentation velocity, and esterase activity measurements. The results of the ancillary studies conducted with respect to the S-MDA resin and S-MDA-mercuripapain agree generally

with those of corresponding studies reported by Goldstein et al. (1970). In addition, the apparent Michaelis constant and k_{cat} of mercuripapain determined at 25°C are similar to documented values (Smith and Parker, 1958; Whitaker and Bender, 1965; Sluyterman and De Graaf, 1969).

As was seen from the kinetic analysis, the reduction in the rate of esterolysis upon immobilization of mercuripapain was reflected by a decrease in the value of k_{cat}, though essentially without change in the value of K_{mapp} (Table IV). These results suggest that the amino acids which form the active site and bind the substrate were not directly or significantly involved with the matrix, and that the observed loss of activity was probably due to steric hindrance of the resin network. The latter inference was similarly made by Goldstein et al. (1970) with respect to S-MDA derivatives of trypsin and subtilopeptidase A, and by Axén and Ernback (1971) regarding Sephadex and agarose conjugates of trypsin, chymotrypsin, and papain. Moreover, the parallelism of the relative decrease in the values of k_{cat} and the specific esterase activity would tend to reinforce this hypothesis.

The apparent absence of 7 arginine and 8 tyrosine residues in acid hydrolysates of the enzyme complex upon analysis (Table V) implicate these amino acids in the formation of the covalent links with diazotized S-MDA resin. (Goldstein et al. (1970) believe 2 lysine residues may additionally be involved). Previous studies have shown that these amino acids can covalently react with diazonium salts of low molecular weight, and that acid hydrolysis does not regenerate the free amino acids from monoazo and bisazo derivatives (Howard and Wild, 1957; Sokolovsky and Vallee, 1967). Furthermore, examination of the three-dimensional structure of the papain molecule (Drenth et al., 1971) reveals that several

tyrosine, arginine, and lysine groups are evidently exposed to the solvent and thus available for reaction.

The preliminary results of the limited proteolysis of cardiac myosin with papain at 0°C are essentially analogous with those of the skeletal system (Lowey et al., 1969), although slightly greater enzyme to mysoin ratios were employed in the present study. In terms of the ultracentrifugal observations, the major aspects of the fragmentation process are summarized as follows. The 5 S component of the water-soluble fraction and a modified form of myosin are initially produced. With further digestion, the apparent quantity of the latter progressively decreases with a concurrent accumulation of the 3 S components of both the water-soluble and water-insoluble fractions. The 5 S subfragment is released prior to the 3 S, water-soluble species. Only the 3 and 5 S material and a small amount of peptide fragments are evident in the final digestion mixtures.

From kinetic analysis, the proteolytic process was found to be characterized by a single first-order reaction. The average values of A_o and k, 290 bonds cleaved per mole of myosin (taking the molecular weight to be 4.7×10^5 gm/mole) and 0.08 min^{-1}, respectively, agree closely with values determined for skeletal myosin digested with papain (Lowey et al., 1969). Previous kinetic investigations of the trypsin-catalyzed peptide bond cleavage of skeletal myosin have established that the overall process follows the sum of two parallel first-order reactions of markedly differing rates (Mihalyi and Harrington, 1959; Segal et al., 1967). Although a detailed comparison of the two enzyme systems cannot be validly made since each involved different enzyme forms, substrate to enzyme ratios, and experimental conditions of digestion, two general

features are evidently similar. One, the value of the first-order rate constant derived with respect to papain corresponds to that of the fast reaction observed in tryptic digestion, though the number of bonds hydrolyzed by papain is appreciably greater. Two, the release of the subfragments is associated with these fast reactions. Furthermore, the results of the present study do not preclude the existence of a second, slower rate of peptide bond cleavage with papain because the kinetic data, which was gathered during routine fragmentation experiments, does not temporally extend past 30 minutes, a time well before manifestation of the slower reaction in, for example, tryptic digestion (Segal et al., 1967).

The major differences found between the amino acid compositions of the trichloroacetic acid-soluble peptides and native myosin were similarly noted by Middlebrook (1959), Segal et al. (1967), and Lowey et al. (1969) with respect to tryptic and papain peptides of skeletal myosin. The release of low molecular weight material rich in proline during the limited fragmentation of cardiac myosin is consistent with the interpretation that proteolysis occurs in regions of disordered secondary structure (Mihalyi and Harrington, 1959). However, the different nature of the subfragments initially produced by trypsin and papain must reflect the particular specificities of the two enzymes and thus, indirectly, the local three-dimensional structure and primary sequence of the mysoin molecule.

In conjunction with the findings that large fragments were released at an early stage of digestion after few bonds had been cleaved, the rather large value of A_o obtained would indicate that a considerable

number of secondary peptide bonds were hydrolyzed by papain. The apparent degradation of the 5 S component initially produced (Figure 27) is reminiscent of the decay in the concentration of HMM-S1 observed by Mueller (1965) during tryptic digestion of rabbit skeletal heavy meromyosin. In addition, the loss of non-protein nitrogen was approximately twice that previously reported for digestion of skeletal myosin with insolubilized papain (Kominz et al., 1965). This degree of degradation was a consequence of adopting a high enzyme to myosin ratio and a lengthy time of digestion. Both the latter conditions were necessary, however, to obtain sizable yields of the more slowly released fragments for subsequent purification and study. In this manner, all the major subfragments were derived from a single preparation of cardiac myosin.

CHAPTER 5

THE PROTEOLYTIC SUBFRAGMENTS

Limited proteolysis of rabbit cardiac myosin was carried out with S-MDA-mercuripapain as described in the previous chapter. The millipore filtrate of final digestion mixtures was routinely dialyzed against low ionic strength buffer to effect separation of the water-soluble and water-insoluble components. Procedures for the isolation and purification of the major fragments and the experimental results of associated ultraviolet optical, amino acid, enzymatic, and physicochemical studies are presented and discussed in this chapter. Based on the similarity of the cardiac subfragments to those derived from limited digestion of skeletal myosin, the purified 3 and 5 S components of the water-soluble fraction are tentatively designated HMM-S2 and HMM-S1, respectively, and the purified 3 S component of the water-insoluble fraction LMM-A.

Methods of Isolation and Purification

LMM-A. Light meromyosin and like fragments were isolated from the water-insoluble fraction and purified using essentially the method of Szent-Györgyi, Cohen, and Philpott (1960). The water-insoluble fraction was dissolved in a small volume of 0.5 M KCl, 0.05 M phosphate buffer, pH 7.0, and reprecipitated by dialysis at 4°C against a liter of 0.05 M KCl, 0.005 M phosphate buffer, pH 7.0. The precipitate was collected by centrifugation for 30 minutes at 2°C and 20 x 10^3 rpm and

redissolved in a minimal volume of 0.6 M KCl, pH 7. Three volumes of 95% ethanol were then added to this solution with gentle mixing, and the alcoholic suspension was allowed to stand for 3 hours at room temperature (23°C). The resulting coalescent precipitate was collected by centrifugation, dispersed in 0.6 M KCl, 0.01 M phosphate buffer, pH 7.0, and dialyzed for at least 12 hours at 4°C against 12 volumes of the same buffer to reduce the ethanol concentration. The dialysate was clarified of insoluble, denatured protein by high-speed centrifugation, and LMM-A precipitated from the supernatant by dialysis at 4°C against 12 volumes of 0.01 M phosphate buffer maintained at pH 6.5. The precipitate was collected by centrifugation and redissolved in 0.6 M KCl, 0.01 M phosphate buffer, pH 7.0. Complete solution was effected by overnight dialysis at 4°C against the same buffer. LMM-A was reprecipitated once at pH 6.5, and the final material dissolved in a minimal volume of 0.5 M KCl, 0.05 M phosphate buffer, pH 7.0, and dialyzed at 4°C against the same buffer prior to experimental examination. The yield of LMM-A routinely obtained was approximately 5 mg per 100 mg cardiac myosin initially digested.

HMM-S1. Subfragment 1 was effectively isolated and purified in a single step upon fractionation of the fragments soluble at low ionic strength by gel filtration. The volume of the water-soluble fraction was reduced to approximately 8 ml under positive nitrogen pressure of 40 psi in an Amicon ultrafiltration cell fitted with a Diaflo UM-10 membrane (Scientific Systems Division, Amicon Corporation, Lexington, Massachusetts). The resulting concentrate was applied to a 2.5 x 85 cm column of Sephadex G-200 pre-equilibrated with the elution solvent. The column was developed by ascending flow with 0.5 M KCl, 0.05 M phosphate

buffer, pH 7.0, at a rate of 8 to 10 ml per hour, and fractions of 4 to 5 ml were collected. The concentrative and chromatographic procedures were conducted at 4°C. The elution results were monitored spectrophotometrically via ultraviolet absorption measurements at 280 nm. In addition, the ATPase activity of selected fractions was determined at 25°C employing pH-stat techniques (described in Chapter 2) with substrate solutions consisting of 0.25 M KCl, 5 mM ATP, 10 mM $CaCl_2$, pH 7.2. A representative elution pattern of the chromatographic separation of the water-soluble fragments thus obtained is shown in Figure 30. The fractions corresponding to the major peak (associated with the ATPase activity) were pooled and clarified of particulate matter by millipore filtration (5 μ pore size), and the volume reduced to approximately 5 ml under positive pressure with Amicon apparatus (40 psi, Diaflo UM-10 membrane). The resulting solution of subfragment 1 was dialyzed at 4°C against 0.5 M KCl, 0.05 M phosphate buffer, pH 7.0, with or without 1 mM DTT depending on the molecular parameter to be subsequently studied. Approximately 20 mg of purified HMM-S1 were generally derived from the proteolytic degradation of 100 mg cardiac myosin.

HMM-S2. Subfragment 2 was recovered from the material initially excluded upon gel filtration of the water-soluble fragments by a method very similar to that for the isolation and purification of LMM-A, incorporating modifications proposed by Lowey et al. (1969). The eluant fractions corresponding to the first small peak (see, for example, Figure 30) were pooled, and the total volume reduced to approximately 5 ml at 4°C under positive pressure with the Amicon apparatus (40 psi, Diaflo UM-10 membrane). Three volumes of 95% ethanol were then added to the concentrate with gentle mixing, and the alcoholic suspension was allowed

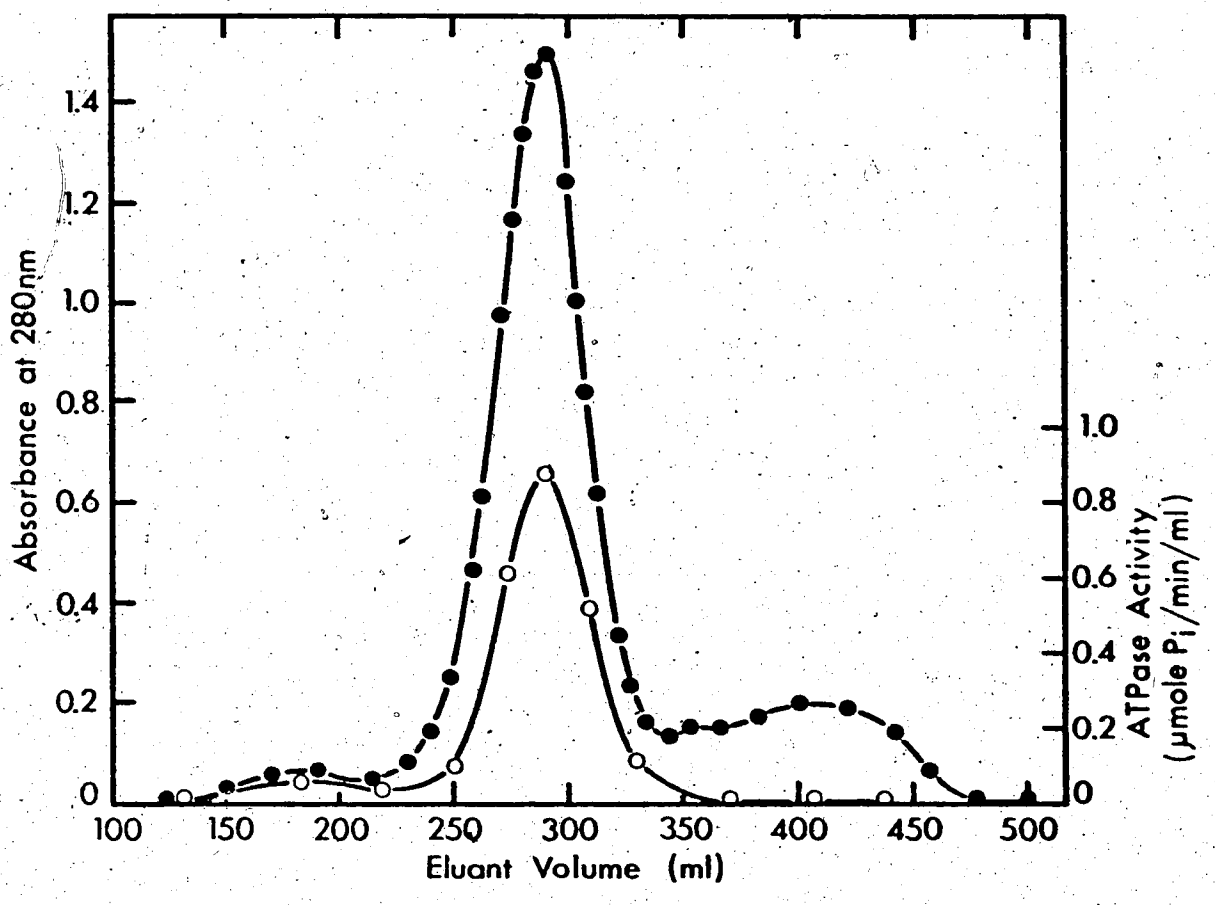

Figure 30. Elution profile of the chromatographic separation of the water-soluble subfragments by gel filtration. The water-soluble fraction, concentrated to 8 ml, was applied to a 2.5 x 85 cm Sephadex G-200 column (void volume ~140 ml) and eluted by ascending flow with 0.5 M KCl, 0.05 M phosphate buffer, pH 7.0, at 4°C and a rate of 9 ml/hr. Fractions of 4.5 ml were collected, and the eluting protein was monitored by absorbance measurements at 280 nm (●—●). The ATPase activity (○—○) of selected fractions was determined at 25°C and pH 7.2 in substrate solutions of 0.25 M KCl, 5 mM ATP, 10 mM $CaCl_2$ employing pH-stat techniques.

to stand for 3 hours at room temperature (23°C). The resulting precipitate was collected by centrifugation for 30 minutes at 2°C and 2.0×10^4 rpm, resuspended in 0.5 M KCl at neutral pH, and dialyzed for at least 12 hours at 4°C against 12 volumes of the same solvent to reduce the concentration of the ethanol. Insoluble, denatured protein was removed from the dialysate by high-speed centrifugation. Subfragment 2 was subsequently precipitated from the supernatant by dialysis at 4°C against 10 volumes of 0.01 M phosphate buffer maintained at pH 4.5. The precipitate was collected by centrifugation and redissolved in 0.5 M KCl, 0.01 M phosphate buffer, pH 7.0. Precipitation of subfragment 2 at pH 4.5 was repeated once, and the final material was dissolved in a minimal volume of 0.5 M KCl, 0.05 M phosphate buffer, pH 7.0 and dialyzed at 4°C against the same buffer prior to analysis. The experimental recovery of HMM-S2 was approximately 1 mg per 100 mg cardiac myosin fragmented.

Results

Final solutions of the purified fragments exhibited single, symmetrical schlieren peaks in the ultracentrifuge upon examination of molecular homogeneity. (Representative patterns are shown later in conjunction with the results of the sedimentation velocity experiments). On this basis the preparations were deemed satisfactory and suitable for further investigation.

With respect to the isolation of HMM-S1, a single chromatographic operation was usually effective in yielding homogeneous material. However, in instances where a large volume of concentrate had been applied to the Sephadex column, the resulting solutions of subfragment 1 were frequently contaminated with HMM-S2. Care was thus taken not to

overload the column, and, in addition, the leading cut of the eluted fractions was routinely made toward the center of the major peak, far removed from the material that was initially excluded.

From area measurements of the chromatographic peaks associated with the water-soluble components (Figure 30), HMM-S1 was found to constitute approximately 75% of the water-soluble fraction. This is of the same order of magnitude as was observed earlier in schlieren patterns of the water-soluble fraction (Figures 26 and 27). The area of the peak corresponding to subfragment 1 in the elution diagrams of whole digestion mixtures (for example, Figure 25) ranged from 30 to 50% of the total. The small, third peak evident in the elution profile of the water-soluble fraction and comprising 15 to 20% of the total area (Figure 30) was ascribed to low molecular weight peptide fragments: the material of this peak was excluded late at three or more void volumes and not precipitated with 15% TCA.

Ultraviolet Optical Properties. The ultraviolet absorption spectra of HMM-S1, HMM-S2, and LMM-A, as determined in 0.5 M KCl, 0.05 M phosphate buffer, pH 7.0, are illustrated in Figure 31. The curves were typical of ultraviolet spectra of most proteins. Maximum absorbance was observed at 280 nm for subfragment 1 and at 278 nm for both subfragment 2 and LMM-A. The extinction coefficients of the purified fragments were determined at the corresponding wavelength of maximum absorbance, in the same solvent system, using several preparations. Since, however, only a small number of trials were performed, the results of each set were not averaged, but rather the values of absorbance were plotted with respect to the corresponding values of protein concentration. A straight line

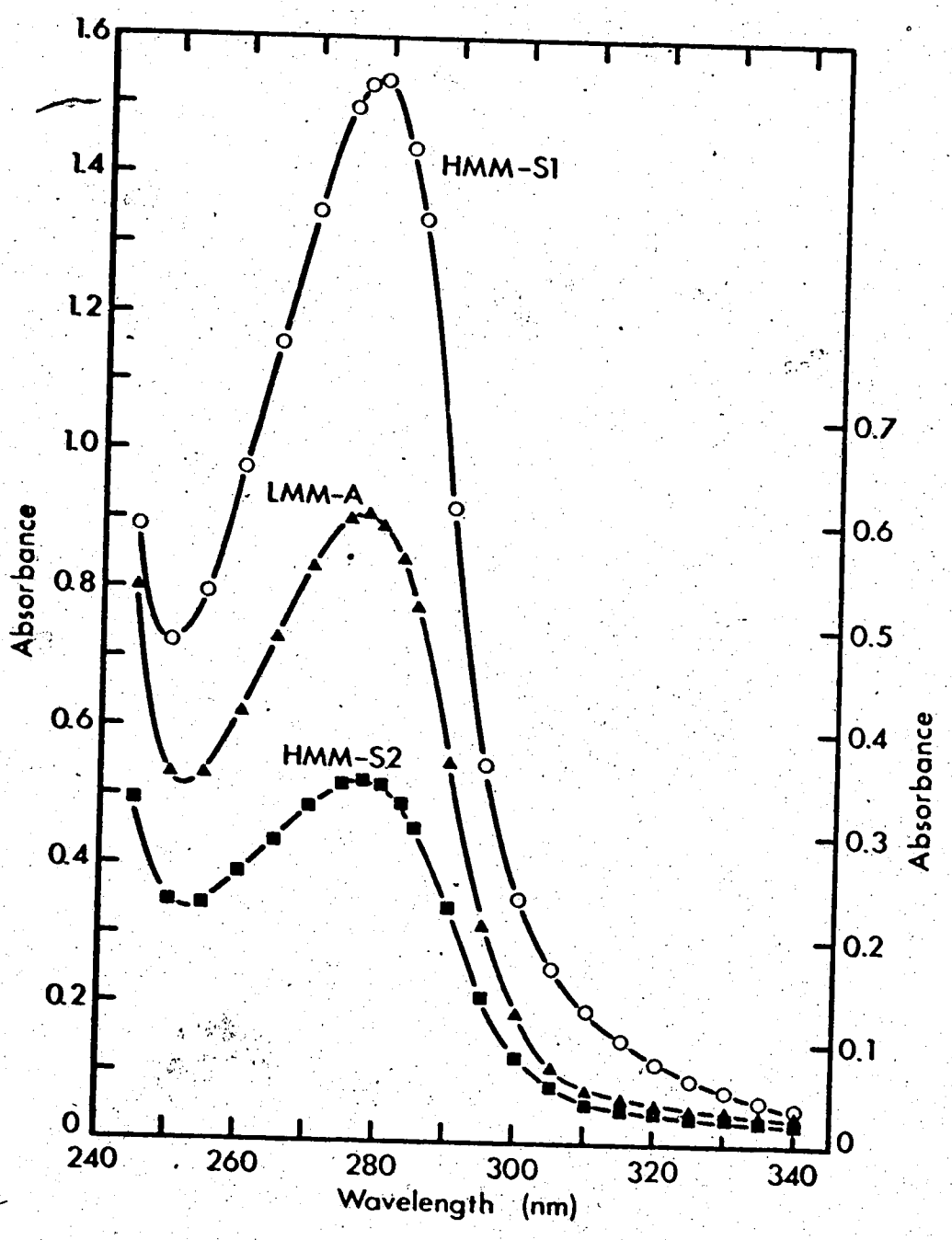

Figure 31. Ultraviolet absorption spectra of HMM-S1 (circles, 1.7 mg/ml), LMM-A (triangles, 2.1 mg/ml), and HMM-S2 (squares, 3.4 mg/ml) in 0.5 M KCl, 0.05 M phosphate buffer, pH 7.0, as determined using a 1 cm path length cuvette and dialysate as the blank. The spectra of LMM-A and HMM-S2 are plotted with respect to the right ordinate scale.

was fitted through the origin and the experimental points, and an "average" extinction coefficient was evaluated from the slope. Values of the protein concentration were standardized by two methods: refractometry and micro-Kjeldahl (using a nitrogen factor of 6.2 for subfragments 1 and 2 (Lowey et al., 1969) and 6.42 for LMM-A (Szent-Györgyi, Cohen, and Philpott, 1960)). The combined results of each data set are graphically summarized in Figure 32. The value of $E^{1\%}_{1\ cm}$ thus determined for HMM-S1, HMM-S2, and LMM-A was 8.20, 0.93, and 2.66, respectively. The apparent linearity of the experimental data in each plot would indicate that the ultraviolet absorption of the purified subfragments adhered to Beer's law (at least up to the highest concentration investigated).

The ultraviolet circular dichroism (CD) of HMM-S1, HMM-S2, and LMM-A was measured in 0.5 M KCl, 0.05 M phosphate buffer, pH 7.0, over the wavelength range 250 to 200 nm. Representative CD spectra are shown in Figure 33. Solutions of the three purified fragments exhibited negative dichroic bands at 221 and 209 nm, though of markedly different intensities. Respective mean residue ellipticity values for HMM-S1 were $^{-}1.47 \times 10^4$ and $^{-}1.35 \times 10^4$ degree·cm^2/dmole; for HMM-S2, $^{-}3.20 \times 10^4$ and $^{-}2.95 \times 10^4$ degree·cm^2/dmole; and for LMM-A, $^{-}4.31 \times 10^4$ and $^{-}3.92 \times 10^4$ degree·cm^2/dmole. In addition, positive trends were evident at the lower wavelengths examined with the crossover points of the spectra occurring at approximately 201 nm. The helical content of each subfragment was not directly estimated from their CD data due to the disparity in reported ellipticity values of standard, helical polyamino acids (Oikawa et al., 1968).

Amino Acid Composition. The amino acid composition of HMM-S1,

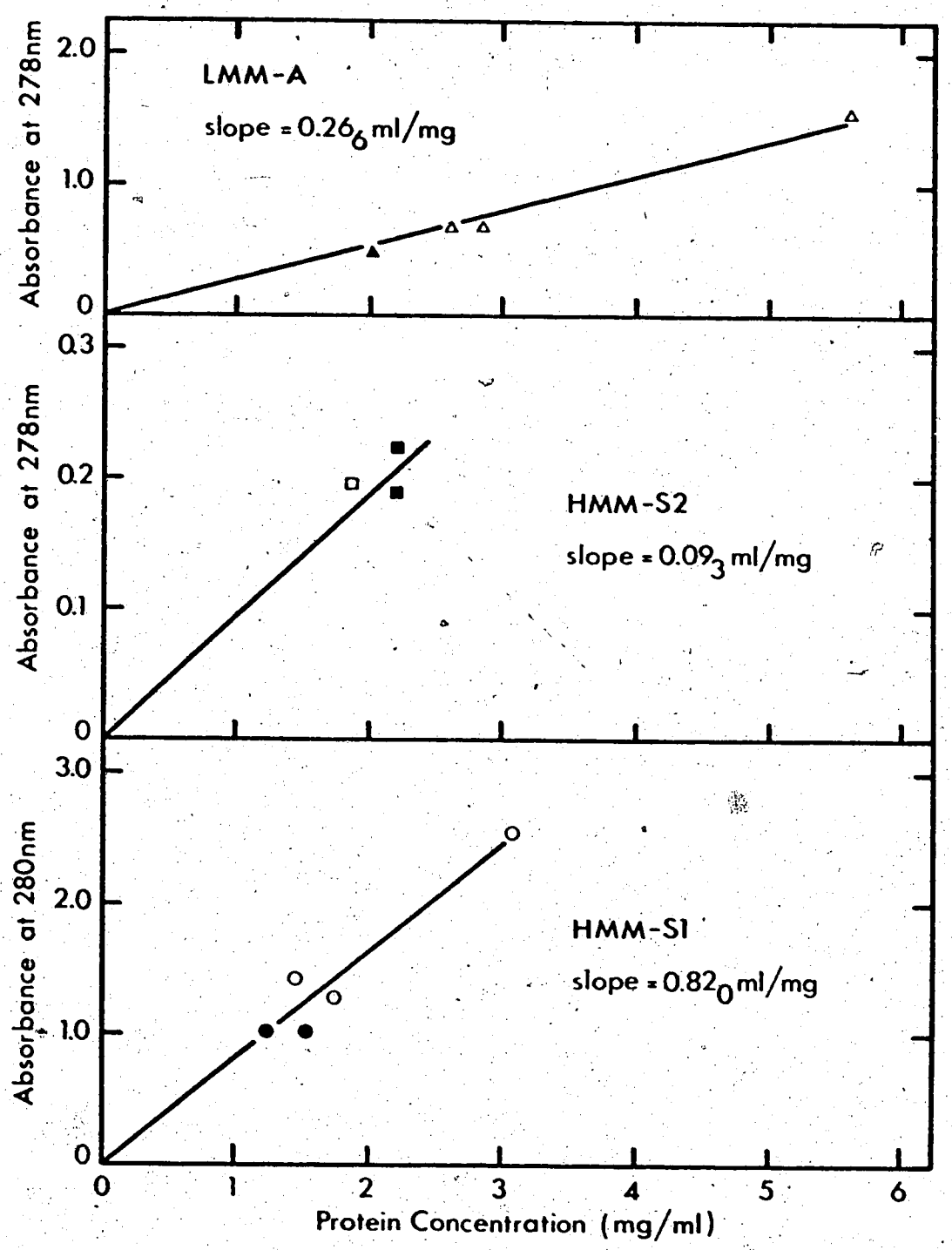

Figure 32. Graphical estimation of the extinction coefficients for LMM-A, HMM-S2, and HMM-S1 in 0.5 M KCl, 0.05 M phosphate buffer, pH 7.0. The UV absorbance was measured using a 1 cm path length cuvette and dialysate as the blank. Protein concentration was standardized by micro-Kjeldahl analysis (open point styles) and by fringe count of c_o interference patterns (closed point styles).

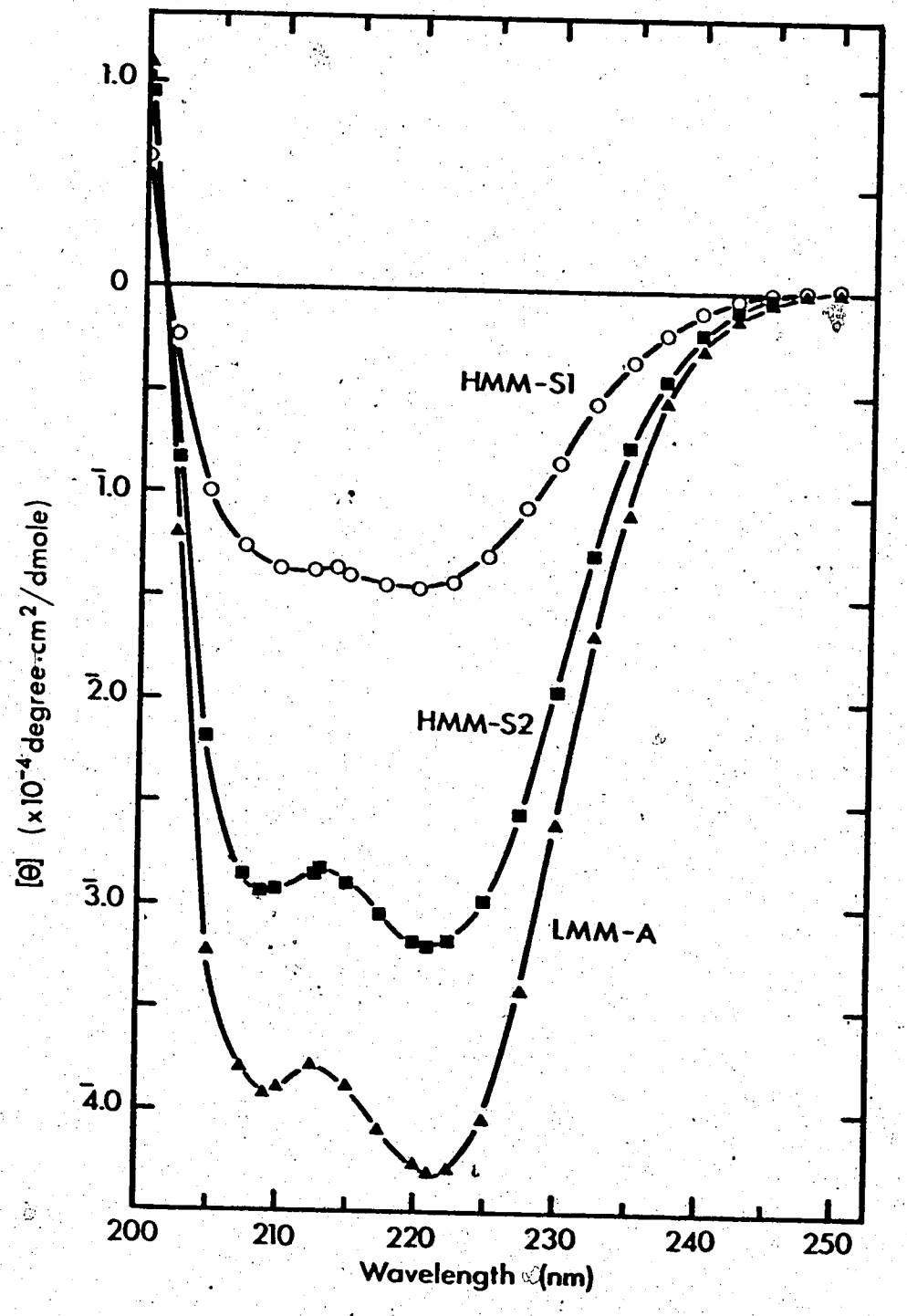

Figure 33. Ultraviolet circular dichroic spectra of HMM-S1 (O—O, 0.43 mg/ml), HMM-S2 (■—■, 0.35 mg/ml), and LMM-A (▲—▲, 0.56 mg/ml) in 0.5 M KCl, 0.05 M phosphate buffer, pH 7.0, as determined at 13.5°C using a 0.0502 cm path length optical cell and dialysate for the solvent base line.

HMM-S2, and LMM-A was determined as described in Chapter 2. Corrected values of the labile residues, threonine, serine, methionine, and tyrosine, were obtained by linear extrapolation to zero hydrolysis time. The analytic values of the 24-, 48-, and 72-hour hydrolysates were averaged for the residues valine, isoleucine, and leucine of HMM-S1 and LMM-A, and for the remaining amino acids of HMM-S2. Average values of the 12-, 24-, 48-, and 72-hour hydrolysate data were calculated for the remaining amino acids of subfragment 1 and LMM-A. The final results, expressed as moles per 10^5 gm protein, are presented in Table VI. The amino acid composition of native cardiac myosin is included in the table for comparison. The general distribution of the amino acids recovered from native myosin was found to be reflected in the analyses of the proteolytic fragments. For example, the average values of lysine, aspartic acid, glutamic acid, alanine, and leucine were relatively high, whereas those of histidine, cysteic acid, and methionine were proportionally low. However, notable differences were observed. LMM-A and HMM-S2 did not contain proline; its level in HMM-S1 was elevated relative to that of myosin. The contents of glutamic acid, alanine, and leucine in LMM-A and subfragment 2 were exceptionally high, while those of tyrosine and phenylalanine were very low. In overall consideration, the amino acid composition of HMM-S2 more closely resembled that of LMM-A than that of either myosin or subfragment 1.

Adenosinetriphosphatase Activity. Of the three purified fragments, only HMM-S1 displayed adenosinetriphosphatase (ATPase) activity. Measurements were conducted at 25°C and pH 8.0 with substrate solutions of 0.4 M KCl, 5 mM ATP using pH-stat methods. The specific activity was expressed as μmoles P_i released per minute per mg protein even though

TABLE VI

AMINO ACID COMPOSITION OF CARDIAC MYOSIN, LMM-A, AND SUBFRAGMENTS 1 AND 2

(moles/10^5 gm protein)

Amino Acid	Myosin	HMM-S1	LMM-A	HMM-S2
Lys	85	83	108	93
His	15	20	13.5	9
Arg	47.5	46	58	44
Asp	82	101	90	82
Thr	42	49	36	38
Ser	40	41	47	47
Glu	163	128	242	215
Pro	23	42	0	0
Gly	39	60	15.5	18
Ala	76	74	90	82
Cya	6.8	11.3	8.7	8.1
Val	40	46	32	28
Met	22.5	29.5	18.5	13
Ile	38	52	27	21
Leu	92	87	122	98.5
Tyr	18	34	6	4
Phe	29	52	7	9

inorganic phosphate was not directly analyzed. The effect of calcium ions on the rate of ATP hydrolysis was examined over a $CaCl_2$ concentration range of 0 to 20 mM, and the results of these experiments, as well as those previously obtained with cardiac myosin, are plotted in Figure 34. As was observed with myosin, the ATPase activity of HMM-S1 was activated in the presence of calcium ions. However, activation was more pronounced with subfragment 1. For example, at 10 mM $CaCl_2$ where the activity of cardiac myosin had reached an apparent maximum of 0.23_5 μmole P_i/min/mg, the activity of HMM-S1 was approximately three times greater equal to 0.90 μmole P_i/min/mg. Moreover, its specific activity was found to increase further to a value of 1.14 μmole P_i/min/mg and level off at a $CaCl_2$ concentration of 20 mM.

Viscosity. Viscometric analyses of LMM-A and subfragments 1 and 2 (in 0.5 M KCl. 0.05 M phosphate buffer, pH 7.0 — the solvent for HMM-S1 additionally contained 1 mM DTT) were carried out following the method outlined in Chapter 2. The protein concentration of the diluted samples was determined spectrophotometrically prior to conducting the viscosity measurements. Graphs of reduced viscosity versus concentration were found to be linear over the concentration range examined, and a straight line was fitted through the experimental points of each data set by the method of least squares (Figure 35). The viscosity of LMM-A exhibited a marked, positive concentration dependence; the slope of the straight line was equal to 4.87 $d\ell^2/gm^2$. In contrast, the slope evident in the data of subfragment 2 was only slightly positive (0.30 $d\ell^2/gm^2$) and that of subfragment 1 was close to zero (0.003_6 $d\ell^2/gm^2$). The values of the intrinsic viscosity and Huggins constant, derived from the results of the least squares analyses, were, respectively, 2.37 [illegible] and

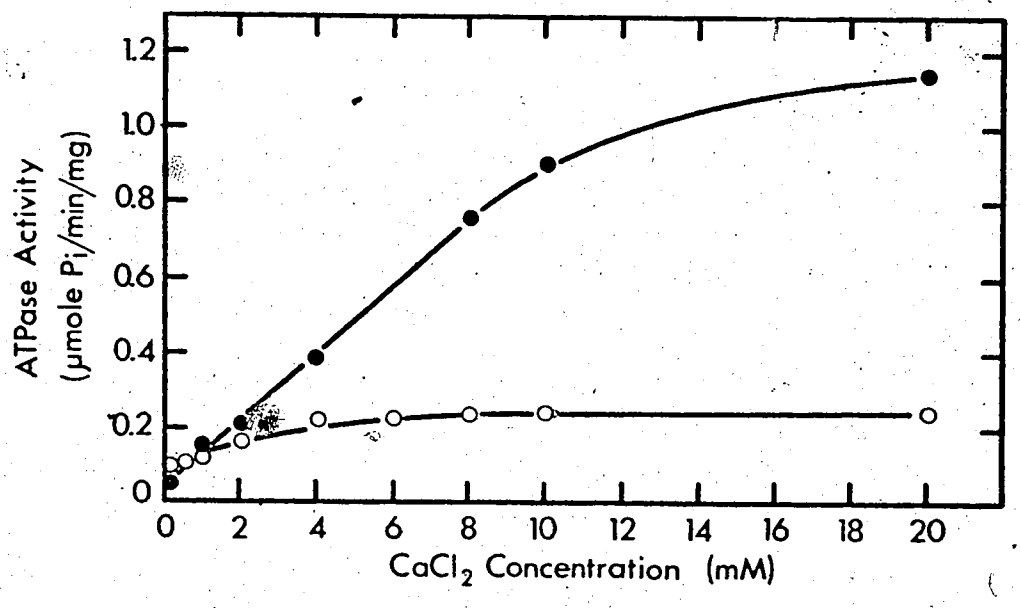

Figure 34. The effect of varying $CaCl_2$ concentration on the specific ATPase activity of HMM-S1 (●—●) and, for comparison, native cardiac myosin (○—○). Measurements were made at 25°C in 0.4 M KCl, 5 mM ATP, pH 8, using 0.6 mg HMM-S1 and 0.95 mg myosin.

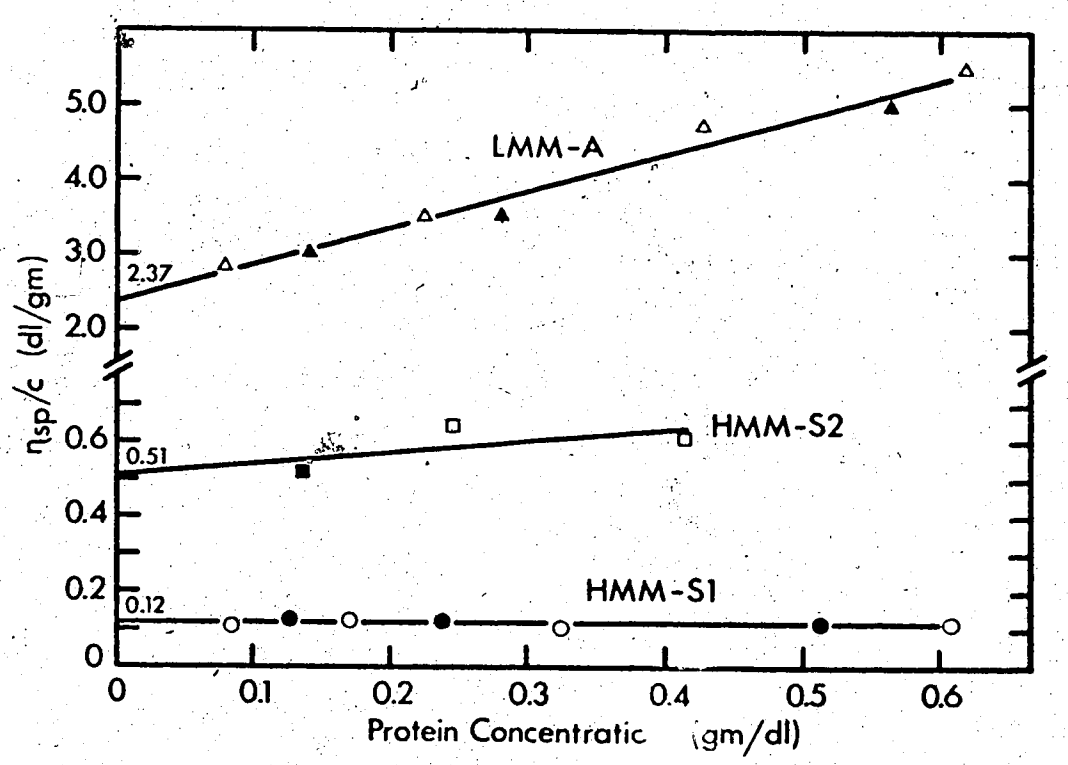

Figure 35. Concentration dependence of the reduced specific viscosity of LMM-A (triangles), HMM-S2 (squares) and HMM-S1 (circles) at 5.0°C in 0.5 M KCl, 0.05 M phosphate buffer, pH 7.0 (the solvent buffer for HMM-S1 additionally contained 1 mM DTT). Open and closed point styles represent results using different preparations of the subfragment considered.

0.87 ± 0.13 for LMM-A, 0.51 ± 0.11 dℓ/gm and 1.16 ± 0.50 for HMM-S2, and 0.12 ± 0.01 dℓ/gm and 0.25 ± 0.02 for HMM-S1.

Sedimentation Velocity. The diluted samples of the purified fragments that had been utilized for viscometric analysis were additionally used in the sedimentation velocity studies. Representative schlieren patterns of LMM-A and subfragments 1 and 2 in 0.5 M KCl, 0.05 M phosphate buffer, pH 7.0 (plus 1 mM DTT in solutions of HMM-S1) are shown on the right side of Figure 36. Observed rates of sedimentation were corrected to standard conditions using a value of 0.728 ml/gm for the apparent partial specific volume of the subfragments (Szent-Györgyi, Cohen, and Philpott, 1960; Lowey et al., 1969) and a value of 1.0309 gm/cm^3, determined pycnometrically, for the density of the solvent buffer at low temperature. Corrected sedimentation coefficients, $s_{20,w}$, were plotted with respect to the corresponding values of protein concentration, and a straight line was fitted through each set of data by the method of least squares. The resultant graphs are illustrated in Figure 36. The sedimentation velocity of the three subfragments was found to vary inversely with respect to the solute concentration. However, the degree of the concentration dependence was different in each case. For example, the value of K_s for LMM-A, HMM-S2, and HMM-S1, calculated from the slope of the appropriate line, was 0.061 ± 0.020, 0.007 ± 0.019, and 0.004 ± 0.002 ml/mg, respectively. From the least squares analysis, the intrinsic sedimentation coefficient of LMM-A was 3.14 ± 0.29 S; of subfragment 2, 3.24 ± 0.18 S; and of subfragment 1, 5.11 ± 0.05 S.

Molecular Weight. The weight-average molecular weight distributions of the purified fragments in 0.5 M KCl, 0.05 M phosphate buffer,

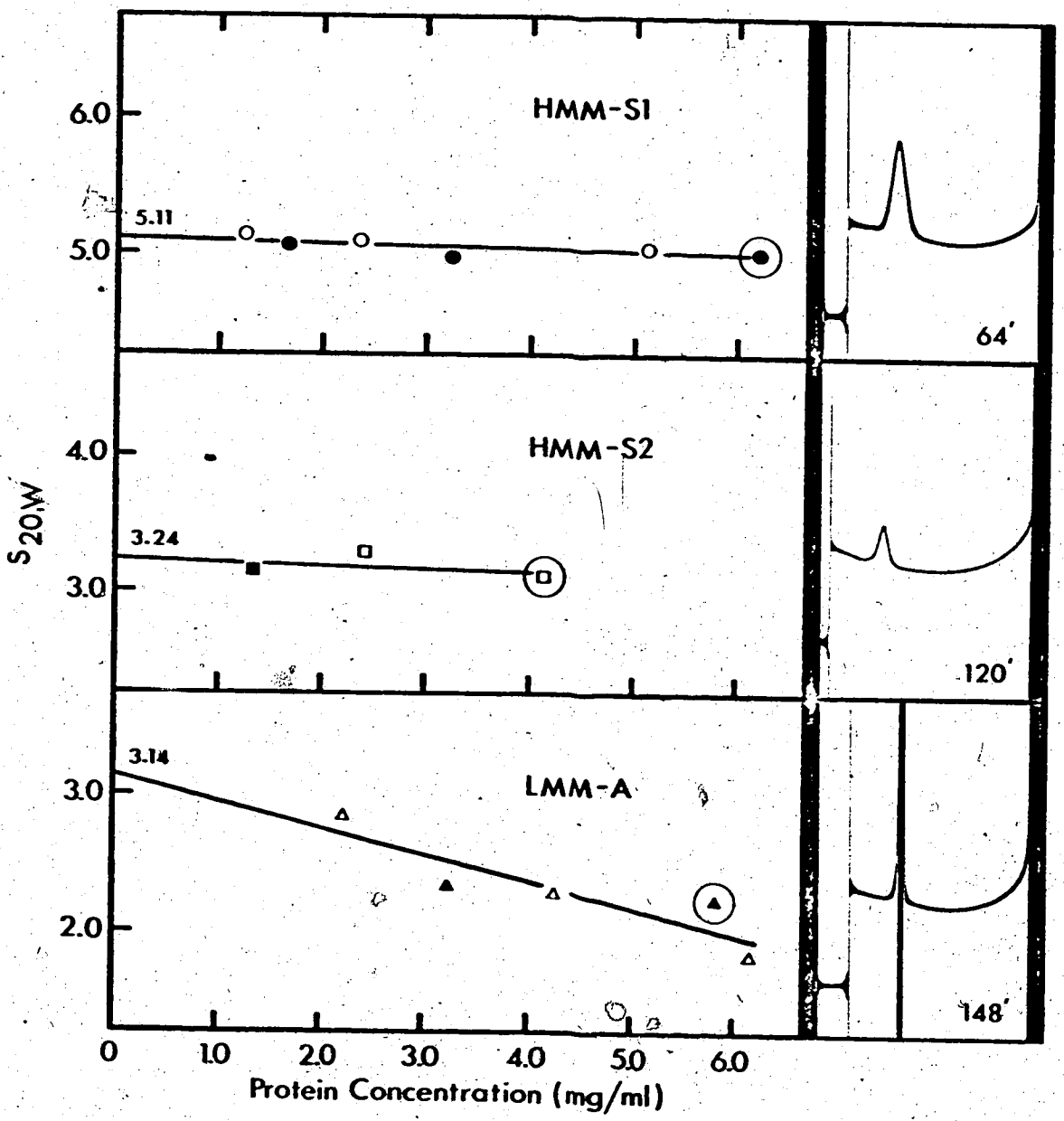

Figure 36. Concentration dependence of $s_{20,w}$ of the major proteolytic subfragments of cardiac myosin. The open and closed point styles represent the results from sedimentation velocity experiments conducted at low temperatures (5 to 7°C) and 60 x 10^3 rpm in 0.5 M KCl, 0.05 M phosphate buffer, pH 7.0, using different preparations of the subfragment concerned. Representative schlieren patterns observed in the ultracentrifuge (bar angle 50°) are shown on the right. The photographs were taken at the time indicated after reaching top speed, and the protein concentration is circled in the plot to the left.

pH 7.0, were determined at low temperature employing sedimentation equilibrium techniques described in Chapter 2. The values of the apparent partial specific volume and the solvent density that were used in the calculations of molecular weight have been given in the previous section concerning sedimentation velocity. In the graphs that follow, the data associated with low- and high-speed sedimentation equilibrium runs are represented by open and closed point styles, respectively.

The final results of sedimentation equilibrium experiments with subfragment 1 are graphically summarized in Figure 37. The low-speed run was conducted at 7.1°C and a set rotor speed of 8.0×10^3 rpm with an initial loading concentration of 6.31 fringes (1.58 mg/ml), as determined by c_o measurements. The high-speed run was carried out at 5.0°C and a set rotor speed of 16×10^3 rpm with an initial loading concentration of approximately 1.5 mg/ml. As seen in Figure 37a, the plots of ln dy versus $r^2/2$ derived from both the low- and high-speed runs were essentially linear throughout. The corresponding values of $\overline{M}_{w,app}$ calculated from the slope of the straight lines drawn in Figure 37a were 1.05×10^5 and 1.16×10^5 gm/mole (low- and high-speed data, respectively). Virtually identical results were obtained with solutions of subfragment 1 containing 1 mM DTT. For example, $\overline{M}_{w,app}$ as determined from a meniscus depletion run conducted at 5°C, 18×10^3 rpm, and an initial HMM-S1 concentration of 1.24 mg/ml was equal to 1.15×10^5 gm/mole. The reciprocal of point weight-average molecular weight values obtained from the experiments described was plotted against computed values of the protein concentration. The combined results are shown in Figure 37b, where, in addition to the point styles previously designated, the data associated with dithiothreitol are represented by closed triangles. Although slight

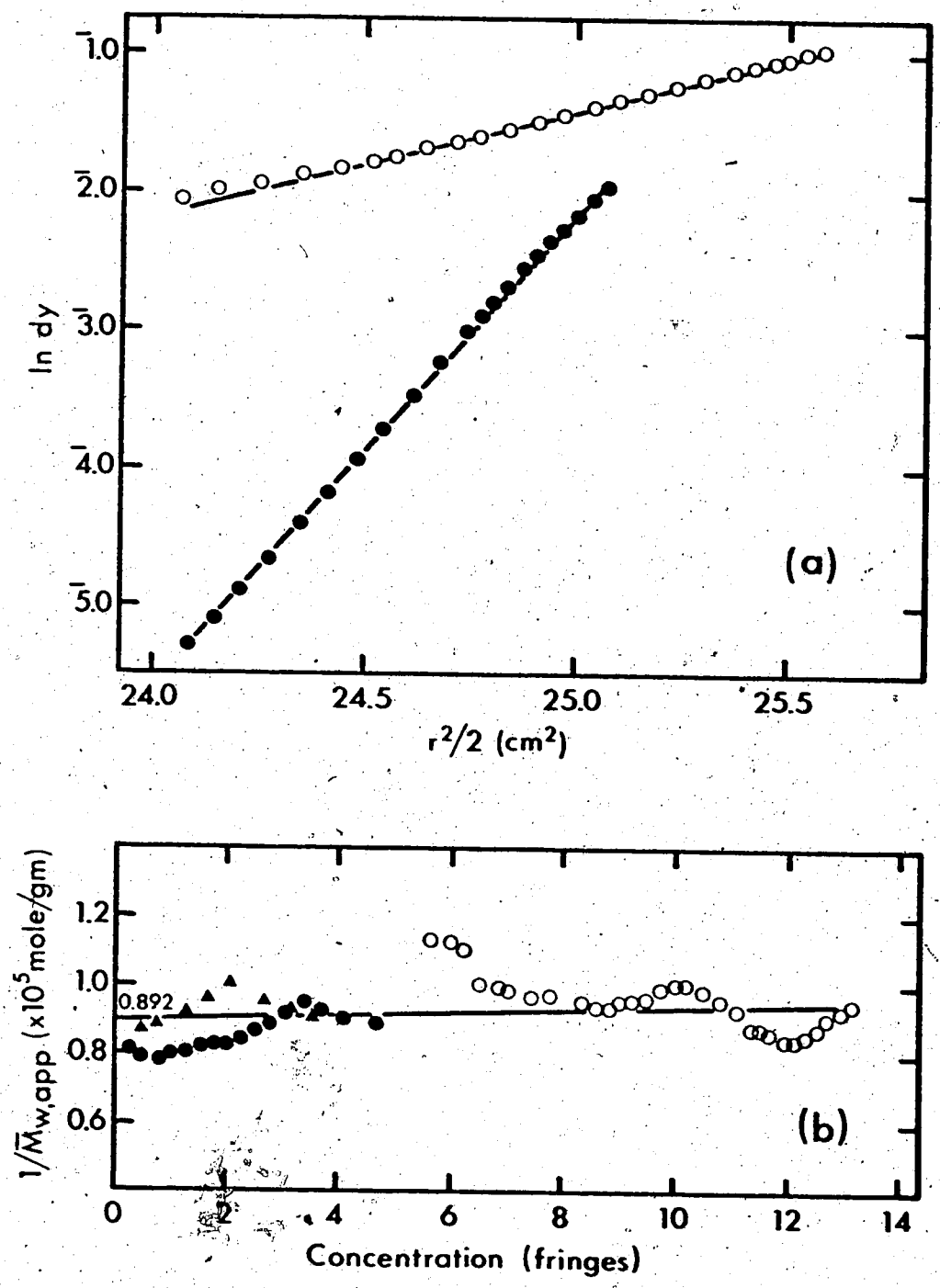

Figure 37. Molecular weight study of cardiac subfragment 1 in 0.5 M KCl, 0.05 M phosphate buffer, pH 7.0. (a) Combined ln dy versus $r^2/2$ plot for high-speed (●—●) and low-speed (○—○) sedimentation equilibrium runs (see text for full experimental details). Many internal data points have not been plotted only for clarity of presentation. (b) Concentration dependence of the reciprocal point weight-average molecular weight values from the data in part (a). (▲—▲) high-speed run in which the solvent buffer additionally contained 1 mM DTT.

perturbation was evident in each of the plots, the general overlap of the curves was good. The composite data was found to be adequately described by a linear relationship over the total concentration range examined; the straight line drawn in Figure 37b was fitted through the experimental points by the method of least squares. The weight-average molecular weight of cardiac subfragment 1 (in the absence or presence of DTT) exhibited little, if any, dependence with respect to concentration. Neither were significant trends evident at either low or high protein concentration. The intrinsic value of $\overline{M}_{w,app}$ for HMM-S1, derived from the results of the least squares analysis, was $1.12 \pm 0.04 \times 10^5$ gm/mole.

The results of a low-speed sedimentation equilibrium experiment with subfragment 2, conducted at 8.7°C and 11×10^3 rpm with an initial loading concentration equivalent to 9.07 fringes, are depicted in Figure 38. Though upward deflection of the initial points was evident in the ln dy versus $r^2/2$ plot, the bulk of the data described a linear function (Figure 38a). This was clearly demonstrated upon plotting the reciprocal of $\overline{M}_{w,app}$ values, determined at each measured radial position, with respect to the corresponding values of concentration (Figure 38b). Moreover, the apparent weight-average molecular weight of HMM-S2 was found to be essentially independent of the solution concentration. A straight line was fitted through the ln dy versus $r^2/2$ data by the method of least squares — that is, through the experimental points at a radial position greater than 24.0 cm^2, which excluded the first eight points of a total of sixty-one. As calculated from the slope of this straight line and the results of the least squares analysis, the weight-average molecular weight of cardiac subfragment 2 was estimated to be $6.3 \pm 0.2 \times 10^4$ gm/mole.

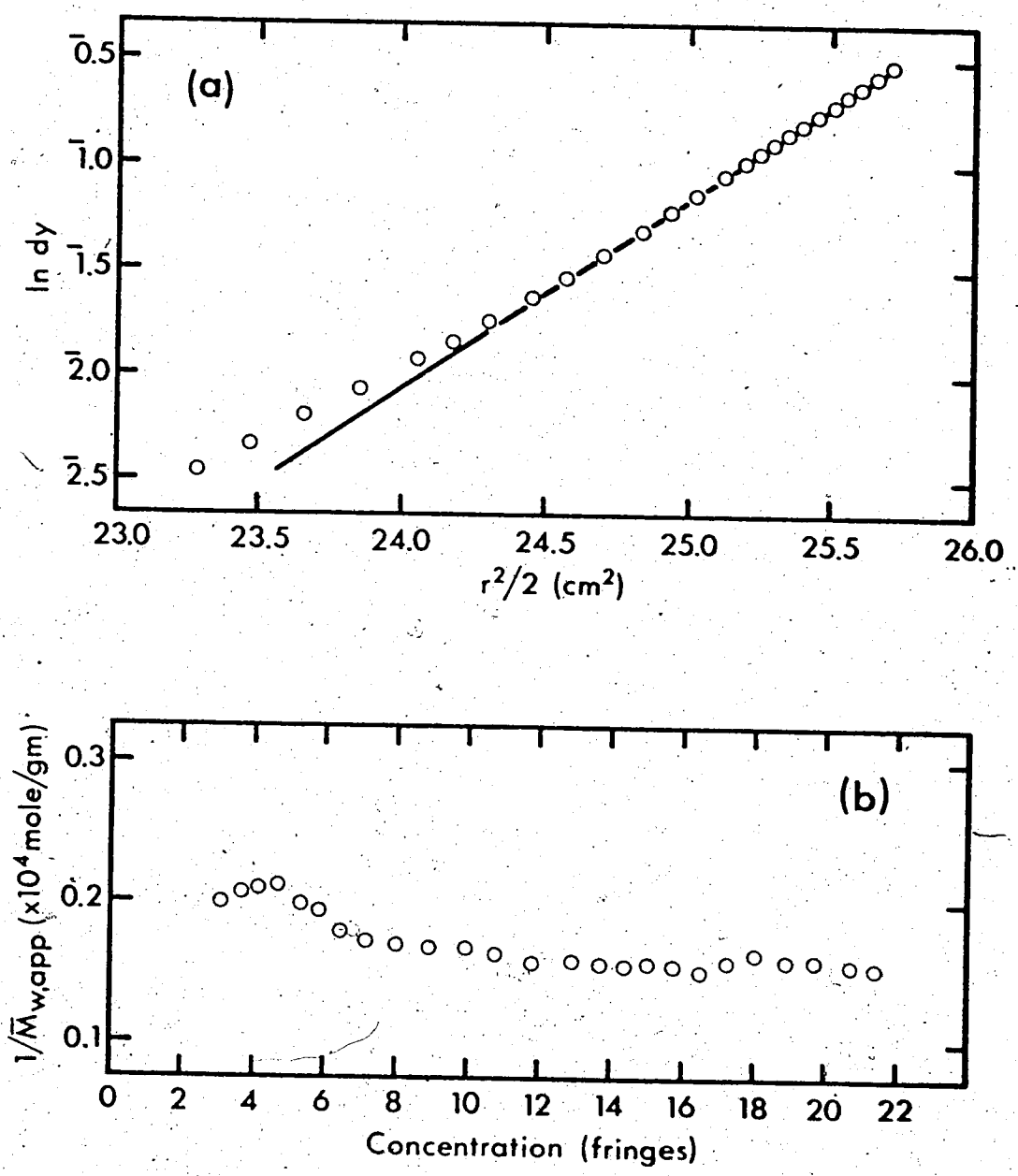

Figure 38. Molecular weight study of cardiac subfragment 2 in 0.5 M KCl, 0.05 M phosphate buffer, pH 7.0. (a) ln dy versus $r^2/2$ plot for a low-speed sedimentation equilibrium run (see text for complete experimental details). Many internal data points have not been included in the graph. (b) Concentration dependence of the reciprocal point weight-average molecular weight values from the data in part (a).

The results of molecular weight studies with respect to solutions of LMM-A are graphically summarized in Figure 39. The low-speed sedimentation equilibrium experiment was conducted at 5°C and a set rotor speed of 7.2×10^3 rpm with an initial loading concentration of 8.30 fringes, as determined by c_o measurements. The high-speed equilibrium run was carried out at 5°C, 17.0×10^3 rpm, and an initial concentration of 1.3 mg/ml. Upon plotting ln dy against $r^2/2$, the resultant graph associated with the high-speed data was found to be entirely linear (Figure 39a). In contrast, that derived from the low-speed data displayed significant upward curvature throughout (Figure 39a). These observations were reflected in the respective plots of point $1/\overline{M}_{w,app}$ values versus protein concentration shown combined in Figure 39b. The molecular weight estimated computed from the results of the meniscus depletion experiment were clearly independent of the solution concentration; the corresponding low-speed values exhibited a marked, nonlinear, negative concentration dependence indicative of a polydisperse system. Furthermore, the overlap of the two plots was observed to occur toward lower molecular weight values in the range (1.1×10^5 to 2.1×10^5 gm/mole) displayed by the low-speed data. Obviously, the high-speed sedimentation equilibrium run yielded molecular weight estimates of the smallest species present in significant amounts in samples of LMM-A. From least squares analysis of the high-speed ln dy versus $r^2/2$ data (the straight line drawn in Figure 39a), this limiting value of the weight-average molecular weight for LMM-A was equal to $1.42 \pm 0.03 \times 10^5$ gm/mole. Although the molecular weight of the largest component present in LMM-A preparations could not be directly determined, a reasonable estimate, based on the asymptotic trend evident at the higher protein concentrations in Figure 39, would

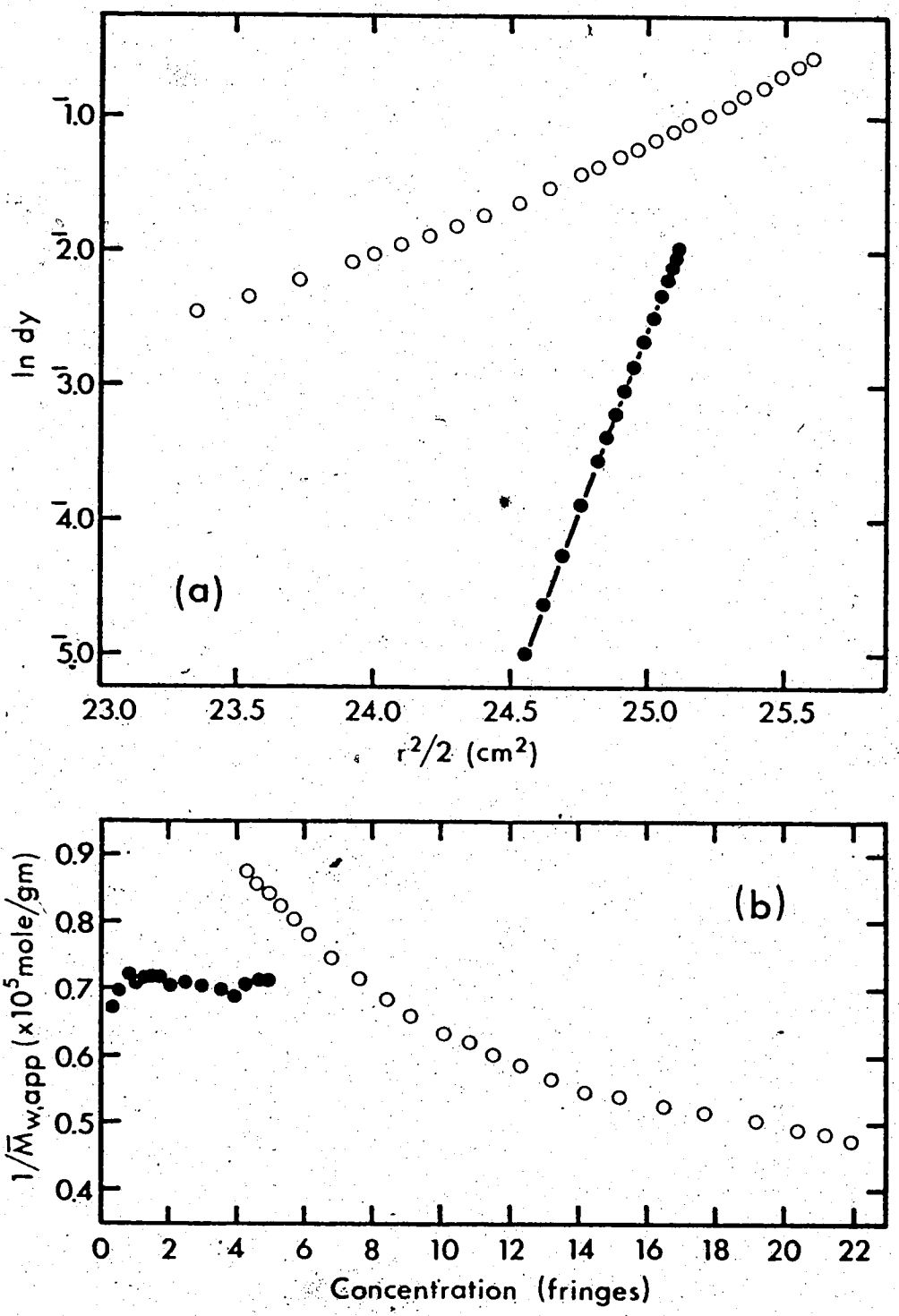

Figure 39. Molecular weight study of LMM-A in 0.5 M KCl, 0.05 M phosphate buffer, pH 7.0. (a) Combined ln dy versus $r^2/2$ plot for high-speed (●—●) and low-speed (○—○) sedimentation equilibrium runs (see text for experimental details). Many internal data points have not been plotted. (b) Concentration dependence of the reciprocal point weight-average molecular weight values from the data in part (a).

be a value slightly greater than 2.1×10^5 gm/mole.

Discussion

In the introduction to this chapter, tentative designations were assigned to the purified components of the water-soluble and water-insoluble fractions based on analogy with the skeletal system. By way of discussing the experimental results, an attempt is thus made to unequivocally establish the identity of these proteolytic subfragments. As was noted from enzymic velocity measurements, the purified 5 S component of the water-soluble fraction was the only isolated fragment to exhibit Ca^{++} ion-activated ATPase activity. Moreover, its specific activity was three to four times higher than that determined with native cardiac myosin under identical conditions. Similar observations have been reported by Mueller (1965) concerning subfragment 1 produced by limited tryptic digestion of rabbit skeletal myosin, by Nihei and Kay (1968) and Lowey et al. (1969) with respect to HMM-S1 obtained by short proteolytic digestion of rabbit skeletal myosin with insolubilized papain, and by Tada et al. (1969) for subfragment 1 prepared by proteolysis of bovine cardiac HMM with soluble papain. The apparent difference observed in the catalytic rates of native cardiac and skeletal myosin (in the presence of calcium ions) was also manifest in their enzymically active subfragments. For example, in substrate solutions containing 5 mM $CaCl_2$, the specific activity of skeletal HMM-S1 was reported to vary between 1.4 and 2.0 μmole P_i/min/mg (Lowey et al., 1969), whereas that of the active cardiac subfragment was approximately one-third , 0.5 μmole P_i/min/mg, as interpolated in Figure 34. Recent investigations have shown that not only are certain light chains associated with subfragment 1

prepared by papain digestion of rabbit skeletal myosin (Weeds and Lowey, 1971) or bovine cardiac myosin (Weeds and Frank, 1973) but also the inclusion of these light chains is essential for expression of biological activity. In consideration of the differences observed between native cardiac and skeletal myosin, particularly with reference to the light chains as discussed in Chapter 3, it is thus not surprising that the subfragments which apparently retain the ATPase active site reflect these differences to a similar extent.

A comparison of the amino acid composition of cardiac and skeletal HMM-S1 is presented in Table VII. Though the overall distribution of the amino acids is generally similar in each of the analyses, the results of the present study most closely resemble those reported by Lowey et al. (1969) for subfragment 1 produced from rabbit skeletal myosin by limited proteolysis with an insolubilized form of papain. Of the total seventeen residues that are tabulated, the corresponding values of thirteen are in excellent agreement, whereas compared with the results of Mueller (1965) for HMM-S1 prepared from rabbit skeletal myosin by tryptic digestion and of Tada et al. (1969) for subfragment 1 obtained from bovine cardiac heavy meromyosin with soluble papain, only the corresponding values of approximately seven amino acids are similar to an equal degree. Considering the source tissues from which the fragments were prepared, these observations may seemingly indicate the existence of species differences between rabbit and bovine cardiac muscle proteins. Care must be taken, however, in making this interpretation since, although a common enzyme was employed for fragmentation, the effect of insolubilization of papain on the production of subfragment 1 has not been fully established. As was shown in the preceding chapter, the activity

TABLE VII

COMPARISON OF THE AMINO ACID COMPOSITION

OF CARDIAC AND SKELETAL SUBFRAGMENT 1*

(moles/10^5 gm protein)

Amino Acid	Cardiac		Skeletal	
	Present Study	Tada et al. (1969)	Mueller (1965)	Lowey et al. (1969)
Lys	83	90	64	83
His	20	17	13	18
Arg	46	42	25	34
Asp	101	99	88	85
Thr	49	40	47	49
Ser	41	39	41	41
Glu	128	175	130	117
Pro	42	25	26	37
Gly	60	44	53	61
Ala	74	72	72	70
Cya	11.3	9.3	10	11
Val	46	34	38	55
Met	29.5	26	27	28
Ile	52	38	37	53
Leu	87	100	71	75
Tyr	34	17	26	34
Phe	52	33	43	52

*The tissue source was rabbit for all the studies but that of Tada et al. (1969), in which subfragment 1 was perpared from bovine heart muscle.

of papain toward a substrate of even small size is reduced upon the immobilization of the enzyme. Soluble papain may hydrolyze peptide bonds not cleaved by insolubilized papain due, for example, to steric hindrance and thus yield subfragments with slightly dissimilar amino acid compositions. Additionally, the actual starting material from which the cardiac fragments were produced was very different in each case: heavy meromyosin obtained by tryptic digestion in the study of Tada et al. (1969) and native myosin in the present study. The degradative action of trypsin on that part of the myosin molecule subsequently liberated by papain has not been assessed. Certainly if peptide bonds were extraneously hydrolyzed in this portion of the molecule and small peptides were released during the production of heavy meromyosin or HMM-S1, the amino acid composition of the resultant fragment would be variant with that of the corresponding fragment obtained from native myosin in a single digestion process. On the other hand, the significantly higher content of arginine, aspartic acid, and leucine evident in the results of Tada et al. (1969) and the present study as compared to that found for skeletal HMM-S1 may be characteristic of the cardiac molecule.

The value of the extinction coefficient, $E^{1\%}_{1\ cm,\ 280\ nm}$, equal to 8.2 determined for rabbit cardiac subfragment 1 also corresponds more closely to values established for rabbit skeletal subfragment 1 than to that found for bovine cardiac HMM-S1: 8.0 (Lowey et al., 1969) and 7.9 (Weeds and Lowey, 1971; Bagshaw et al., 1973) for the skeletal fragment, prepared by limited proteolysis of native myosin with insolubilized papain, and 6.4 for the bovine cardiac fragment (Tada et al., 1969). As concluded upon reexamination of the amino acid composition data presented in Table VII, the ultraviolet absorption properties of cardiac

and skeletal subfragment 1 essentially reflect the respective contents of the aromatic residues. For instance, the corresponding quantities of tyrosine and phenylalanine evident in the analyses of Lowey et al. (1969) and the present study are identical, and in turn, approximately one and one-half times greater than the amounts reported by Tada et al. (1969) for bovine cardiac HMM-S1. Although the helical content of the cardiac subfragment was not directly evaluated with reference to circular dichroic parameters of standard, α-helical polyamino acids, an estimate based on the ratio of the mean residue ellipticity values for rabbit cardiac HMM-S1 at 221 and 209 nm to the corresponding values for LMM-A is 34%. Assuming LMM-A is completely α-helical (Oikawa et al., 1968), this estimate is in very good agreement with the helical content reported for rabbit skeletal HMM-S1 as derived from optical rotatory dispersion measurements (Lowey et al., 1969). Furthermore, this result would suggest that the overall secondary structure of the two fragments is very much alike.

The intrinsic values of the viscosity, sedimentation velocity, and weight-average molecular weight equal to 0.12 dℓ/gm, 5.11 S, and 1.12×10^5 gm/mole, respectively, obtained with rabbit cardiac subfragment 1 are very similar to published values for the skeletal system. For example, [η] ranges from 0.064 dℓ/gm (Lowey et al., 1969) to 0.125 dℓ/gm (Young et al., 1965), $s^{\circ}_{20,w}$ from 5.4 S (Nihei and Kay, 1968) to 5.95 S Mueller (1965), and $\bar{M}_w$ from 1.10×10^5 gm/mole (Nihei and Kay, 1968) to 1.17×10^5 gm/mole (Young et al., 1965). The apparent independence of these parameters with respect to the solution concentration of cardiac HMM-S1 is also consistent with reported observations concerning the skeletal fragment (Lowey et al., 1969). Furthermore, the very low

values of the Huggins constant and K_s experimentally derived suggest that cardiac subfragment 1 is a relatively compact, spherical macromolecule (Creeth and Knight, 1965; Bradbury, 1970).

The amino acid composition of rabbit cardiac and skeletal LMM, LMM-like fragments, and HMM-S2 (produced by limited digestion of native myosin with insolubilized papain) are presented for comparison in Table VIII. The general distribution of the amino acids in each of the analyses is remarkably similar: for example, notably high quantities of lysine, aspartic acid, glutamic acid, alanine, and leucine, relatively low amounts of the aromatic residues, and the absence of proline. Upon stringent comparison of the corresponding values of individual amino acids, however, the composition of LMM-A is found to most closely resemble that of skeletal rods, and the composition of cardiac subfragment 2 to resemble that of skeletal HMM-S2. As evident in Table VIII, the estimated levels of the sulfhydryl content were generally higher for the cardiac fragments. In addition, the recovery of glutamic acid and leucine in analyses of LMM-A was exceptionally high, whereas that of lysine, glutamic acid, and methionine in present analyses of subfragment 2 was correspondingly low (in comparison to the data for skeletal rods and HMM-S2, respectively). The significance of these observations is not presently known; these differences may very well be characteristic of the cardiac molecule.

Certainly, the rather low values of the ultraviolet extinction coefficient found for LMM-A and HMM-S2 directly reflect the low aromatic residue content of these cardiac fragments. As expected from the apparent homology of the amino acid compositions, the value of $E^{1\%}_{1\ cm,\ 278\ nm}$ equal to 2.66 determined for LMM-A is not significantly different from

TABLE VIII

COMPARISON OF THE AMINO ACID COMPOSITION OF RABBIT CARDIAC AND SKELETAL LMM-LIKE FRAGMENTS AND SUBFRAGMENT 2

(moles/10^5 gm protein)

Amino Acid	LMM-A Present Study	HMM-S2 Present Study	LMM Fr.1 Lowey & Cohen (1962)	Myosin Rods Lowey et al. (1969)	HMM-S2 Lowey et al. (1969)
Lys	108	93	94	107	121
His	13.5	9	21	15	9
Arg	58	44	60	56	37
Asp	90	82	83	88	87
Thr	36	38	33	38	43
Ser	47	47	34	39	35
Glu	242	215	210	219	242
Pro	0	0	0	0	0
Gly	15.5	18	18	20	19
Ala	90	82	81	85	87
Cya	8.7	8.1	4.0	4.6	6.4
Val	32	28	38	33	24
Met	18.5	13	19	23	26
Ile	27	21	39	36	34
Leu	122	98.5	96	99	99
Tyr	6	4	9	5.9	2.6
Phe	7	9	4	7.0	8.6

that of 2.40 reported for chromatographed skeletal LMM fraction 1 (Szent-Györgyi, Cohen, and Philpott, 1960); neither is the parallel value for cardiac subfragment 2, 0.93, dissimilar to that of 0.7 established by Lowey et al. (1969) for skeletal HMM-S2 (though at the wavelength of 280 nm). Consistent with the interpretations derived from optical rotatory dispersion data made by Szent-Györgyi, Cohen, and Philpott (1960) with respect to skeletal LMM Fr. 1 and by Lowey et al. (1969) concerning skeletal LMM and rods, the excellent agreement of the mean residue ellipticity values for LMM-A at 221 and 209 nm ($^{-}4.31 \times 10^4$ and $^{-}3.92 \times 10^4$ degree·cm^2/dmole, respectively) with corresponding values for skeletal light meromyosin fraction 1 ($^{-}4.44 \times 10^4$ and $^{-}4.13 \times 10^4$ degree·cm^2/dmole, respectively (Oikawa et al.,1968)) would suggest that LMM-A is also entirely α-helical in aqueous solutions. Based on the ratio of the mean residue ellipticity values for cardiac subfragment 2 at 221 and 209 nm to the corresponding values for LMM-A, the α-helical content of HMM-S2 is estimated to be approximately 75%, which is very similar to that evaluated for skeletal subfragment 2 from optical rotatory dispersion measurements (Lowey, Goldstein, and Luck, 1966).

The intrinsic values of the reduced viscosity, sedimentation coefficient, and weight-average molecular weight determined for rabbit cardiac subfragment 2 (0.51 dℓ/gm, 3.24 S, and 6.3×10^4 gm/mole, respectively) are additionally analogous with published values for the corresponding skeletal fragment (for example, 0.4 dℓ/gm, 2.7 S and 6.2×10^4 gm/mole, respectively (Lowey et al., 1969)). The very high value of the Huggins constant obtained (1.16) would indicate that the molecular structure of cardiac subfragment 2 is relatively rigid and asymmetric (Bradbury, 1970), though the apparent independence of the physicochemical

parameters with respect to the protein concentration would suggest, in turn, that the interaction of the macromolecules in solution is not proportionally great.

The viscometric properties of LMM-A are very similar to those reported for rabbit skeletal rods (Lowey et al., 1969). Both the weight intrinsic viscosity (2.37 dℓ/gm) and Huggins constant (0.87) are significantly high, consistent with the interpretation that aqueous solutions of LMM-A are comprised of rigid and highly asymmetric macromolecules. The relatively large, negative concentration dependence additionally observed in the sedimentation velocity studies (K_s equal to 0.061 ml/mg) would tend to support this conclusion. The intrinsic sedimentation coefficient found for LMM-A (3.14 S) is within the range of documented values for cardiac and skeletal LMM Fr. 1 (2.80 S (Theiner, 1963) to 3.36 S (Young et al., 1964)) and for skeletal rods (3.4 S (Lowey et al., 1969)). However, since the range of reported values is very narrow, LMM cannot be readily distinquished from rods on a basis of $s^{\circ}_{20,w}$ values alone — these fragments are too much alike in this respect. The results of the molecular weight studies clearly demonstrated that preparations of LMM-A were truly mixtures of at least two species of LMM-like fragments: material with a minimum weight-average molecular weight of 1.42 x 10^5 gm/mole, corresponds to the molecular weight of cardiac and skeletal light meromyosin (Mueller et al., 1964; McCubbin and Kay, 1968; Lowey et al., 1969), and a heavier component with a molecular weight in the order of 2.1 x 10^5 gm/mole, which is similar to the molecular weight of intact skeletal rods (Lowey et al., 1969; Biró et al., 1973). Moreover, as collectively inferred from the results of the separate studies, LMM-A consists mainly of intact rods (or aggregate material) plus a small

proportion of light meromyosin (hence the appellation "LMM-A", where "A" designates neither rod nor fraction 1 particles but rather the alcohol precipitation method of purification). Mixtures of LMM and intact myosin rods have been similarly obtained upon limited digestion of rabbit skeletal myosin (in solution) with insolubilized papain (Lowey et al., 1969), and the formation of total rods has even been observed in early tryptic digests of cardiac and red myosins (Bíró et al., 1973).

CHAPTER 6

FINAL DISCUSSION

The present study has included a thorough examination of the enzymic, ultraviolet optical, amino acid, and physicochemical properties of rabbit cardiac myosin. It has demonstrated that the native cardiac molecule can be systematically fragmented into distinct components by limited proteolytic digestion with S-MDA-mercuripapain. Moreover, the process of degradation has been analyzed both kinetically and ultracentrifugally, and the major fragments have been isolated and characterized. The various physical and chemical parameters experimentally determined for cardiac myosin and the subfragments are collectively shown in Table IX. Final conclusions drawn with respect to the molecular structure of native cardiac myosin, in light of the results of the fragmentation study, are discussed briefly in this chapter. Possible topics for continued research are additionally considered in question form at the end of the discussion.

The results of the present investigation are consistent with the currently favored model for native skeletal myosin: superficially, a highly asymmetric, rodlike molecule with globular protrusions at one end (Lowey et al., 1969). General features of the cardiac molecule and its subfragments are schematically illustrated in Figure 40. The semi-rigid and asymmetric nature of myosin is reflected, for example, by the marked concentration dependence of its hydrodynamic parameters. The high value of the weight intrinsic viscosity and rather low intrinsic sedimentation

TABLE IX

PHYSICAL AND CHEMICAL PARAMETERS OF RABBIT CARDIAC MYOSIN AND THE PROTEOLYTIC SUBFRAGMENTS*

Parameter	Myosin	HMM-S1	LMM-A	HMM-S2
$\overline{M}_w$ ($\times 10^{-5}$)	4.77	1.12	1.42 - 2.1	0.63
$s^\circ_{20,w}$ (S)	6.08	5.11	3.14	3.24
[η] (dℓ/gm)	2.04	0.12	2.37	0.51
ATPase Activity ($\mu m\ P_i$/min/mg)	0.23_5	0.90	none	none
$E^{1\%}_{1cm}$ at λ_{max} (nm)	6.06 280	8.20 280	2.66 278	0.93 278
$[\Theta]_{221nm}$ ($\times 10^{-4}$)	$^{-}2.69$	$^{-}1.47$	$^{-}4.31$	$^{-}3.20$
$[\Theta]_{209nm}$ ($\times 10^{-4}$) (deg.cm^2/dmole)	$^{-}2.56$	$^{-}1.35$	$^{-}3.92$	$^{-}2.95$

*All parameters, except that of specific ATPase activity, were determined in 0.5 M KCl, 0.05 M phosphate buffer, pH 7.0, at low temperatures. The activity values tabulated were measured at pH 8 and 25°C with substrate solutions consisting of 0.4 M KCl, 5 mM ATP, 10 mM $CaCl_2$.

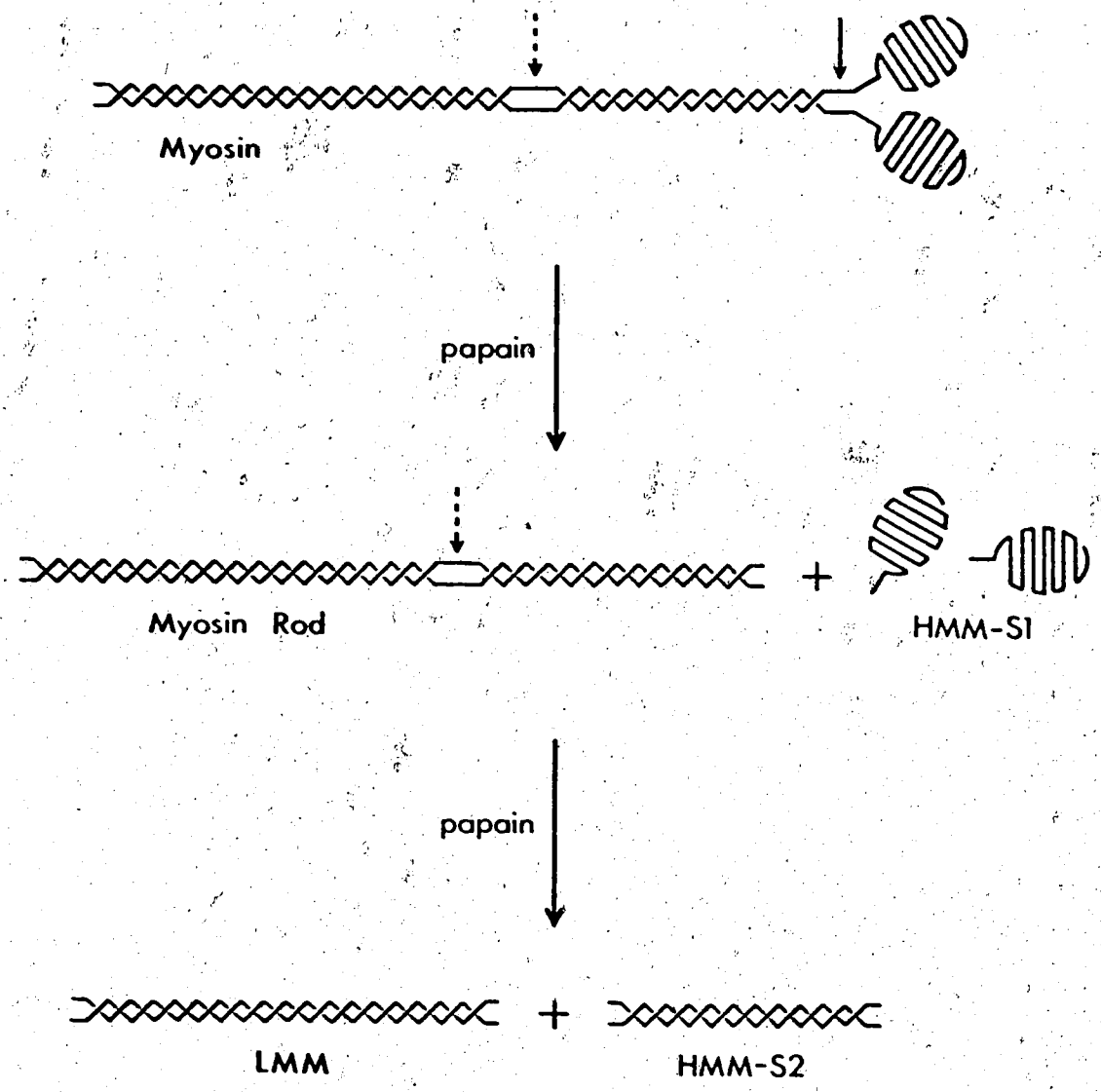

Figure 40. Schematic representation of the cardiac myosin molecule and the major proteolytic subfragments, illustrating the principal steps of the digestion process with insolubilized papain.

coefficient in proportion to the molecular weight are additional manifestations of these structural features. Taking the monomer molecular weight of cardiac myosin to be 4.7×10^5, then each native molecule must be comprised of only two heavy polypeptide chains (each approximately 2.0×10^5 in molecular weight (Brahms and Kay, 1963)) and a minimum of three light chains (two 2.7×10^4 and one 1.8×10^4 in molecular weight (Mani and Kay, 1973)). The helical intertwinement of the two heavy chains, indicated in the rodlike portion of the molecule (Figure 40), is tentatively inferred from the circular dichroic data of those purified subfragments which display a high degree of molecular asymmetry similar to native myosin (for example, myosin rod and light meromyosin). Even though both cardiac and skeletal myosin have been examined by electron microscopy (Mueller et al., 1964; Lowey et al., 1969), details with respect to the actual mode of interaction of the heavy chains have not been observed.

Additionally depicted in Figure 40 are the principal steps of the fragmentation reaction assumed to have occurred with insolubilized papain. At least two regions exist within the myosin molecule which are readily susceptible to attack by proteolytic enzymes: one located along the rodlike portion, and the other at the attachment point of the globules. These are diagrammatically indicated in Figure 40 by small arrows. It is not to be construed from the drawing, however, that lability to proteolytic cleavage is attributable solely (if at all) to disruption of the helical folding of the two heavy polypeptide chains. Certainly this is a very plausible explanation which was originally proposed by Mihalyi and Harrington (1959). However, the apparent absence of proline in the amino acid analyses of LMM-A and HMM-S2 and the different subfragments

initially released by proteolytic enzymes of dissimilar specificities would tend to support the hypothesis that proteolysis occurs in regions of particular amino acid content (Lowey et al., 1969). Distinction between these two possibilities cannot be made unequivocally at the present time. The real answer is likely some combination of both explanations: peptide bonds may initially be hydrolyzed at specific amino acids which are favorably oriented through the tertiary structure to proteolytic attack.

Irrespective of the molecular basis of this phenomenon, the S-MDA-papain complex was found to cleave native cardiac myosin principally in the two regions described, though at apparently different rates. As illustrated in Figure 40, subfragment 1 is predominately produced during the initial stages of the fragmentation process, and myosin rod is released concurrently. Analogous observations have been reported by Nihei and Kay (1968) and Lowey et al. (1969) with respect to papain digestion of rabbit skeletal myosin. With further time of proteolysis, the intact rods are additionally cleaved yielding light meromyosin and subfragment 2 (Figure 40). Clearly, if this myosin model and reaction scheme are correct, the late buildup of HMM-S2 that was experimentally observed would be actually expected. Since this fragment constitutes an internal part of the myosin molecule, the heavy chains must be proteolytically broken in at least two areas to effect its release. In contrast, theoretically each of the other major subfragments can be liberated in a single digestion step. Proteolytic cleavage of the cardiac myosin molecule in the centrally located region (indicated by the broken small arrow in Figure 40) does not appear to occur to any great extent. This conclusion is based on two observations: one, heavy meromyosin was

not evident in significant amounts during early stages of the fragmentation process, and two, final solutions of LMM-A were found to consist of myosin rods and light meromyosin — the former in greater proportion. Obviously, if fragmentation proceeded at the two "sites" at a similar rate, heavy meromyosin would not be produced and LMM-A would be essentially light meromyosin. On the otherhand, if cleavage occurred preferentially in the central region (as recognized with trypsin (Young et al., 1964, for example)), heavy and light meromyosin would be released in approximately equal amounts, and the results clearly distinguishable from those of the present study. Recent investigations have shown that prolonged tryptic digestion of skeletal light meromyosin and intact rods result in the production of a series of new fragments (Bálint et al., 1968; Biró et al., 1973). Although evidence to this effect was not obtained in the present study, the existence of additional regions along the cardiac myosin molecule susceptible to proteolytic attack by papain cannot be entirely ruled out. Certainly under the milder experimental conditions that were employed here (for example, low temperature and limited duration of the reaction), the final quantities of these fragments, if released, would have been very small.

In the context of the model considered for cardiac myosin (Figure 40), the values of the weight-average molecular weight determined for the purified subfragments are arithmetically consistent with that established for the native molecule. Thus adding together the molecular weight values for light meromyosin (1.42×10^5), subfragment 2 (6.3×10^4), and twice that for subfragment 1 (2.24×10^5), the total is 4.29×10^5 which agrees reasonably well with the corresponding value of the molecular weight determined for cardiac myosin (4.7×10^5), taking

into consideration the rather extensive loss of non-protein nitrogen. Similarly, the sum of the molecular weight values estimated for the total rod (2.1×10^5) and twice that for subfragment 1 (2.24×10^5), equal to 4.34×10^5, numerically accounts for most of the molecular weight of myosin. Moreover, the value of the weight-average molecular weight of light meromyosin (1.42×10^5) plus that of subfragment 2 (6.3×10^4) very closely approximates the molecular weight estimate for total rods (2.1×10^5). If the apparent accuracy of the latter observation is more real than fortuitous, then the extent of the secondary degradation in the central region must have been minimal. This would imply that most of the labile peptides released during proteolysis originated from the globular portion of the myosin molecule. It has been reported, for instance, that the light chains evidently not essential for the expression of ATPase activity are partially, if not totally, destroyed in preparing subfragment 1 from either rabbit skeletal or bovine cardiac myosin by brief papain digestion (Weeds and Lowey, 1971; Weeds and Frank, 1973).

An important limitation in the preparation of the myosin subfragments by proteolysis is thus the extensive internal cleavage which occurs during the release of these fragments. This has been commonly observed with several proteolytic enzymes of widely different specificities which have been utilized to fragment skeletal myosin: for example, trypsin (Mihalyi and Harrington, 1959), chymotrypsin (Segal et al., 1967), and papain (Kominz et al., 1965). The rather high value of non-protein nitrogen experimentally obtained in this study and the appearance of multiple bands upon preliminary electrophoresis of the purified fragments on SDS-polyacrylamide gels (not shown) would certainly indicate that the subfragment molecules were severely nicked. Although this

secondary type of degradation probably cannot be fully prevented, it can be minimized. In future preparations of rabbit cardiac HMM-S1 and total rods, for example, employing the methods described in the present study, the duration of the digestion at low temperature could be reduced to approximately 10 minutes, with possibly a corresponding reduction in the enzyme to myosin ratio. Stone and Perry (1973) have recently shown that the extent of degradation evident in the light chains of skeletal myosin is directly related to the papain/myosin ratio used. However, these modifications cannot be applied if high yields are desired of the more slowly released subfragments such as HMM-S2; unfortunately their production by lengthy proteolysis must come at the expense of the other subfragments.

That the ATPase activity of cardiac myosin is associated with the globular portion of the molecule (that is, subfragment 1) has been clearly demonstrated in the present study. However, the native molecule contains two subfragment 1 particles, and the question exists as to whether each component is independently active, or whether the ATPase activity of only a single globule is actually expressed. Numerous investigations have shown, for instance, that skeletal myosin and heavy meromyosin possess two nucleotide binding sites per unit (Schliselfeld and Bárány, 1968; Murphy and Morales, 1970; Morita, 1971) and that skeletal HMM-S1 has only one such site per unit (Young, 1967; Eisenberg and Moos, 1970). On the other hand, it has been reported that only one globule is in fact active in skeletal myosin or heavy meromyosin at a time (Rizzino et al., 1968; Lowey et al., 1969; Eisenberg and Kielley, 1973; Tonomura et al., 1973). Assuming that the inherent enzymatic properties of the cardiac HMM-S1 globules were not altered by the proteolytic

treatment of myosin with papain, three possibilities and their immediate consequences in terms of the relative specific ATPase activity can be hypothesized. If both globules are independently active in native myosin, then the resulting specific activity of HMM-S1 would be approximately two times greater than that determined for myosin, since two subfragment 1 particles constitute one-half the native molecule by weight. Likewise, if only one of the two globules is catalytically active, attached or not, the apparent specific activity of HMM-S1 would be approximately twice that of myosin. However, if only one globule is active in native myosin but both express full ATPase activity when proteolytically released, then the specific activity of HMM-S1 would be about four times that obtained with myosin under similar conditions. Although the Ca^{++} ion-activated ATPase activity of cardiac subfragment 1 was not analyzed kinetically, the apparent three- to fourfold increase in the specific activity of HMM-S1 over that of cardiac myosin, experimentally observed at optimum levels of $CaCl_2$, may thus imply that with respect to the native molecule, only one globule exhibits enzymatic activity at a time. Obviously this is but a tentative conclusion; definitive resolution of the original question must await further kinetic and substrate binding studies c cardiac myosin and its enzymically active subfragments.

Suffice it to say, many pertinent questions remain to be swered through continued research. Their solution constitutes a necessary prerequisite to understanding the mechanism of muscular contraction at the molecular level. A few of these questions have been alluded to in previous discussion. For example, what is the exact nature of the association behavior of native cardiac myosin in terms of the virial coefficient and association constants? Is this reaction, observed in vitro

at high ionic strength, responsible for the in vivo assembly of cardiac myosin monomers into the thick filaments, as suggested by Harrington et al. (1973) with regard to the skeletal system? And what role does the rodlike portion of the native molecule play in the answers to these questions? The interaction of the light and heavy chains of myosin has been shown to be essential for the expression of biological activity (Stracher, 1969; Dreizen and Gershman, 1970); however, very little is known as to the exact manner in which the essential light chains and relevant areas of the heavy chains interact to form the enzymatic active site in subfragment 1, or even myosin. Is the mode of interaction different in the cardiac and skeletal molecules, and if so, to what extent does this account for the differences observed between their specific ATPase activities? And what of the minor peptide fragments also released during proteolysis? For instance, do they originate from hinge-like regions in the native molecule? Are they involved in the attachment of the subfragment 1 globules to the myosin rod and in some way mediate the possible allosteric effect? Perhaps their significance in the contractile process has hitherto been underestimated.

These are but a very few of the many questions which remain to be resolved experimentally. The production of smaller, intact portions of cardiac myosin which retain their inherent molecular properties has been clearly shown by the present study to be practical for routine use. Opportunity now exists to closely examine and analyze individual fragments in ways which would not be applied to the native molecule, due to its large size and tendency to aggregate.

BIBLIOGRAPHY

Adams, E.T., Jr. (1967), Fractions No. 3, Beckman Instruments Inc., Palo Alto, California.

Archibald, W.J. (1947), J. Phys. and Colloid Chem. 51, 1204.

Asai, H. (1963), Biochemistry 2, 458.

Axén, R., and Ernback, S. (1971), Eur. J. Biochem. 18, 351.

Babul, J., and Stellwagen, E. (1969), Anal. Biochem. 28, 216.

Bagshaw, C.R., Eccleston, J.F., Trentham, D.R., Yates, D.W., and Goody, R.S. (1973), Cold Soring Harbor Symp. Quant. Biol. 37, 127.

Bailey, K. (1942), Biochem. J. 36, 121.

Bálint,M., Fekete, Gy., Szilágyi, L., Blazsó, M., and Biró, N.A. (1968), J. Mol. Biol. 37, 317.

Bárány, M., Gaetjens, E., Bárány K., and Karp, E. (1964), Arch. Biochem. Biophys. 106, 280.

Biró, N.A., Szilágyi, L., and Bálint, M. (1973), Cold Spring Harbor Symp. Quant. Biol. 37, 55.

Bradbury, J.H. (1970), in Physical Principles and Techniques of Protein Chemistry Part B (S.J. Leach, ed.), Academic Press, Inc., New York, New York, p. 99.

Brahms, J., and Kay, C.M. (1962), J. Mol. Biol. 5, 132.

Brahms, J., and Kay, C.M. (1963), J. Biol. Chem. 238, 198.

Carney, J.A., and Brown, A.L., Jr. (1966), J. Cell. Biol. 28, 375.

Conway, G.F., and Roberts, J.L. (1965), Am. J. Physiol. 208, 243.

Creeth, J.M., and Knight, C.G. (1965), Biochim. Biophys. Acta 102, 549.

Dreizen, P., and Gershman, L.C. (1970), Biochemistry 9, 1688.

Dreizen, P., Gershman, L.C., Trotta, P.P., and Stracher, A. (1967), J. Gen. Physiol. 50(Part 2), 85.

Dreizen, P., and Richards, D.H. (1973), Cold Spring Harbor Symp. Quant. Biol. 37, 29.

Drenth, J., Jansonius, J.N., Koekoek, R., and Wolthers, B.G. (1971), Advan. Protein Chem. 25,79.

Ebashi, S., Makoto, E., and Ohtsuki, I. (1969), Quart. Rev. Biophys. 2, 351.

Eisenberg, E., and Kielley, W.W. (1973), Cold Spring Harbor Symp. Quant. Biol. 37, 145.

Eisenberg, E., and Moos, C. (1970), J. Biol. Chem. 245, 2451.

Erlander, S.R., and Babcock, G.E. (1961), Biochim. Biophys. Acta 50, 205.

Finck, H. (1965), Biochim. Biophys. Acta 111, 221.

Gazith, J.S., Himmelfarb, S., and Harrington, W.F. (1970), J. Biol. Chem. 245, 15.

Gellert, M.F., von Hippel, P.H., Schachman, H.K., and Morales, M.F. (1959), J. Am. Chem. Soc. 81, 1384.

Gergely, J. (1953), J. Biol. Chem. 200, 543.

Gershman, L.C., Stracher, A., and Dreizen, P. (1969), J. Biol. Chem. 244, 2726.

Glazer, A.N., and Smith, E.L. (1961), J. Biol. Chem. 236, 2948.

Godfrey, J.E., and Harrington, W.F. (1970), Biochemistry 9, 894.

Goldstein, L., Pecht, M., Blumberg, S., Atlas, D., and Levin, Y. (1970), Biochemistry 9, 2322.

Gratzer, W.B., and Lowey, S. (1969), J. Biol. Chem. 244, 22.

Gurd, F.R.N. (1950), in Protein Methods and Procedures, Dept. Phys. Chem. Harvard Medical School, Boston, Massachusetts, ch. 12.

Hanson, J., and Huxley, H.E. (1960), in Structure and Function of Muscle (G.H. Bourne, ed.), Academic Press, Inc., New York, New York, vol. 1, p. 183.

Hanson, J., and Lowy, J. (1963), J. Mol. Biol. 6, 46.

Harrington, W.F., and Burke, M. (1972), Biochemistry 11, 1448.

Harrington, W.F., Burke, M., and Barton, J.S. (1973), Cold Spring Harbor Symp. Quant. Biol. 37, 77.

Howard, A.N., and Wild, F. (1957), Biochem. J. 65, 651.

Huggins, M.L. (1942), J. Am. Chem. Soc. 64, 2716.

Huszar, G., and Elzinga, M. (1972), J. Biol. Chem. 247, 745.

Huxley, H.E. (1953), Biochim. Biophys. Acta 12, 387.

Huxley, H.E. (1963), J. Mol. Biol. 7, 281.

Huxley, H.E., and Brown, W. (1967), J. Mol. Biol. 30, 383.

Huxley, H.E., and Hanson, J. (1954), Nature 173, 973.

Jacobsen, C.F., Léonis, J., Linderstrøm-Lang, K., and Ottesen, M. (1957), Methods of Biochemical Analysis 4, 171.

Katz, A.M. (1970), Physiol. Rev. 50, 63.

Kay, C.M. (1960), Biochim. Biophys. Acta 38, 420.

Kay, C.M., Green, W.A., and Oikawa, K. (1964), Arch. Biochem. Biophys. 108, 89.

Kielley, W.W., and Bradley, L.B. (1956), J. Biol. Chem. 218, 653.

Kimmel, J.R., and Smith, E.L. (1958), Biochem. Preparations 6, 61.

Klainer, S.M., and Kegeles, G. (1955), J. Phys. Chem. 59, 952.

Kominz, D.R., Mitchell, E.R., Nihei, T., and Kay, C.M. (1965), Biochemistry 4, 2373.

Lansing, W.D., and Kraemer, E.O. (1935), J. Am. Chem. Soc. 57, 1369.

Leonis, J. (1948), Compt. rend. trav. lab. Carlsberg Sér. chim. 26, 315.

Locker, R.H., and Hagyard, C.J. (1967), Arch. Biochem. Biophys. 122, 521.

Lowey, S., and Cohen, C. (1962), J. Mol. Biol. 4, 293.

Lowey, S., Goldstein, L., and Luck, S. (1966), Biochem. Z. 345, 248.

Lowey, S., and Holtzer, A. (1959), Biochim. Biophys. Acta 34, 470.

Lowey, S., and Risby, D. (1971), Nature 234, 81.

Lowey, S., Slayter, H.S., Weeds, A.G., and Baker, H. (1969), J. Mol. Biol. 42, 1.

Lowry, O.H., Rosebrough, N.J., Farr, A.L., and Randall, R.J. (1951), J. Biol. Chem. 193, 265.

Luchi, R.J., Kritcher, E.M., and Conn, H.L. (1965), Circulation Res. 16, 74.

Mani, R.S., and Kay, C.M. (1973), Can. J. Biochem. 51, 178.

McCubbin, W.D., and Kay, C.M. (1968), Biochim. Biophys. Acta 154, 239.

McCubbin, W.D., Kay, C.M., and Oikawa, K. (1967), Biopolymers 5, 236.

McCubbin, W.D., Willick, G.E., and Kay, C.M. (1973), Biochem. Biophys. Res. Commun. 50, 926.

Middlebrook, W.R. (1959), Science 130, 621.

Mihalyi, E., and Harrington, W.F. (1959), Biochim. Biophys. Acta 36, 447.

Mihalyi, E., and Szent-Györgyi, A.G. (1953), J. Biol. Chem. 201, 189.

Mitchel, R.E.J., Chaiken, I.M., and Smith, E.L. (1970), J. Biol. Chem. 245, 3485.

Mommaerts, W.F.H.M. (1966), J. Mol. Biol. 15, 377.

Moore, S. (1963), J. Biol. Chem. 238, 235.

Moore, S., and Stein, W.H. (1963), Methods Enzymol. 6, 819.

Morell, S.A., and Bock, R.M. (1954), Am. Chem. Soc., 126th Meeting, New York, Div. of Biol. Chem. Abstracts, p. 44C.

Morita, F. (1971), J. Biochem. 69, 517.

Morrison, R.T., and Boyd, R.N. (1966), Organic Chemistry, Allyn and Bacon, Inc., Boston, Massachusetts, p. 570.

Mueller, H. (1964), J. Biol. Chem. 239, 797.

Mueller, H. (1965), J. Biol. Chem. 240, 3816.

Mueller, H., Franzen, J., Rice, R.V., and Olson, R.E. (1964), J. Biol. Chem. 239, 1447.

Mueller, H., and Perry, S.V. (1962), Biochem. J. 85, 431.

Murphy, A.J., and Morales, M.F. (1970), Biochemistry 9, 1528.

Nihei, T., and Kay, C.M. (1968), Biochim. Biophys. Acta 160, 46.

Oikawa, K., Kay, C.M., and McCubbin, W.D. (1968), Biochim. Biophys. Acta 168, 164.

Ouellet, L., Laidler, K.J., and Morales, M.F. (1952), Arch. Biochem. Biophys. 39, 37.

Perry, S.V. (1960), Biochem. J. 74, 94.

Peterson, E.A., and Sober, H.A. (1962), Methods Enzymol. 5, 3

Richards, E.G., Chung, C.S., Menzel, D.B., and Olcott, H.S. (1967), Biochemistry 6, 528.

Richards, E.G., Teller, D.C., and Schachman, H.K. (1968), Biochemistry 7, 1054.

Rizzino, A.A., Eisenberg, E., Wong, K.K., and Moos, C. (1968), Federation Proc. 27, 519.

Roark, D.E., and Yphantis, D.A. (1969), Proc. N. Y. Acad. Sci. 164, 245.

Sarkar, S. (1973), Cold Spring Harbor Symp. Quant. Biol. 37, 14.

Sarkar, S., Sreter, F.A., and Gergely, J. (1971), Proc. Natl. Acad. Sci. U.S. 68, 946.

Schachman, H.K. (1959), Ultracentrifugation in Biochemistry, Academi Press Inc., New York, New York.

Schliselfeld, L.H., and Bárány, M. (1968), Biochemistry 7, 3206.

Segal, D.M., Himmelfarb, S., and Harrington, W.F. (1967), J. Biol. Chem. 242, 1241.

Seidel, J.C. (1967), J. Biol. Chem. 242, 5623.

Slayter, H.S., and Lowey, S. (1967), Proc. Natl. Acad. Sci. U.S. 58, 1611.

Sluyterman, L.A. Æ., and DeGraaf, M.J.M. (1969), Biochim. Biophys. Acta 171, 277.

Smith, E.L., and Parker, M.J. (1958), J. Biol. Chem. 233, 1387.

Sokolovsky, M., and Vallee, B.L. (1967), Biochemistry 6, 700.

Sreter, F.A., Seidel, J.C., and Gergely, J. (1966), J. Biol. Chem. 241, 5772.

Stone, D., and Perry, S.V. (1973), Biochem. J. 131, 127.

Stracher, A. (1969), Biochem. Biophys. Res. Commun. 35, 519.

Stracher, A., and Dreizen, P. (1966) in Current Topics in Bioenergetics (D.R. Sanadi, ed.), Academic Press Inc., New York, New York, p. 153.

Svedberg, T., and Pedersen, K.O. (1940), The Ultracentrifuge, Oxford Univ. Press, Johnson Reprint Corporation, New York, New York.

Szent-Györgyi, A. (1951), Chemistry of Muscular Contraction, 2nd edition, Academic Press, Inc., New York, New York.

Szent-Györgyi, A.G. (1953), Arch. Biochem. Biophys. 42, 305.

Szent-Györgyi, A.G., Cohen, C., and Philpott, D.E. (1960), J. Mol. Biol. 2, 133.

Tada, M., Bailin, G., Bárány, K., and Bárány, M. (1969), Biochemistry 8, 4842.

Tanford, C. (1961), Physical Chemistry of Macromolecules, John Wiley and Sons, Inc., New York, New York., p. 390.

Theiner, M. (1963), Ph.D. Dissertation, University of Pittsburgh, Penn.

Tonomura, Y., Appel, P., and Morales, M. (1966), Biochemistry 5, 515.

Tonomura, Y., Hayashi, Y., and Inoue, A. (1973), Cold Spring Harbor Symp. Quant. Biol. 37, 169.

Van Holde, K.E. (1967), Fractions No. 1, Beckman Instruments Inc., Palo Alto, California.

Van Holde, K.E., and Baldwin, R.L. (1958), J. Phys. Chem. 62, 734.

Verpoorte, J.A., and Kay, C.M. (1966), Arch. Biochem. Biophys. 113, 53.

Vierling, J., Roberts, J.L., Conway, G., and Heazlitt, R. (1968), Biochim. Biophys. Acta 160, 53.

Weeds, A.G., and Frank, G. (1973), Cold Spring Harbor Symp. Quant. Biol. 37, 9.

Weeds, A.G., and Lowey, S. (1971), J. Mol. Biol. 61, 701.

Weeds, A.G., and Pope, B. (1971), Nature 234, 85.

Whitaker, J.R., and Bender, M.L. (1965), J. Am. Chem. Soc. 87, 2728.

Williams, J.W., Van Holde, K.E., Baldwin, R.L., and Fujita, H. (1958), Chem. Rev. 58, 715.

Woods, E.F., Himmelfarb, S., and Harrington, W.F. (1963), J. Biol. Chem. 238, 2374.

Young, M. (1967), J. Biol. Chem. 242, 2790.

Young, D.M., Himmelfarb, S., and Harrington, W.F. (1964), J. Biol. Chem. 239, 2822.

Young, D.M., Himmelfarb, S., and Harrington, W.F. (1965), J. Biol. Chem. 240, 2428.

Yphantis, D.A. (1964), Biochemistry 3, 297.

APPENDICES

Computer Programs

Appendix 1. SDCF. The program SDCF is a translation of the mathematical expressions and numerical procedures described in Chapter 2 into APL programming language and form, and is routinely used for the calculation of sedimentation coefficients.

Input for SDCF consists of the following parameters:

X	a vector of the horizontal distances (cm) from the maximum ordinate position of the boundary to the inner edge of either reference hole image, as measured on the schlieren plate,
T	a vector of the times (min) at which the photographs were taken,
REF	the true radial distance (cm) from the axis of rotation to the inner edge of the reference hole considered,
MF	the reciprocal of the cell to plate magnification,
RPM	the rotor speed (revolutions/min),
BARV	the partial specific volume (ml/gm),
RHOT	the solvent density (gm/ml) at the temperature of the sedimentation velocity run,
NNO	the relative viscosity of the solvent to that of water,
NTN20	the relative viscosity of water at the temperature of the run to that at 20°C.

Output consists of S0BS, the observed sedimentation coefficient, and S20W, the corrected sedimentation coefficient, both in units of seconds.

The program SDCF is printed on the following page.

```
     ∇ X SDCF T;E;Y
[1]    →(REF>6)/SET
[2]    E←1
[3]    →CALS
[4]    SET:E←¯1
[5]    CALS:SLOPE←(((ρT)×+/T×Y)-(+/T)×+/Y←⊛REF+E×X×MF)÷((ρT)
       ×+/T*2)-(+/T)*2
[6]    ('SOBS ';SOBS←SLOPE×60÷(RPM×6.2832)*2)
[7]    ('S20W ';SOBS×NTN20×NNO×(1-BARV×0.9982)÷1-BARV×RHOT)
     ∇
```

Appendix 2. LSDQM, HSDQM, MNZY2, and LSPFIT. The APL programs HSDQM and LSDQM are written on a basis of the theory and mathematical relationships presented in Chapter 2. They are designed for the reduction of high- and low-speed sedimentation equilibrium data and for the subsequent calculation of the apparent weight-average molecular weights at individual radial positions. MNZY2 extends these computations and is used to calculated the number-, z-, and y_2-average molecular weight moments at the same positions. The polynomial least squares program, LSPFIT, is employed extensively as a subroutine in HSDQM, LSDQM, and MNZY2.

The Input for HSDQM consists of the following parameters:

X	a vector of the horizontal comparator readings (cm) derived with respect to the principal interference pattern,
Y	a vector of the average vertical fringe displacements (cm) associated with the radial positions considered in X,
YW	a vector of the variance values of the Y readings,
BX	a vector of the horizontal comparator readings (cm) of the base-line patterns,
BY	a vector of the average vertical fringe displacements (cm) associated with the radial positions considered in BX,
BW	a vector of the variance values of the BY readings,
XOR	the horizontal comparator reading (cm) for the inner edge of the outer reference hole fringes,
MAG	the cell to photographic plate magnification,

RCR — the true radial distance (cm) from the axis of rotation to the inner edge of the outer reference hole,

T — the absolute temperature (°K) of the sedimentation equilibrium run,

VT — the variance of temperature control,

BARV — the partial specific volume (ml/gm),

VBARV — the variance of the value taken for the partial specific volume,

RHO — the solution density (gm/ml) at the temperature of the equilibrium run,

VRHO — the variance of the density value,

RPM — the rotor speed (revolutions/min),

VRPM — the variance of rotor speed control,

FDEL — the vertical distance (cm) between fringes as measured in a plateau region,

VFDEL — the variance of the FDEL measurement,

J — the power of the polynomial to which the data in the central region of the column is to be fitted by the sliding least squares routine (1, 2, or 3).

The Output is a table with the following columns: $r^2/2$ (one-half the square of the corrected radial distances in order of increasing radii), ln dy (natural logarithm of the smoothed fringe displacement corresponding to each radial position), the estimated propagated error in the ln dy values, the concentration (in terms of fringes) at each radial position, the apparent weight-average molecular weight at each radial position, and the propagated experimental error in the $\overline{M}_{w,app}$ values. HSDQM also prints out the calculated value of the constant term, $RT/(1 - \bar{\nu}\rho)\omega^2$, and the meniscus concentration (in fringes), as well as an estimate of the propagated errors.

A copy of the program HSDQM is shown on the next two pages.

```
     ∇ HSDQM;DELY;DY;DYDR2;I;IND;M;N;Q;S;VDYDR2;VYO;W;WS
[1]    SGW←VSGW←SMY←VSMY←R2←DY←ι S←K←¯1+N←1
[2]    R2←R2,0.5×(RCR-(XOR-X[N])≠MAG)*2
[3]    DY←DY,Y[N]-Y[1]
[4]    →((N←N+1)>ρY)/8
[5]    →(X[N]≠X[N-1])/2
[6]    Y[1]←Y[1]-Y[N-1]-Y[N]
[7]    →4
[8]    Y←BY
[9]    X←0.5×(RCR-(XOR-BX)≠MAG)*2
[10]   W←1≠BW
[11]   0 LSPFIT 3
[12]   →(0=+/BY←(DY←DY-(R2∘.*0,ι3)+.×CF)≥0.015)/85
[13]   WW←YW
[14]   →((N←BYι1)<9)/85
[15]   BX←(3ρ1),(ιB),3ρB←N-6
[16]   BW←(ι3),(Bρ4),4+ι3
[17]   DYDR2←VDYDR2←ι¯1+I←1
[18]   X←R2[(IND←BX[I]+0,ι6)]
[19]   Y←DY[IND]
[20]   W←1≠WW[IND]
[21]   3 LSPFIT 2
[22]   DYDR2←DYDR2,SLP[BW[I]]
[23]   VDYDR2←VDYDR2,VSLP[BW[I]]
[24]   →((((N-2)>I)∧I>4),(((N≥I)∧I≥N-2)∨4≥I←I+1))/ 18 22
[25]   X←DY[ιN]
[26]   Y←DYDR2
[27]   W←1≠VDYDR2
[28]   K LSPFIT 1
[29]   →(0=+/BY←(DY←DY-DY[1]-DELY←CF[1]≠CF[2])≥0.025)/85
[30]   →(1<K←K+1)/42
[31]   →(0<M←⌊/DY[(B←ιN←BYι1)])/33
[32]   S←0.0001+|M
[33]   Y←⊕BY←DY[B]+S
[34]   X←R2[B]
[35]   W←1≠YW[B]
[36]   2 LSPFIT 2
[37]   W←1≠YW[B]+(BY-*LSY)*2
[38]   2 LSPFIT 3
[39]   WW←YW[B]+(DY[B]-BY←(*LSY)-S)*2
[40]   BY←BY≥0.018
[41]   →14
[42]   VYO←(VA×(1≠CF[2]*2))+(CF[1]*2)×VB×1≠CF[2]*4
[43]   N←(DY≥0.005)ι1
[44]   →(0=+/M←DY≥0.06)/48
[45]   →(15>M←1+(Mιi)-N)/49
[46]   M←15
[47]   →51
[48]   M←1+(ρDY)-N
[49]   →((9≤M←¯1+2×⌈M≠2),(9>1+(ρDY)-N))/ 51 85
[50]   M←9
[51]   BY←(3ρ1),((ρS)ρ1),(Q←ι1+B-M),(1+B-⌽S←7+2×¯1+ι(M-7)≠2),
       3ρ¯6+B←1+(ρDY)-N
```

```
[52]  BX←(3ρ7),S,((ρQ)ρM),(ϕS),3ρ7
[53]  BW←(ι3),(⌈S÷2),((ρQ)ρ⌈M÷2),(⌈ϕS÷2),4+ι3
[54]  DY←(-B)↑DY
[55]  R2←(-B)↑R2
[56]  YW←WW←(-B)↑YW
[57]  WS←ιK←0
[58]  I←1
[59]  Q←((BX[I]≠7),(BX[I]=7))/(J,2)
[60]  Y←⊕DY[(IND←BY[I]+0,ιBX[I]-1)]
[61]  X←R2[IND]
[62]  W←1÷WW[IND]
[63]  K LSPFIT Q
[64]  →(K=3)/70
[65]  WS←WS,WW[I]+(DY[I]-+(X[BW[I]]∘.*0,ιQ)+.×CF)*2
[66]  →((((B-2)>I)∧I>4),(((B≥I)∧I≥B-2)∨4≥I←I+1))/ 59 65
[67]  K←3
[68]  WW←WS
[69]  →58
[70]  SGW←SGW,SLP[BW[I]]
[71]  VSGW←VSGW,VSLP[BW[I]]
[72]  SMY←SMY,LSY[BW[I]]
[73]  VSMY←VSMY,VSLP[BW[I]]
[74]  →((((B-2)>I)∧I>4),(((B≥I)∧I≥B-2)∨4≥I←I+1))/ 59 70
[75]  M←(B,6)ρ0
[76]  M[;1]←R2
[77]  M[;4]←(*M[;2]←SMY)÷FDEL
[78]  M[;3]←VSMY*0.5
[79]  M[;5]←SGW×K←83140000×T÷(BVR←1-BARV×RHO)×W2←((RPM÷60)
      ×6.2832)*2
[80]  M[;6]←K×(VSGW+(SGW*2)×VK←(VT÷T*2)+(((VBARV×RHO*2)+VRHO
      ×BARV*2)÷BVR*2)+4×VRPM÷RPM*2)*0.5
[81]  '     R2/2(CM*2)          LNDY              +/-
       C(FRINGES)          MWAPP             +/-'
[82]  M
[83]  ('   CNST= ';K;' +/- ';K×VK*0.5;'  MENISCUS CONC. ';
      DELY÷FDEL;' +/- ';((VYO+(VFDEL×DELY*2)÷FDEL*2)*0.5)÷
      FDEL;' FRINGES ')
[84]  →0
[85]  'INSUFFICIENT FRINGE DISPLACEMENT OR DATA POINTS SPAN
      FOR ANALYSIS'
∇
```

Other than the different methods involved in determining the concentration at each radial position, the computation of apparent molecular weight values from low-speed sedimentation equilibrium data is essentially identical to that from high-speed data. Thus, the Input for LSDQM is the same as that listed for HSDQM, but with one additional parameter, YO, the fringe displacement corresponding to the initial cell-

loading concentration ultracentrifugally calibrated via a separate c_o run. Likewise, the Output of LSDQM is the same except that the estimated value of the meniscus concentration is not printed.

The program LSDQM is reproduced below.

```
     ∇ LSDQM;DIS;DY;I;IND;M;N;Q;S;W;WS
[1]    SGW←VSGW←SMY←VSMY←R2←DY←WS←⍳K←¯1+N←1
[2]    R2←R2,0.5×(RCR-(XOR-X[N])÷MAG)*2
[3]    DY←DY,Y[N]-Y[1]
[4]    →((N←N+1)>⍴Y)/8
[5]    →(X[N]≠X[N-1])/2
[6]    Y[1]←Y[1]-Y[N-1]-Y[N]
[7]    →4
[8]    Y←BY
[9]    X←0.5×(RCR-(XOR-BX)÷MAG)*2
[10]   W←1÷BW
[11]   0 LSPFIT 3
[12]   →(0=+/M←(DY←DY-(R2∘.*0,⍳3)+.×CF)≥0.06)/16
[13]   →(15>M←M⍳1)/17
[14]   M←15
[15]   →19
[16]   M←⍴DY
[17]   →((9≤M←¯1+2×⌈M÷2),(9>⍴DY))/ 19 51
[18]   M←9
[19]   DIS←DY+YO-((R2[⍴DY]×DY[⍴DY])-0.5×+/(R2[1+IND]+R2[IND])
       ×DY[1+IND]-DY[IND←⍳(⍴DY)-1])÷(R2[⍴DY]-R2[1])
[20]   WW←YW
[21]   BY←(3⍴1),((⍴S)⍴1)⍪(Q←⍳1+B-M),(1+B-⌽S←7+2×¯1+⍳(M-7)÷2),
       3⍴¯6+B←⍴DY
[22]   BX←(3⍴7),S,((⍴Q)⍴M),(⌽S),3⍴7
[23]   BW←(⍳3),(⌈S÷2),((⍴Q)⍴⌈M÷2),(⌈⌽S÷2),4+⍳3
[24]   I←1
[25]   Q←((BX[I]≠7),(BX[I]=7))/(J,2)
[26]   Y←⊕DIS[(IND←BY[I]+0,⍳BX[I]-1)]
[27]   X←R2[IND]
[28]   W←1÷WW[IND]
[29]   K LSPFIT Q
[30]   →(K=3)/36
[31]   WS←WS,WW[I]+(DIS[I]-*(X[BW[I]]∘.*0,⍳Q)+.×CF)*2
[32]   →(((B-2)>I)∧I>4),(((B≥I)∧I≥B-2)∨4≥I←I+1))/ 25 31
[33]   K←3
[34]   WW←WS
[35]   →24
[36]   SGW←SGW,SLP[BW[I]]
[37]   VSGW←VSGW,VSLP[BW[I]]
[38]   SMY←SMY,LSY[BW[I]]
[39]   VSMY←VSMY,VLSY[BW[I]]
[40]   →(((B-2)>I)∧I>4),(((B≥I)∧I≥B-2)∨4≥I←I+1))/ 25 36
[41]   M←(B,6)⍴0
```

```
[42]  M[;1]←R2
[43]  M[;4]←(*M[;2]←SMY)÷FDEL
[44]  M[;3]←VSMY*0.5
[45]  M[;5]←SGW×K←83140000×T÷(BVR←1-BARV×RHO)×W2←((RPM÷60)
      ×6.2832)*2
[46]  M[;6]←K×(VSGW+(SGW*2)×VK←(VT÷T*2)+(((VBARV×RHO*2)+VRHO
      ×BARV*2)÷BVR*2)+4×VRPM÷RPM*2)*0.5
[47]  '   R2/2(CM*2)          LNDY              +/-
       C(FRINGES)          MWAPP             +/-'
[48]  M
[49]  ('   CNST= ';K;' +/- ';K×VK*0.5)
[50]  →0
[51]  'INSUFFICIENT DATA POINT SPAN FOR ANALYSIS'
      ∇
```

The Input for MNZY2 consists of the following parameters, commonly derived from the final computations of either HSDQM or LSDQM:

R2	a vector of $r^2/2$ values,
SMY	a vector of the smoothed ln dy values associated with the radial positions considered in R2,
VSMY	a vector of the variances of the smoothed ln dy values,
SGW	a vector of the effective reduced weight-average molecular weights (as defined by Yphantis, 1964),
VSGW	a vector of the calculated variances of the SGW values,
WW	a vector of the final weighing factors computed in LSDQM or HSDQM,
K	the value of the constant term $RT/(1 - \bar{v}\rho)\omega^2$,
VK	the variance estimate of the constant term,
J	the power of the polynomial to which the data in the central region of the column is to be fitted by the sliding least squares routine (1, 2, or 3).

The Input for MNZY2 also includes the vectors BX, BY, and BW, established in LSDQM or HSDQM, which control the sliding least squares and smoothing routines.

The Output is a table of the apparent number-, z-, and y_2-average molecular weight values calculated at each radial position plus an estimate of the associated propagated error.

The program MNZY2 is prir ed below.

```
     ∇ MNZY2;C;I;IND;IT;M;Q;S;   M;T;W;X;Y
[1]    SGZ←VSGZ←SGN←VSGN←ISY2-   3Y2←ιSUM←¯1+I←1
[2]    C←*SMY
[3]    S←1÷SGW
[4]    Y←S[IND]×X←1÷C[(IND←BY[I]+0,ιBX[I]-1)]
[5]    W←1÷WW[IND]
[6]    3 LSPFIT J
[7]    SGZ←SGZ,(ISY2←ISY2,SLP[BW[I]])[I]×Q←SGW[I]*2
[8]    VSGZ←VSGZ,Q×((VISY2←VISY2,VSLP[BW[I]])[I]×Q)+4×(ISY2[I]
       *2)×VSGW[I]
[9]    →(I>1)/13
[10]   T←C[1]÷SGN←SGN,0.5×(3×SGW[1])-SGZ[1]
[11]   VSGN←VSGN,0.25×VSGZ[1]+9×VSGW[1]
[12]   →16
[13]   SGN←SGN,C[I]÷IT←T+0.5×SUM←SUM+(C[I]+C[I-1])×R2[I]-R2[I
       -1]
[14]   M←((VSMY[1]×*2×SMY[1])×VSGN[1]×(C[1]*2)÷SGN[1]*2)×(C[I]
       *2)÷SGN[1]*2
[15]   VSGN←VSGN,(M+((IT-0.5×C[I]×R2[I]-R2[I-1])*2)×VSMY[I]×*
       2×SMY[I])÷IT*4
[16]   →((((B-2)>I)∧I>4),(((B≥I)∧I≥B-2)∨4≥I←I+1))/ 4 7
[17]   M←(B,6)ρ0
[18]   M[;1]←SGN×K
[19]   M[;2]←K×(VSGN+VK×SGN*2)*0.5
[20]   M[;3]←SGZ×K
[21]   M[;4]←K×(VSGZ+VK×SGZ*2)*0.5
[22]   M[;5]←K÷ISY2
[23]   M[;6]←(K×(VK+VISY2÷ISY2*2)*0.5)÷ISY2
[24]   '       MNAPP                +/-              MZAPP
         +/-              MY2APP'              +/-'
[25]   M
     ∇
```

The auxiliary program LSPFIT fits a power series polynomial through a collection of given points by the method of least squares utilizing matrix inversion techniques. To facilitate its use as a subroutine and thus minimize extraneous computations in a given situation, the program is designed to evaluate the many variables and statistical parameters associated with the coefficients of the fitted polynomial in successive stages. Control is exercised by the appropriate specification of an option parameter, OPTN. If OPTN is set equal to zero, only

the coefficients of the fitted polynomial are calculated. If OPTN equals 1, then the variances of the coefficients are additionally evaluated. If OPTN is set equal to 2, the least squares values of the independent variable and their associated variances are also determined. Any other specification of OPTN will result in the computation of all of these plus the value of the slope at each independent variable and the estimated variance of this value.

Input for LSPFIT consists of the following parameters:

X	a vector of the independent variables,
Y	a vector of the dependent variables associated with X,
W	a vector of the numerical weighing factors,
N	the degree of the polynomial to be fitted.

The Output of LSPFIT is not printed directly in keeping with its role as a subroutine. Following are the results that can be specifically called:

CF	the coefficients of the fitted polynomial in ascending order of the powers of the independent variable,
VA,VB	the variances of the coefficients in the same order,
LSY	the least squares values of the independent variable,
VLSY	the variances of the LSY values,
SLP	the value of the first derivative solved for each independent variable,
VSLP	the variances of the SLP values.

A copy of the program LSPFIT is presented below.

```
    ∇ OPTN LSPFIT N;A;I;K;M;MY;NY;R;S;SW;U;WT
[1]   WT←⍉(N,K)⍴W←(K←⍴W)×W÷+/W
[2]   NY←Y-MY←(+/W×Y)÷SW←+/W
[3]   CF←(MY-+/R×M),R←(S←⌹(⍉A)+.×A×WT)+.×U←NY+.×WT×A←A-(K,N)
      ⍴M←(+/[1] WT×A←X∘.*⍳N)÷SW
[4]   →(OPTN=0)/0
[5]   VB←(1 1 ⍉S)×SG2←((NY+.×NY×W)-R+.×U)÷K-N+1
```

```
[6]    VA←SG2×(÷SW)+(M+.×S)+.×M
[7]    →(OPTN=1)/0
[8]    LSY←(X∘.*0,ιN)+.×CF
[9]    VLSY←SG2×(÷SW)+(1 1 ⌹(A+.×S)+.×⍉A×WT)
[10]   →(OPTN=2)/0
[11]   SLP←VSLP←ι0
[12]   A←((K,N)ριN)×X∘.*0,ιN-I←1
[13]   M←(2×(ιN)∘.<ιN)+(ιN)∘.=ιN
[14]   SLP←SLP,R+.×A[I;]
[15]   VSLP←VSLP,+/+/SG2×S×M×A[I;]∘.×A[I;]
[16]   →(K≥I←I+1)/14
       ∇
```

Appendix 3. ARCH and RND. The APL program ARCH, intended for the numerical analysis of data from Archibald experiments, incorporates the mathematical expressions and procedures presented in Chapter 2. In conjunction with the rounding program RND, ARCH is used to calculate the apparent weight-average molecular weight and solution concentration at the meniscus position.

The Input for ARCH consists of the following parameters:

ZN	a vector of vertical distances (cm) from the base line to the gradient curve, as measured on the schlieren plate in order from the meniscus to the plateau region,
RN	the comparator distance (cm) from the inner edge of the inner reference hole image to the meniscus,
DX	the width of the horizontal interval (cm),
MAG	the cell to plate magnification,
T	the absolute temperature (°K) of the Archibald run,
BARV	the partial specific volume (ml/gm),
RHO	the solution density (gm/ml),
RPM	the rotor speed (revolutions/min),
CO	the calibrated value (in units of area) of the initial concentration of the sample solution.

The Output consists of MM, the apparent weight-average molecular weight (rounded to the nearest hundred), and CM, the concentration

of the solution estimated at the meniscus (rounded to the third decimal place).

Following is the program ARCH.

```
     ∇ ARCH;CNST;DF;XN
[1]    XN←(5.7÷RN÷MAG)+(DF←DX÷MAG)×(⍳(⍴ZN))-1
[2]    CNST←83140000×T÷(1-BARV×RHO)×((RPM÷60)×6.2832)*2
[3]    MM←CNST×ZN[1]÷XN[1]×CM←CO-(1÷XN[1]*2)×DF×+/ZN×XN*2
[4]    (' MM EQUALS ';¯2 RND MM;' CM EQUALS ';3 RND CM)
     ∇
```

[redacted] for RND is X, the number to be rounded, and N, the decimal [redacted] which the rounding is to take place. The rounded number is the Output. RND is defined as:

```
     ∇ R←N RND X
[1]    R←(10*-N)×⌊0.5+X×10*N
     ∇
```